STUDIES ON TWO NOVEL SHRIMP RESPONSE PROTEINS TO YELLOW HEAD VIRUS AND DEVELOPMENT OF A PROTEIN INTERACTION NETWORK FOR SHRIMP TAURA SYNDROME VIRUS

THANAWAT SRIPHAIJIT

A THESIS SUBMITTED IN PARTIAL FULFILLMENT
OF THE REQUIREMENTS FOR
THE DEGREE OF DOCTOR OF PHILOSOPHY
(BIOTECHNOLOGY)
FACULTY OF GRADUATE STUDIES
MAHIDOL UNIVERSITY
2014

Thesis
entitled

STUDIES ON TWO NOVEL SHRIMP RESPONSE PROTEINS TO YELLOW HEAD VIRUS AND DEVELOPMENT OF A PROTEIN INTERACTION NETWORK FOR SHRIMP TAURA SYNDROME VIRUS

.....
Mr. Thanawat Sriphaijit
Candidate

.....
Prof. Amornrat Phongdara,
Dr.Eng.
Co-advisor

.....
Prof. Timothy W. Flegel,
Ph.D.
Major advisor

.....
Prof. Watanalai Panbangred,
Dr.Eng.
Co-advisor

.....
Miss Saengchan Senapin,
Ph.D.
Co-advisor

.....
Prof. Banchong Mahaisavariya,
M.D., Dip Thai Board of Orthopedics
Dean
Faculty of Graduate Studies
Mahidol University

.....
Assoc. Prof. Chuenchit Boonchird,
Ph.D.
Program director
Doctor of Philosophy Program in
Biotechnology
Faculty of Science
Mahidol University

Thesis
entitled

STUDIES ON TWO NOVEL SHRIMP RESPONSE PROTEINS TO YELLOW HEAD VIRUS AND DEVELOPMENT OF A PROTEIN INTERACTION NETWORK FOR SHRIMP TAURA SYNDROME VIRUS

was submitted to the Faculty of Graduate Studies, Mahidol University
for the degree of Doctor of Philosophy (Biotechnology)
on
March 3, 2014

.....
Mr. Thanawat Sriphaijit
Candidate

.....
Prof. Amornrat Phongdara,
Dr.Eng.
Member

.....
Asst. Prof. Somchai Chauvatcharin,
Ph.D.
Chair

.....
Prof. Watanalai Panbangred,
Dr.Eng.
Member

.....
Prof. Timothy W. Flegel,
Ph.D.
Member

.....
Mr. Triwit Rattanarojpong,
Ph.D.
Member

.....
Miss Saengchan Senapin,
Ph.D.
Member

.....
Prof. Banchong Mahaisavariya,
M.D., Dip Thai Board of Orthopedics
Dean
Faculty of Graduate Studies
Mahidol University

.....
Prof. Skorn Mongkolsuk,
Ph.D.
Dean
Faculty of Science
Mahidol University

ACKNOWLEDGEMENTS

I would like to express my gratitude to all those who gave me the possibility to complete this thesis. First, my sincere gratitude and deep appreciation are expressed to my advisor, Prof. Timothy Flegel for his invaluable advice and discussion, patient proof reading, and giving me opportunities to do this research. My sincere appreciation is also expressed to Dr. Saengchan Sanapin, my co-advisor, for her guidance, continuous discussion, and many suggestions for make me to carry out my study successfully.

I would like to express my great thanks to Prof. Amornrat Phongdara and Prof. Watanalai Panbangred for her valuable advice and supports on my thesis work.

I would like to thank to the member in room K444 for their help, friendship, and hospitality which make me happy for being the member of CENTEX SHRIMP.

I would like to acknowledge the support from a Royal Golden Jubilee Ph.D. Program by Thailand Research Fund and a Thailand Graduate Institute of Science and Technology Scholarship.

Finally, I would like to express my deepest appreciation to my parent, for their concern, love, and encouragement throughout my graduate study and my life.

Thanawat Sriphaijit

STUDIES ON TWO NOVEL SHRIMP RESPONSE PROTEINS TO YELLOW HEAD VIRUS AND DEVELOPMENT OF A PROTEIN INTERACTION NETWORK FOR SHRIMP TAURA SYNDROME VIRUS

THANAWAT SRIPHAIJIT 4837119 SCBT/D

Ph.D. (BIOTECHNOLOGY)

THESIS ADVISORY COMITTEE: TIMOTHY W. FLEGEL, Ph.D., SAENGCHAN SENAPIN, Ph.D., AMORNRAT PHONGDARA, Dr. Eng., WATANALAI PANBANGRED, Dr. Eng.

ABSTRACT

Shrimp farming is an important business in many Asian countries including Thailand. Despite their economic importance, relatively little is known about the shrimp themselves and about their interaction with pathogens (especially viral pathogens). This is due in part to the lack of continuous shrimp cell lines for conducting molecular and cellular studies. This research focused on interactions between shrimp and viral proteins and among shrimp virus proteins themselves. Using a yeast two-hybrid (Y2-H) screen between yellow head virus (YHV) proteins and hemocyte proteins of the black tiger shrimp *Penaeus monodon*, two interacting shrimp proteins were discovered. One was the C-terminal region of SPH516 (SPH516-C) that interacted with a putative metal ion binding domain (MIB) encoded by ORF1b of the YHV genome. Subsequently, the full-length of SPH516 (*PmSPH516*) cDNA was obtained using 5' rapid amplification of cDNA ends (5' RACE) and it also bound specifically to the MIB domain only. *Pm*SPH516 domain features included a putative signal peptide, glycine-rich repeat motifs, a clip domain, an HDG triad and a trypsin-like serine protease domain. *PmSPH516* transcripts were highly expressed in hemocytes and gills and were found to be down-regulated after YHV infection. Immunohistochemistry using a polyclonal antibody raised against heterologously expressed SPH516-C protein revealed that it was present almost exclusively in shrimp hemolymph. The second YHV-interacting protein found was a leucine-rich repeat (*PmLRR*) sequence that also bound to the MIB domain. However, identification of this first full-length *PmLRR* from shrimp revealed that the initial partial sequence was not in-frame with the AD domain of pGADT7 plasmid used in the yeast two-hybrid assay. Thus, interaction was not observed between the full-length *Pm*LRR and YHV MIB domain. The deduced protein of *Pm*LRR contained a high proportion of leucine residues (17%) and had sixteen tandem LRR motifs of 23-24 amino acids in length in the primary sequence. The computed 3D structure revealed a horseshoe shape consisting of alternately repeated strand and helical domains. *PmLRR* expression was tissue-specific (i.e., highest in hemocytes, the intestine and lymphoid organ) suggesting that it may play some role in shrimp defense against pathogens. A preliminary test suggested that *PmLRR* was down-regulated after viral challenges. A second Y2-H screen using the BIR domain of Taura syndrome virus (TSV) as bait yielded the first reported *Pm*Amidase from shrimp, but this was only partially characterized. With respect viral-viral protein interactions, a protein-protein interaction (PPI) network for TSV was established using 81 pairwise protein interaction tests that yielded 19 positive interactions. The TSV PPI map was visualized by cytoscape software and revealed a total number of 6 proteins (nodes) involved in 14 interactions (edges). Interestingly, the BIR and VP1 proteins had the highest number of interactions (5 edges) in the map, possibly suggesting important roles in the TSV life cycle. By *in vitro* pull-down assays, it was shown that the structural proteins alone (VP1, VP2 and VP3) could not form a complex without Hel protein involvement.

KEY WORDS: TSV / YHV / YEAST TWO-HYBRID / PmLRR / PmSPH516

127 pages

การศึกษายีนสองชนิดในกุ้งที่ตอบสนองต่อการติดเชื้อไวรัสหัวเหลือง และการสร้างแผนที่ปฏิสัมพันธ์สำหรับโปรตีนของไวรัสทอร่า
STUDIES ON TWO NOVEL SHRIMP RESPONSE PROTEINS TO YELLOW HEAD VIRUS AND DEVELOPMENT OF A PROTEIN INTERACTION NETWORK FOR SHRIMP TAURA SYNDROME VIRUS

ธนวัฒน์ ศรีไพจิตร์ 4837119 SCBT/D

ปร.ด . (เทคโนโลยีชีวภาพ)

คณะกรรมการที่ปรึกษาวิทยานิพนธ์: ทิมโมที ฟลีเกล, Ph.D., แสงจันทร์ เสนาปิน, Ph.D., อมรรัตน์ พงศ์ดารา, Dr. Eng., วัฒนาลัย ปานบ้านเกร็ด, Dr. Eng.

บทคัดย่อ

อุตสาหกรรมการเลี้ยงกุ้งมีความสำคัญต่อเศรษฐกิจของประเทศในแถบภูมิภาคเอเชียรวมทั้งประเทศไทยด้วย แต่ความรู้ความเข้าใจในกลไกของกุ้งต่อการตอบสนองเชื้อโรคโดยเฉพาะเชื้อไวรัสยังมีอยู่จำกัด ส่วนหนึ่งเป็นเพราะการที่ไม่มีเซลล์กุ้งที่เลี้ยงได้อย่างถาวรสำหรับใช้เพื่อศึกษาวิจัยด้านชีวโมเลกุล งานวิจัยนี้มีจุดประสงค์ในการศึกษาปฏิสัมพันธ์ระหว่างโปรตีนของกุ้งและโปรตีนของไวรัสรวมถึงปฏิสัมพันธ์ระหว่างโปรตีนของไวรัสด้วยกันเอง โดยใช้เทคนิค yeast two-hybrid screen ผลการหาปฏิสัมพันธ์ระหว่างโปรตีนของไวรัสหัวเหลืองและโปรตีนจากเม็ดเลือดกุ้งกุลาดำทำให้พบโปรตีนสองชนิดที่จับได้กับโดเมน metal ion binding domain (MIB) ของไวรัสหัวเหลืองซึ่งสร้างมาจากยีนในส่วน ORF1b ของไวรัส โดยโปรตีนชนิดแรกนั้น เป็นส่วนของปลายซี (C-terminus) ของโปรตีน serine protease homolog (SPH516) ต่อมาได้หาลำดับนิวคลีโอไทด์ที่สมบูรณ์ของยีน *PmSPH516* ด้วยเทคนิค 5’ rapid amplification of cDNA ends (5’ RACE) ซึ่งยังพบว่าโปรตีน SPH516 ที่สมบูรณ์มีปฏิสัมพันธ์กับโปรตีน MIB ของไวรัส ลักษณะที่สำคัญของโปรตีน *Pm*SPH516 คือมีส่วนของ signal peptide, มีบริเวณที่มีกรดอะมิโนไกลซีนซ้ำๆ (glycine-rich repeat), มีโดเมน clip, โดเมน HDG triad และโดเมน trypsin-like serine protease การศึกษาการแสดงออกของยีน *PmSPH516* พบว่ามีมากในเม็ดเลือดและเหงือกกุ้ง แต่จะลดลงเมื่อกุ้งติดเชื้อไวรัสหัวเหลือง ผลการศึกษาทางอิมมูโนวิทยาโดยใช้แอนติบอดีที่จำเพาะต่อโปรตีน SPH516 ด้านปลายซี พบว่าโปรตีน SPH516 อยู่ในน้ำเลือดกุ้ง โปรตีนชนิดที่สองที่ทำการศึกษา เริ่มจากการพบลำดับนิวคลีโอไทด์บางส่วนที่มีความเหมือนกับยีนที่สร้างโปรตีนที่มีกรดอะมิโนลิวซีนซ้ำๆ (leucine-rich repeat, LRR) แต่เมื่อหาลำดับนิวคลีโอไทด์ที่สมบูรณ์ของยีน *PmLRR* แล้ว ทำให้พบว่าลำดับนิวคลีโอไทด์บางส่วนที่พบแต่แรกนั้นไม่ได้เชื่อมต่อตรงกับโดเมน AD ของพลาสมิด pGADT7 เมื่อทดสอบปฏิสัมพันธ์ของโปรตีนจึงไม่พบการมีปฏิสัมพันธ์ระหว่างโปรตีน *Pm*LRR ที่สมบูรณ์กับโปรตีน MIB ของไวรัสหัวเหลือง ลักษณะเฉพาะของโปรตีน *Pm*LRR คือมีกรดอะมิโนลิวซีนสูงถึง 17 เปอร์เซ็นต์ และมีโดเมน LRR ที่มีความยาว 23-24 กรดอะมิโน จำนวน 16 โดเมน การจำลองโครงสร้างสามมิติของโปรตีน *Pm*LRR พบว่ามีโครงสร้างเป็นรูปเกือกม้าที่ประกอบด้วยสายโปรตีนแบบแผ่นสลับกับแบบเกลียว การศึกษาการแสดงออกของยีนพบว่า *PmLRR* มีการแสดงออกสูงในเนื้อเยื่อที่เกี่ยวกับภูมิคุ้มกันในกุ้ง เช่น เม็ดเลือด ลำไส้และต่อมน้ำเหลือง ซึ่งอาจเป็นไปได้ว่า *PmLRR* มีความเกี่ยวข้องกับการต่อต้านเชื้อโรคในกุ้ง เมื่อทดสอบในกุ้งที่ติดเชื้อไวรัสหัวเหลือง พบว่ามีการแสดงออกของยีน *PmLRR* ลดลง การศึกษาปฏิสัมพันธ์ระหว่างโดเมน BIR ของไวรัสทอร่า (Taura syndrome virus) และโปรตีนของกุ้ง ทำให้พบยีนที่ยังไม่เคยมีรายงานในกุ้งมาก่อน คือ *Pm*Amidase ส่วนการศึกษาปฏิสัมพันธ์ระหว่างโปรตีนของไวรัสทอร่าด้วยกันเองนั้น พบปฏิสัมพันธ์ของโปรตีน 19 คู่ จากการทดสอบทั้งหมด 81 คู่ เมื่อสร้างแผนที่ปฏิสัมพันธ์ด้วยโปรแกรม Cytoscape พบว่าในแผนที่ประกอบด้วยโปรตีน 6 ชนิด ซึ่งมีปฏิสัมพันธ์กันจำนวน 14 ปฏิสัมพันธ์ โดยโปรตีน BIR และโปรตีน VP1 เป็นโปรตีนที่มีปฏิสัมพันธ์กับโปรตีนชนิดอื่นมากที่สุดถึง 5 ปฏิสัมพันธ์ อาจกล่าวได้ว่าโปรตีนทั้งสองชนิดนี้มีความสำคัญต่อไวรัสทอร่า จากการใช้เทคนิค pull-down assays พบว่าโปรตีนโครงสร้างของไวรัสได้แก่ โปรตีน VP1, VP2 และ VP3 ไม่สามารถมีปฏิสัมพันธ์กันได้โดยปราศจากโปรตีน Hel

127 หน้า

CONTENTS

CONTENTS (cont.)

CONTENTS (cont.)

CONTENTS (cont.)

CONTENTS (cont.)

LIST OF TABLES

LIST OF FIGURES

LIST OF FIGURES (cont.)

LIST OF FIGURES (cont.)

LIST OF ABBREVIATION

%	Percent
bp	Base pair
°C	Degree Celsius
cDNA	Complementary deoxyribonucleic acid
DMSO	Dimethylsulfoxide
dsDNA	Double stranded deoxyribonucleic acid
dsRNA	Double stranded ribonucleic acid
Fig	Figure
GAL4 AD	GAL4 Activation domain
GAL4 BD	GAL4 DNA binding domain
g	Gram
x g	Gravity force
h	Hour
H&E	Hematoxylin and Eosin
IgG	Immunoglobulin G
IPTG	Isopropyl-beta-D-thiogalactopyranoside
kDa	Kilo Dalton
m	Metre
M	Mole
mA	Milliamp
mg	Milligram
min	Minute
ml	Millilitre
mm	Millimetre
mM	Millimole
MW	Molecular weight

LIST OF ABBREVIATION (cont.)

µg	Microgram
µl	Microlitre
µm	Micrometre
nm	Nanometre
OD	Optical density
ORF	Open reading frame
PCR	Polymerase chain reaction
rpm	Round per minute
sec	Second
SPF	Specific pathogen free
TSV	Taura syndrome virus
U	Unit
V	Volt
v/v	Volume by volume
w/v	Weight by volume
WSD	White spot disease
WSSV	White spot syndrome virus
YHD	Yellow head virus
YHV	Yellow head disease

CHAPTER I
INTRODUCTION

Shrimp farming is an important industry worldwide and has been developed rapidly over the past several decades. For example, global, cultivated penaeid shrimp production reached approximately 4 million metric tons in 2011 compared to approximately 1 million metric tons from the capture fishery (FAO). Currently, the major species for culture are Pacific white shrimp *Penaeus vannamei* and the black tiger shrimp *Penaeus monodon*. In Asia, the leading producers are from China, Thailand, Vietnam, Indonesia and India (FAO, 2011). However, disease outbreaks particularly from viral pathogens such as white spot syndrome virus (WSSV), yellow head virus (YHV), and Taura syndrome virus (TSV) have caused massive mortality and losses to the shrimp industry (see review by Lightner et al., 2012; Flegel, 2012). In Asia, during the 1990s, shrimp production dropped due to massive mortality caused predominantly by WSSV, causing losses of approximately 6 billion US dollars. In Thailand in 1991, YHV was reported to have caused economic loss of about 0.5 billion US dollars. Six genotypes of YHV (Wijegoonawardane et al., 2008) have been discovered but the most virulent type YHV-1 has so far caused serious disease outbreaks only in Thailand. In Ecuador in 1992, disease cause by Taura syndrome virus (TSV) was first reported in *P. vannamei*. Since its emergence, in the Americas, economic losses have been estimated to be 1-2 billion US dollars. In Asia in 1999, TSV outbreaks caused economic losses estimated at 0.5-1 billion US dollars (see review by Lightner et al., 2012). Currently, control of viral pathogens in shrimp aquaculture relies essentially on biosecurity measures focused on exclusion and the use of therapeutics such as may be applied for diseases of bacteria, fungi and protozoa are not yet available. However, innovative methods for treatment such as use of double-stranded RNA to induce RNA interference (RNAi) are now being explored. Some of viral genes from YHV and WSSV have been shown to be suppressed and to result in improved survival after viral challenge by using the RNAi strategy (see

review by Hirono et al., 2011; Robalino et al., 2007). However, the work has been done mainly at the experimental laboratory scale and no successful field applications have yet been implemented.

Understanding the shrimp immune response to pathogens has became a top priority in shrimp research with the hope of establishing improved, innovative methods to control viral diseases and of eventually developing therapeutic approaches. So far, no shrimp genome has been completely sequenced and this hampers the study on immune-related genes and proteins. Thus, other molecular approaches are being used to search for the relevant shrimp genes and proteins. These include development of expressed sequence tag (EST) libraries, microarray studies and proteomic studies (see review by Tassanakajon et al., 2012). This has led to the discovery of numerous immune related molecules including antimicrobial peptides, serine proteinases and inhibitors, phenoloxidases, oxidative enzymes, clottable proteins and pattern recognition proteins (see review by Tassanakajon et al., 2012). Identification must be followed by the more difficult task of determining their functions and importance in the complex network of immunological responses. In this thesis work two novel genes that might be involved in the shrimp immune response to viral pathogens have been identified. Their transcriptional expression patterns were investigated in various normal shrimp tissues and in response to viral challenges. In addition, host-viral protein interactions were also investigated. This included an investigation of proteomic interactions among the proteins of TSV itself using the yeast two-hybrid system, a powerful tool to study protein-protein interactions. In summary, the main objectives of the thesis were were:

1. To identify and characterize a gene encoding a leucine-rich repeat protein from the giant tiger shrimp *P. monodon*.

2. To study the protein interaction between a shrimp serine protease homolog protein and yellow head virus proteins.

3. To develop and analyze a TSV protein-protein interaction (PPI) map.

CHAPTER II
LITERATURE REVIEW

2.1 Shrimp aquaculture and viruses

Cultivated shrimp is an important commodity in international trade. For example, during 2011, the global production of penaeid shrimp by aquaculture was approximately 4 million metric tons. This contrasted with approximately 1 million metric tons for captured shrimp (FAO, 2012). During 2006-2010, shrimp production in Asian countries was reported to be increasing with an average annual growth rate of more than 5% (Fig. 2.1). Nevertheless, this growth rate was slower than that recorded during 2000-2006, when the average annual growth rates reached 18%. The decreased rate was at least partly due to the impact of a new wave of diseases. The largest declines were seen in China, Thailand, Vietnam and Malaysia, where production was expected to drop 5, 7, 21 and 36% per year, respectively, between 2011 and 2012 (GOAL, 2012). For example, in Thailand, there was drop in production in 1995 that continued till 1997 and there was another drop in 2003 due to yellow head disease (YHD) and white spot disease (WSD) outbreaks. Moreover, introduction of Pacific whiteleg shrimp, *Penaeus vannamei* into Asia to replace formerly cultured black tiger shrimp *P. monodon* was also the vehicle for transferring new viral diseases. The most of the important shrimp viruses in Asia include white spot syndrome virus (WSSV), yellow head virus (YHV), Taura syndrome virus (TSV), infectious hypodermal and hematopoietic necrosis virus (IHHNV) and infectious myonecrosis virus (IMNV) (Table 2.1). After WSSV emerged in the early 1990s, there have been continuous, large scale mortalities in farmed shrimp. The next most severe pathogen is probably YHV that causes high and rapid mortality with both *P. monodon* and *P. vannamei*. Two other deadly viruses, IMNV and TSV are of importance for *P. vannamei* but not for *P. monodon*. Another important virus is IHHNV that can cause high mortality in the American blue shrimp *P. stylirostris* and stunted growth in *P. vannamei*. However,

it also has little, if any, effect on *P. monodon* (see review by Flegel, 2006). The estimated losses due to these shrimp viruses are summarized in Table 2.2.

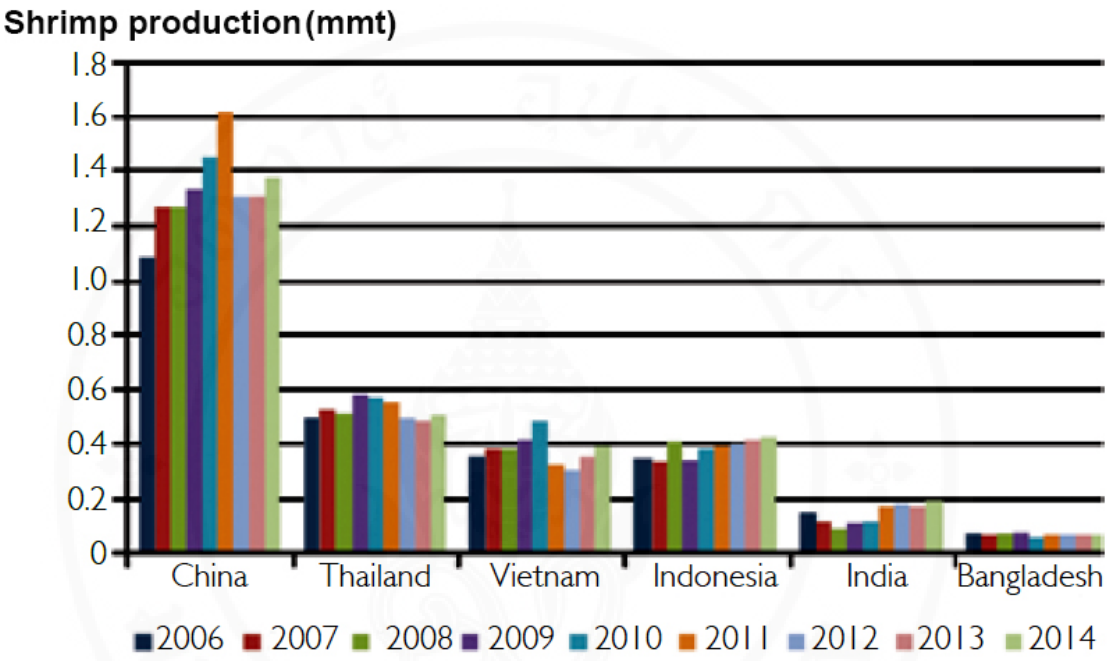

Figure 2.1 Production of farm-raised shrimp in major farming nations in Asia. China data include marine and freshwater production of *P. vannamei* (picture from GOAL, 2013).

Table 2.1 OIE listed penaeid shrimp diseases as of 2010 (table from Lightner et al., 2012).

Disease name	Pathogen type	Pathogen name and acronym	Principal host group
Taura syndrome	ssRNA virus	Taura syndrome virus (TSV)	Penaeid shrimp
White spot disease	dsDNA virus	White spot syndrome virus (WSSV)	Penaeid shrimp
Yellow head disease	ssRNA virus	Yellow head virus (YHV) & Gill-associated virus (GAV)	Penaeid shrimp
Infectious hypodermal and hematopoietic necrosis (IHHN)	ssDNA virus	IHHN virus, IHHNV	Penaeid shrimp
Infectious myonecrosis (IMN)	dsRNA virus	IMN virus (IMNV)	Penaeid shrimp

Table 2.2 Estimated losses due to certain OIE listed virus diseases since their emergence and/or discovery (table from Lightner et al., 2012).

Virus – region	Year of emergence	Product loss to industry
IHHNV – Americas	1981	$0.5–1 billion
YHV – Asia	1991	$0.5 billion
TSV – Americas	1991/92	$1–2 billion
TSV – Asia	1999	$0.5–1 billion
WSSV – Asia	1992/93	$6 billion
WSSV – Americas	1999	$1–2 billion
IMNV – Americas	2004	$100–200 million
IMNV – Asia	2006	$1 billion (estimated)

2.2 Yellow head virus

Yellow head virus (YHV) is the causative agent of yellow head disease (YHD) that can cause massive losses on shrimp farms within a few days after appearance of the first signs of disease in a pond. It first emerged in the black tiger shrimp *P. monodon* in Thailand in 1990. Since then various types have been reported in other countries in Asia, including India, Indonesia, Malaysia, the Philippines, Sri Lanka, Vietnam and Taiwan (Chantanachookin et al., 1993; Walker et al., 2001). Six different genotypes of YHV are recognized but only YHV type-1 has caused major disease losses and only in Thailand (Wijegoonawardane et al., 2008). Australian gill-associated virus (GAV) or YHV type-2 has been linked to less severe disease outbreaks described as mid-crop mortality syndrome (Spann et al., 1997; Walker et al., 2001). Other low virulence strains of YHV has been found in wild and farmed *P. vannamei* in western Mexico (de la Rosa-Vélez et al., 2006; Castro-Longoria et al., 2008; Cedano-Thomas et al., 2009; Sánchez-Barajas et al., 2009). No severe YHD outbreaks have been reported in the Americas or East Africa according to the World Organization for Animal Health (OIE Aquatic Animal Health Code, 2010).

The black tiger shrimp *P. monodon* is a natural host for YHV. Shrimp post larvae and juveniles of 20-25 days are highly susceptible to YHV infection while postlarvae younger than 15 days are apparently resistant. Nevertheless, other penaeid and palemonid shrimp species have also been shown to be susceptible to experimental infection, though YHV is rarely detected in other penaeid shrimp (Walker et al., 2009). The symptoms of YHD include initially abnormal high food consumption followed by abrupt cessation in feeding. The moribund shrimp swim slowly near the edges of the rearing ponds where they die. Mass mortality up to 100% can occur within 2-4 days after the first occurrence of gross signs of disease. The gross signs include a pale and yellowish cephalothorax and gills with general bleaching of body color (Fig. 2.2). The appearance of a yellowish cephalothorax is the result of the underlying yellow hepatopancreas and swollen digestive gland showing through the translucent carapace (Chantanachookin et al., 1993). YHV can be transmitted horizontally by injection, ingestion of infected tissue, immersion in membrane-filtered tissue extracts or cohabitation with infected shrimp. Vertical transmission occurs from both male and

female parents, possibly via surface infection or contamination of tissue surrounding fertilized eggs.

YHV-infected shrimp show widespread cellular degeneration in the gills, connective tissues, hemocytes, hematopoietic organs and lymphoid organ, suggesting preferential infection of cells of ectodermal or mesodermal origin (Boonyaratpalin et al., 1993; Chantanachookin et al., 1993). Experimentally YHV-infected whiteleg shrimp *P. vannamei* also showed this distribution of YHV in various organs of moribund shrimp. The infected tissues included the branchial portion of the gills, nerve cord, lymphoid organ, heart, connective tissue of the midgut and hepatopancreas, head soft tissues, abdominal muscles and eyestalks with varying quantities of viral particles (Lu et al., 1994). The viral particles were concentrated largely within the cytoplasm of infected gill cells within a short period after challenge (i.e., 4 day post challenge). Hemocytes and the LO were more rapidly infected than other tissues, suggesting that they were the primary targets for YHV infection and multiplication (Lu et al., 1994).

By transmission electron microscopy (Fig. 2.3), negatively stained, purified viral particles were found to be enveloped and bacilliform measuring 50-60 X 190-200 nm. The internal helical nucleocapsid is closely surrounded by an envelope studded with prominent surface spikes approximately 11 nm in length. Nucleocapsids have helical symmetry with a diameter of 13-18 nm, apparently consisting of coiled tubular structures arranged perpendicular to the ventral axis (Nadala et al., 1997; Wongteerasupaya et al., 1995).

According to the extensive analysis of YHV genome sequences, YHV has been classified into the order *Nidovirales*, family *Roniviridae* and genus *Okavirus* (Cowley et al., 1999; 2000; 2002; Sittidilokratna et al., 2002). The genome of YHV is positive-sense, single-stranded RNA (Nadala et al., 1997; Tang et al., 1999; Wongteerasupaya et al., 1995). The complete YHV genome comprises 26,662 nucleotides containing five long open reading frames (ORF) designated as ORF1a, ORF1b, ORF2, ORF3 and ORF4 (Fig. 2.4). ORF1a and ORF1b overlap at a ribosomal frame-shift site (AAAUUUU) and encode polyproteins, from which replicase proteins are derived by proteolytic cleavage (Sittidilokratna et al., 2002, 2008). The ORF1b contains RNA-dependent RNA polymerase (pol), helicase (Hel) and metal ion binding

domains (MIB) that are characteristic of nidoviruses (Sittidilokratna et al., 2002). ORF2 encodes the 146 amino-acid p20 nucleocapsid (N) protein (Cowley et al., 2004; Sittidilokratna et al., 2006). ORF3 encodes a 1666 amino-acid polyprotein containing six hydrophobic regions, which are predicted to be transmembrane (TM) domains (Jitrapakdee et al., 2003). This polyprotein undergoes post-translational cleavage to produce an N terminal 228 amino-acid polypeptide of unknown function, as well as envelope glycoproteins gp116 (899 amino acids) and gp64 (539 amino acids) (Jitrapakdee et al., 2003). YHV ORF4 (20 amino acids) is truncated by multiple stop codons. The YHV structural proteins have been identified from purified virions and consist of three major structural proteins gp116 (116 kDa), gp64 (64 kDa) and p20 (20 kDa), respectively (Jitrapakdee et al., 2003).

The envelope proteins gp116 and gp64 have been reported to be glycosylated by sugar moieties detected by ECL glycoprotein staining and thymol (Jitrapakdee et al., 2003). It has also been revealed that gp116 and gp64 envelope glycoproteins possess N-linked rather than O-linked glycans (Soowannayan et al., 2010). It was indicated that glycans linked to gp64 are mannose-rich, whilst glycans linked to gp116 possess terminal N-acetylgalactosamine and N-acetylglucosamine in addition to terminal mannose-type sugars (Soowannayan et al., 2010). Topology prediction of gp64 revealed a type I transmembrane glycoprotein anchored in the viral envelop at the C-terminus. By contrast, gp116 has been predicted to be a type III transmembrane glycoprotein anchored in the envelope at the C terminus but with both the C terminus and N terminus external (Jitrapakdee et al., 2003). Both gp116 and gp64 are suggested to form envelope glycoproteins of YHV virions (Jitrapakdee et al., 2003) whereas p20 comprises the nucleocapsid protein (Soowannayan et al., 2003).

Diagnosis of YHD can be done by histological examination. Haematoxylin and eosin staining of sectioned infectious tissue shows intensely basophilic cytoplasmic inclusions that consist of virogenic stromata and pyknotic/karyorrhectic nuclei (Fig. 2.5). However, gross signs of infection and histopathology are not entirely reliable indicators of YHD. Thus, it is recommended that molecular such as RT-PCR (Kiatpathomchai et al., 2004; Wonteerasupaya et al., 1997), real-time RT-PCR (Mouillesseaux et al., 2003), multiplex nested RT-PCR (Cowley et al., 2004) or loop-mediated isothermal amplification (Jaroenram et al., 2012) be used for confirmation.

Additionally, polyclonal (Assavalapsakul et al., 2005) and monoclonal antibodies (Sithigorngul et al., 2000; 2002; 2007) against structural proteins of YHV have been produced and developed for immunodetection.

Figure 2.2 Gross signs of yellow head disease (Chantanachookin et al., 1993) are seen here in the 3 shrimp on the right. They are generally bleached in color with a yellowish discoloration of the cephalothorax ("head") region when compared to shrimp of normal appearance on the left (picture from Flegel, 2006).

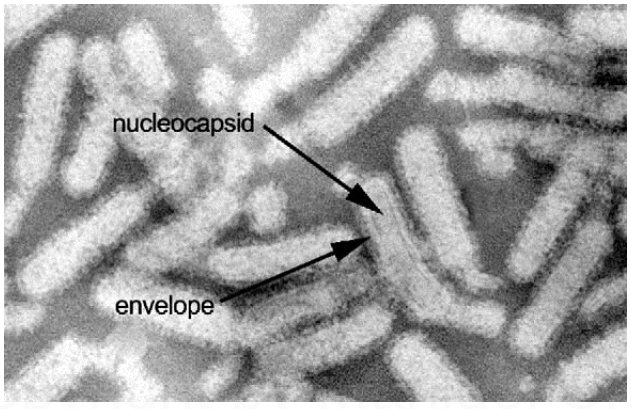

Figure 2.3 Transmission electron micrograph of negatively stained purified virions of YHV (picture from Flegel, 2006).

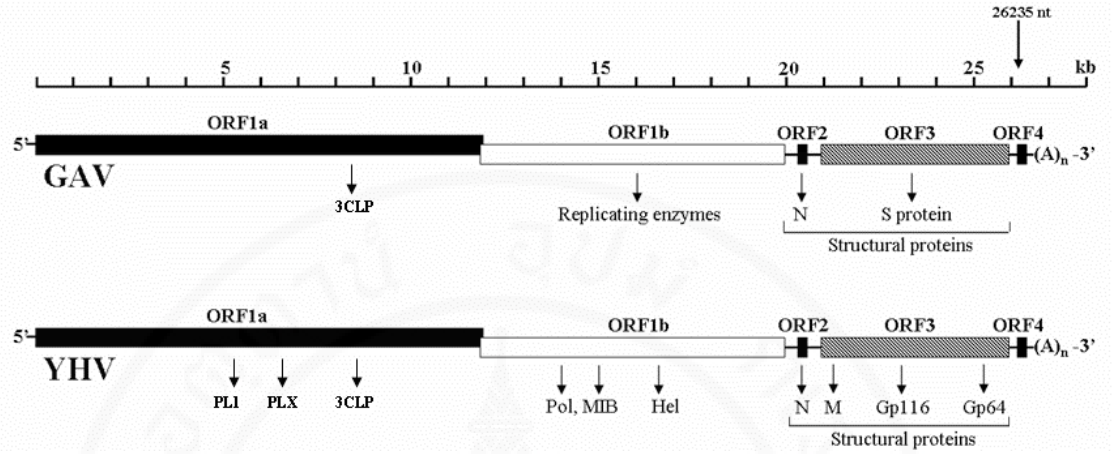

Figure 2.4 Schematic diagram of the organization of GAV and YHV genomes. Boxes represent the ORF of the approximately 26 kb genomic RNA. The discontinuous boxes show ORF1a and ORF1b with an overlapping (-1) ribosomal frame shift site. PL1: a putative papain-like protease; PLX: a homology domain to PL1 but lacking the canonical α+β fold; 3CLP: 3C-like protease; N: nucleocapsid; S protein: structural protein; Pol: polymerase domain; MIB: metal ion-binding domain; Hel: helicase domain; M: M protein; Gp116: glycoprotein 116 kda; Gp64: glycoprotein 64 kDa (Modified from Sittidilokratna et al, 2002; 2008 and Jitrapakdee et al., 2003).

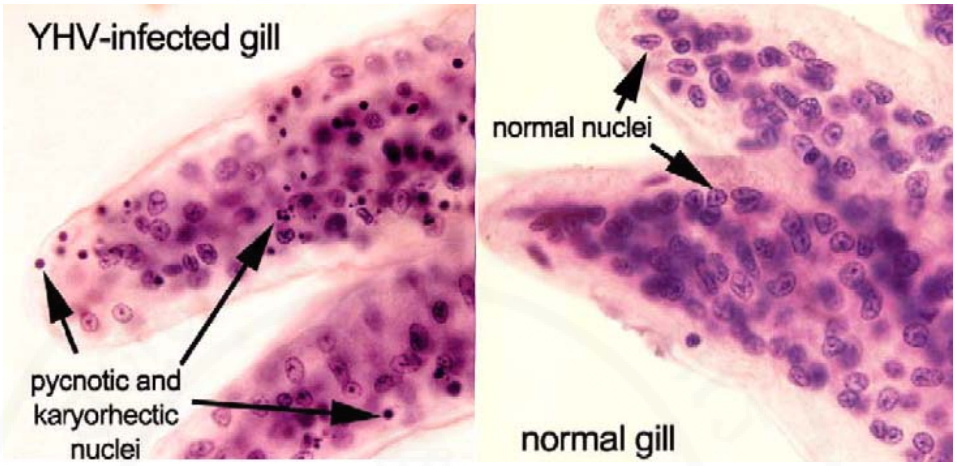

Figure 2.5 Gills of YHV infected shrimp stained with H&E. The densely stained purple (basophilic) inclusions contrast sharply with the normal nuclei that are larger and show more diffuse staining of the chromatin (picture from Flegel, 2006).

2.3 Taura syndrome virus

Taura syndrome virus (TSV) is the causative agent of Taura syndrome (TS) that emerged in Ecuador in 1991. The disease was recognized as a major new disease of farmed *P. vannamei* in the Americas by early 1992 but its viral etiology was not established until 1994 (see review by Flegel, 2006; Lightner, 2011). Since its discovery, disease has now been found in most shrimp farming countries in Asia, the Middle East, and North, South and Central America. According to the guidelines by OIE in 2010, only Australia, Africa and some specific zones or compartments can be considered free of TS (see review by Lightner et al., 2012). By molecular analysis, it has been revealed that there are four distinct TSV strains from the Americas, Venezuela, South East Asia and Belize (Wertheim et al., 2009).

TS is virulent for the Pacific white shrimp, *P. vannamei* with cumulative mortalities varying from 40 to more than 90% from the stages of PL to juveniles to subadults. It is known as a disease of the nursery because it generally attacks small juveniles (0.05-5.0 g) within 14 to 40 days after stocking PL into grow-out ponds. TSV can also infect Western Hemisphere penaeid species including *Litopenaeus*

stylirostris, *L. setiferus* and *L. schmitti* that sometimes show no sign of disease (Brock et al., 1997; Overstreet et al., 1997). Although they do not develop clinical signs of disease, some species such as *Fenneropenaeus chinensis*, *P. monodon*, and *Marsupenaeus japonicas* are also susceptible to TSV by experimental infection (Brock et al., 1997; Overstreet et al., 1997; Flegel, 2006).

Disease signs are shown as shrimp become lethargic and cease feeding. Moribund shrimp gather at the pond edge where they die. The distinctive gross signs of TS are divided into the acute phase, the transition (or recovery) phase and the chronic phase. In the acute phase, disease signs are weakness and soft shells, empty stomachs and pale-red body surfaces from expansion of red chromatophores in the appendages and especially the uropods (Fig. 2.6). During molting, shrimp with the severe acute phase usually die. However, if they survive, they enter the recovery phase characterized by irregularly shaped and randomly distributed melanised (dark) cuticular lesions (Fig. 2.6). These shrimp may also die during subsequent molting, but if they survive the molt, they regain normal appearance (i.e., they lose the black lesions). Although shrimp look normal, they are in the chronic phase of infection and can transmit the virus to other shrimp. Transmission of TSV is horizontal through cannibalism and water contamination. Although vertical transmission from infected adult broodstock to their offspring is suspected, it has not been experimentally confirmed (see review by Lightner, 2011).

By histopathology, disease lesions can be distinguished in acute and transition phases. During the acute phase, the virus mainly infects the sub-cuticular epithelium of the foregut, hindgut, gills and appendages, and often connective tissues, hematopoietic tissues and the antennal gland. No signs of infections are seen in the hepatopancreas, midgut, heart, striated muscle and the ventral nerve cord (see review by Lightner, 2011). Lesions in the cuticular epithelium are characterized by necrosis and increased eosinophilia of the cytoplasm together with pyknotic or karyorrhectic nuclei. Although the lymphoid organ may appear normal in the transition phase, *in situ* hybridization with a specific cDNA probe and immunohistochemistry with specific TSV antibodies can clearly show large quantities of TSV in the lymphoid organ tubules (see review by Flegel, 2006; Lightner, 2011). Shrimp in the chronic phase of TS display no gross signs of infection.

Morphologically, TSV is a small, unenveloped 32 nm icosahedral virus (Fig. 2.7). Its genome is a linear, positive sense single-stranded RNA of approximately 10.2 kb comprising two large ORFs (Fig. 2.8). ORF 1 encodes a nonstructural polyprotein, a sequence motif of a baculovirus IAP repeat (BIR), a helicase, a protease and an RNA-dependent RNA polymerase. ORF 2 contains the sequences of the TSV structural proteins, including the three major capsid proteins VP1, VP2 and VP3 (55, 40, and 24 kDa, respectively) (Bonami et al., 1997; Mariet al., 1998, 2002; Robles-Sikisaka et al., 2001). Based on its characteristics, TSV has been assigned by the International Committee on Taxonomy of Viruses (ICTV) to the newly created genus *Cripavirus* in the new family *Dicistroviridae* (in the ‘‘superfamily” of picornaviruses) (Mayo, 2002a,b).

Although histological analysis is the classical method for TSV diagnosis, it cannot confirm the disease during the chronic phase of infection since shrimp do not show any gross signs of disease. According to OIE (2006), the *in situ* hybridization assay using a specific DIG-labeled cDNA probe to TSV can provide a definitive diagnosis for TSV infection including acute, transition and chronic phases. In addition, monoclonal and polyclonal antibodies against TSV have been produced to detect the virus by immunohistochemistry (Poulos et al., 1999; Chaivisuthangkura et al., 2006). Numerous one step and nested reverse transcriptase (RT-PCR) methods have been developed for detection of TSV, and some are commercially available (Mari et al., 1998; Nunan et al., 1998, 2004; Phalitakul et al., 2006). More recently, a rapid and sensitive loop-mediated isothermal amplification (LAMP) method has been described (Kiatpathomchai et al., 2007; 2008).

Figure 2.6 Gross signs of Taura syndrome. A tail fan of *P. vannamei* with reddish necrotic areas (arrow) indicated acute phase signs (left). The right photo shows black lesions in the cuticle characteristic of the recovery stage of TSV infection (Lightner, 1996).

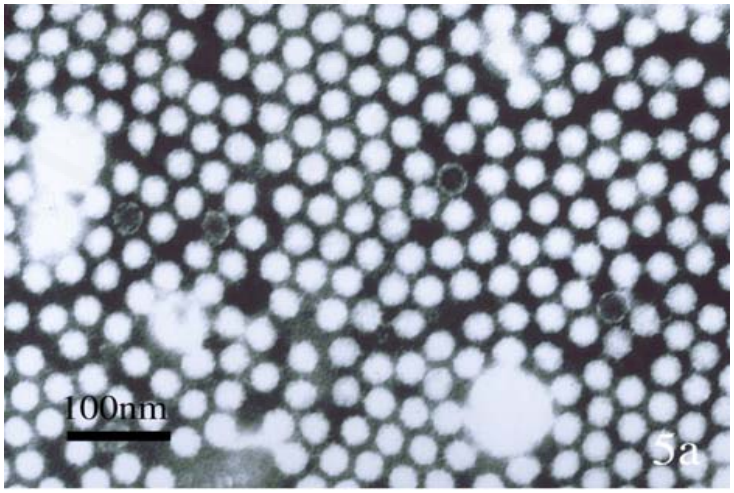

Figure 2.7 Transmission electron micrograph of purified TSV from cesium chloride gradient ultracentrifugation. Most of the hexagonal appearing (in profile) icosahedral particles are full, but several particles lack the viral genome and show only empty capsids (picture from Lightner, 2011).

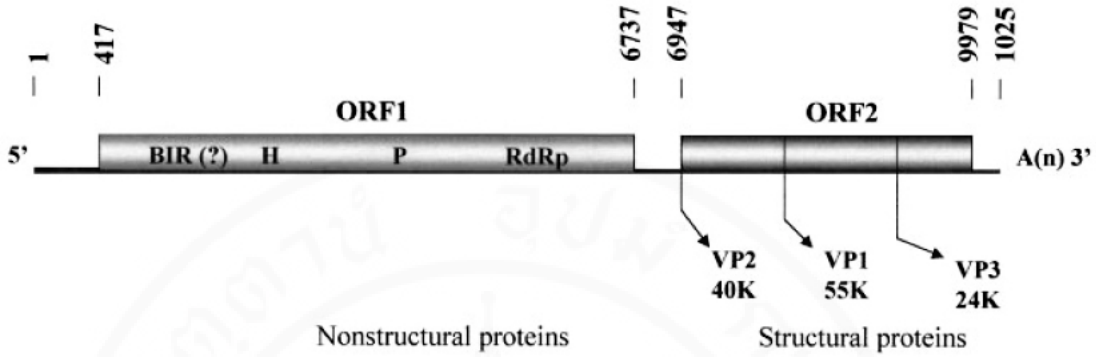

Figure 2.8 Schematic diagram of the genome organization of TSV. Numbers indicate nucleotide positions. ORFs 1 and 2 are shown as open boxes and UTRs as a single line. The approximate positions of the BIR-like sequence (BIR), helicase (H), protease (P) and RNA-dependent RNA polymerase (RdRp) are indicated. Arrows represent the N termini of the capsid proteins (picture from Mari et al., 2002).

2.4 Protein-protein interaction through the yeast two-hybrid system

Protein-protein interactions are important molecular processes for biological functions. Thus understanding them is the key to understanding any biological system. A powerful technique that can be used to study protein-protein interactions is the yeast two-hybrid system. It was first described in 1989 by Fields and Song. It is a genetic system where the interaction between two proteins of interest is detected via activation of reporter genes under the control of a specific transcription factor (Fields and Song, 1989). Transcription factor proteins usually contain separable DNA-binding domains (BD) that are capable of binding to upstream activating DNA sequences (UAS), and transcriptional activation domains (AD) that are capable of activating transcription of corresponding promoters. As shown in Fig. 2.9, a protein X is expressed as a fusion protein to BD domain commonly called the bait. This bait is bound to the UAS of a reporter gene, but does not activate it because of lacking an AD domain. A second protein Y is expressed as a fusion protein to the AD domain named

the prey. The prey protein alone cannot activate transcription since it has no affinity for the UAS of the promoter (Fig. 2.9). However, if the bait and prey interact (bind together), then a functional transcription factor is reconstituted at the promoter site in order to activate transcription of the reporter gene. In the yeast two-hybrid system, protein interaction is measured through the activation of one or several reporter genes. The transcription factor that is the most commonly used in yeast is GAL4 (Fields and Song, 1989) that activates the transcription of the reporter gene, *lacZ*. In addition, genes such as *HIS3* and *ADE2* are now regularly used as reporter genes, in conjunction with *lacZ*, to provide a more stringent assay for protein-protein interactions (see review by Causier and Davies, 2002). In addition to interaction between the two proteins of interest, the prey is usually constructed as a collection of unknown proteins expressed from a cDNA or genomic library. Screening of a prey library with specific baits may then lead to identification of novel interaction partners.

Although yeast the two-hybrid system provides many advantages including simplicity, rapidity and inexpensiveness, the technique still has its limitations. For example, some proteins such as proteins containing transmembrane domains may be excluded from the nucleus where the system operates. Also, false positives may be observed with some proteins (such as transcriptional activators) that can activate reporter genes without protein-protein interaction. Several approaches have been developed to avoid false positives. These include modification of the yeast strain and utilization of multiple reporters. False negatives can also happen when physiological protein-protein interactions cannot be detected by the technique. Instability of proteins or failure of nuclear localization can also cause false negative results (see review by Causier and Davies, 2002).

According to the availability of complete genomes of numerous organisms, many new approaches have been developed to study their biology. Large-scale protein-protein interaction studies via the yeast two-hybrid assay constitute one of the important approaches that have been used to establish protein interaction networks. Those networks have been revealed for viruses (McCraith et al., 2000; Uetz et al., 2006; Flajolet et al., 2000; Calderwood et al., 2007), *Helicobacter pylori* (Rain et al., 2001), budding yeast (Uetz et al, 2000; Ito et al., 2001), *Plasmodium falciparum* (LaCount et al., 2005), *Caenarhabitis elegans* (Li et al., 2004), *Drosophila* (Giot et al.,

2003; Stanyon et al., 2004; Formstecher et al., 2005) and humans (Rual et al., 2005; Stelzl et. al., 2005). For large-scale protein interaction screenings, two approaches are generally used. The library screening approach is used for library screening with multiple baits while the matrix approach employs an array of defined preys instead of a library (see review by Causier, 2004; Auerbach and Stagljar, 2005).

In the library approach (Fig. 2.10), a particular bait is expressed in a yeast with the mating strain type a, whereas a collection of preys or the library is transformed into a yeast with the mating strain type α. The bait is then mated with the mixture of library, and interactions were measured from yeast clones isolated on selective media. To determine the interacting partners, the prey plasmid is first isolated from yeast and amplified in the bacterium *Escherichia coli*. The prey is then identified by sequencing. However, the library approach is technically challenging when screening a large collection of baits, since a lot of clones have to be picked up, isolated and sequenced. In addition, false-positive interactors are common in library screens and they may generate preys that can activate reporter genes without actually binding to the bait. Nevertheless, several vectors and yeast strains have been improved to reduce the occurrence of false positive interactions (Walhout et al., 2000; Ito et al., 2001). In the matrix approach (Fig. 2.10), each prey is separately cloned and transformed into yeast clones as an array format on plates. The bait generated in the opposite mating type is then mated with every prey in the array and the resulting diploid strains are selected onto selective medium. The replicative diploid is used to screen for interactions via growth on selective media. In contrast to the library approach, the identity of the prey is determined by its position in the array, and no plasmid isolation and sequencing are required. Essentially, the matrix approach has the advantage of easy reduction in false positive results which may be generated either by nonspecific interactions or self-activating prey. For instance, repeated screenings will allow for identification of false-positive interactors present in the array. Such preys become apparent after several screens and can then be discarded.

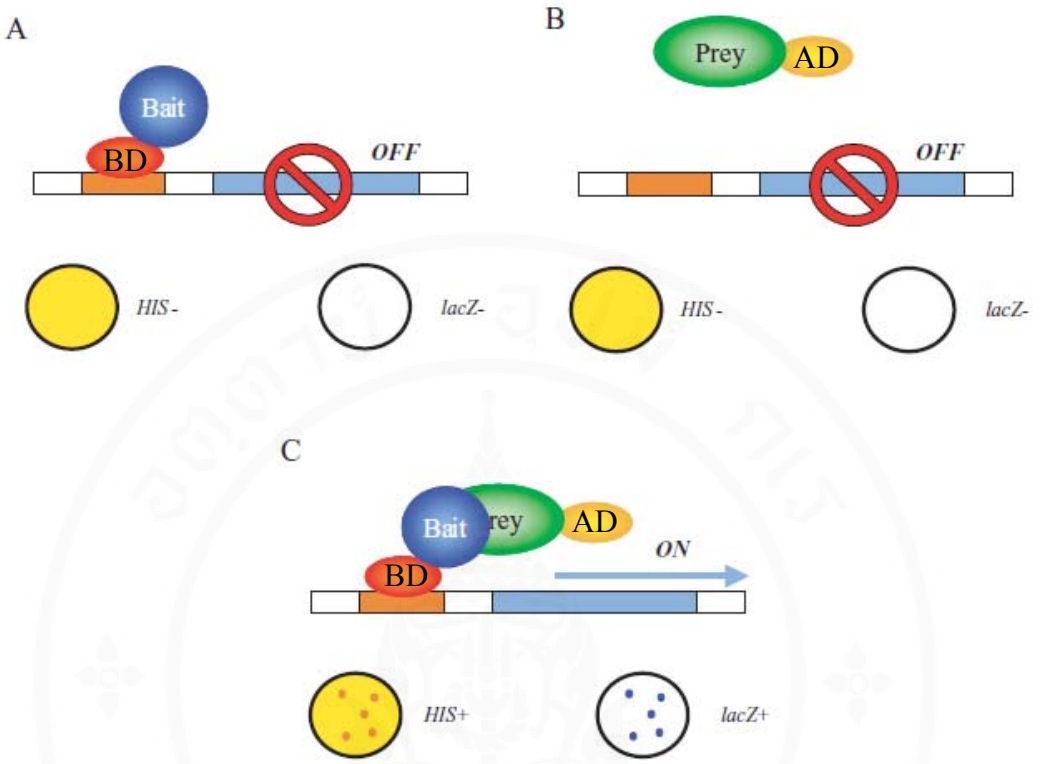

Figure 2.9 The yeast two-hybrid system. (A) A bait is expressed as a fusion to a DNA binding domain (BD). The BD-bait binds to the operator sequences present in the promoter region upstream of the reporter gene but does not activate its transcription since the BD-bait does not contain an activation domain. (B) A prey is expressed as a fusion to an activation domain (AD). The AD-prey fusion has the capability to activate transcription in yeast but because it is not actively targeted to the promoter it does not activate transcription of the reporter gene. (C) The interaction between bait and prey targets the AD-prey fusion protein to the promoter, thereby reconstituting an active transcription factor. The hybrid transcription factor is bound to the promoter upstream of the reporter gene and therefore activates transcription. The readout of the activated reporter gene is measured either as growth on selective medium (auxotrophic selection markers, such as *HIS3*, *URA3*, or *ADE2)* or in a color reaction *(lacZ*). Yeast expressing only the DBD-bait or the AD-prey on its own do not grow on selective medium (*HIS*-) and do not display blue staining in a color assay (*lacZ*-), whereas yeast harboring an interacting DBD-bait and AD-prey display growth (*HIS*+) and blue color (*lacZ*+) (picture from Auerbach and Stagljar, 2005).

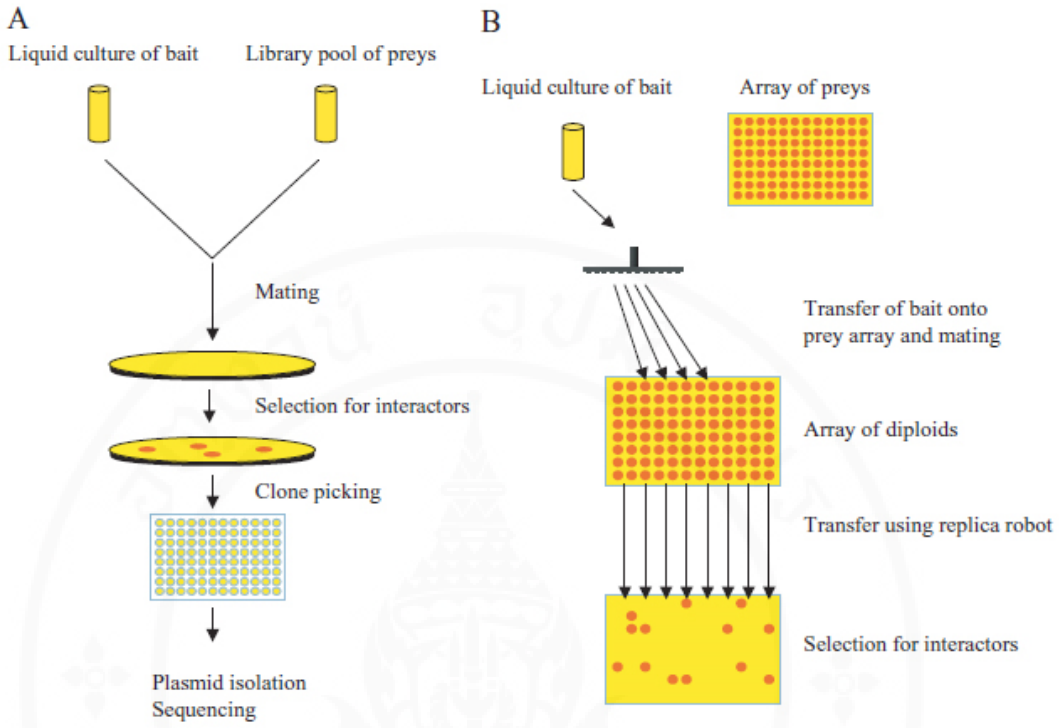

Figure 2.10 High-throughput approaches utilizing the yeast two-hybrid system. (A) The library screening approach. A yeast strain expressing a bait under investigation is mixed with a collection of yeast strains each expressing a random prey from a library. Incubation in rich medium allows the two strains to mate and diploids expressing bait and prey are selected. The diploids are then transferred to selective medium to isolate those clones containing interacting baits and preys (selection for interactors). Yeast clones that display growth on selective medium are picked up, transferred into multiwell plates, and processed for plasmid isolation and insert sequencing to identify the interacting prey. (B) The matrix or array approach. An array of preys is prepared by spotting yeast clones each expressing a known prey onto plates. The colonies on the array are then picked up by a robot and mated with a yeast strain expressing the bait under investigation. An exact replica of the array is transferred to a fresh plate to select for diploids expressing bait and prey and then to selective medium to select for interacting baits and preys. The identity of the prey in colonies that grow under selection is determined by its position within the array (picture from Auerbach and Stagljar, 2005).

CHAPTER III
MATERIALS AND METHODS

3.1 Bacterial strains

Escherichia coli, XL1-Blue (*recA1 endA1 gyrA96 thi-1 hsdR17 supE44 relA1 lac* [F′ *proAB lacI*^{q}*ZMΔ15* Tn*10* (Tet^{r})]) was used as the host for plasmid propagation. *E. coli*, BL21 pLysS (DE3) (F^{-} *ompT hsdSB*(r_B^- m_B^-) *gal dcm* (DE3) pLysS (Cam^{r}) was used for protein expression of inserted genes in vectors.

3.2 Yeast strains

Saccharomyces cerevisiae, AH109 (*MATa, trp1-901, leu2-3, 112, ura3-52, his3-200, gal4*Δ*, gal80*Δ*,,LYS2: : GAL1*$_{UAS}$*-GAL1*$_{TATA}$*-HIS3, GAL2*$_{UAS}$*-GAL2*$_{TATA}$*-ADE2, URA3: :MEL1*$_{UAS}$*-MEL1*$_{TATA}$*-lacZ,MEL1*) and Y187 (*MAT*α*, ura3-52, his3-200, ade2-101, trp1-901, leu2-3, 112, gal4*Δ*, met*$^{-}$*, gal80*Δ *,URA3: : GAL1*$_{UAS}$*-GAL1*$_{TATA}$*-lacZ, MEL1*) from Clontech were used in yeast two-hybrid assays.

3.3 Shrimp and viruses

Live juvenile black tiger shrimp *Penaeus monodon* (25-30 g body weight), were obtained from an experimental farm in Nakornsrithammarat, sounthern Thailand. The shrimp were specific pathogen free (SPF) for white spot syndrome virus (WSSV) and yellow head virus (YHV) for six generations. They were acclimatized in artificial sea water at 15 ppt for 24 h before used in experiments. YHV, WSSV and Taura syndrome virus (TSV) stocks were kindly provided by Charoen Pokphand Company.

3.4 Plasmid vectors

The plasmid vector used for cloning of PCR products was pDrive vector (QIAGEN) (Fig. 3.1). Plasmid vectors used for yeast two-hybrid assay were pGBKT7 and pGADT7 (Clontech) (Figs. 3.2 and 3.3, respectively). The pET-15b vector (Novagen) and pGEX-4T-1 vector (GE Healthcare, formerly Amersham Biosciences) were used for protein expression in the bacterial system. The cloning/expression region under T7 promoter of pET-15b and tac promoter of pGEX-4T-1 are shown in the Fig. 3.4 and 3.5, respectively.

3.5 Culture media

E. coli, XL1-blue or BL21 pLysS (DE3) was cultured in LB medium (Difco^{TM}). *S. cerevisiae* was cultured in YPD medium (2 % (w/v) peptone, 1% (w/v) yeast extract, and 2% (w/v) glucose). Yeast selective medium was minimal synthetic dropout medium (SD medium, Clontech) supplemented with amino acids (Clontech) that depended on each selection.

3.6 Oligonucleotides

Oligonucleotide primers were custom-ordered from BIO BASIC INC., Canada. All primers used in this study were listed in Table 3.1.

3.7 Chemical reagents and enzymes

All common chemicals and reagents used in this study were purchased from Merck: Germany, Fluka: Switzerland, and Sigma: USA. Restriction enzymes and other modification enzymes were purchased from New England Biolabs, Invitrogen, Fermentas, and QIAGEN. A protease inhibitor cocktail was purchased from Roche.

3.8 Antibodies

A mouse anti-His antibody was purchased from GE Healthcare. A goat anti-mouse IgG- horseradish peroxidase (HRP) conjugate was purchased from Sigma. A rabbit anti-GST antibody and a goat anti-rabbit IgG-alkaline phosphatase (AP) conjugate were purchased from Zymed.

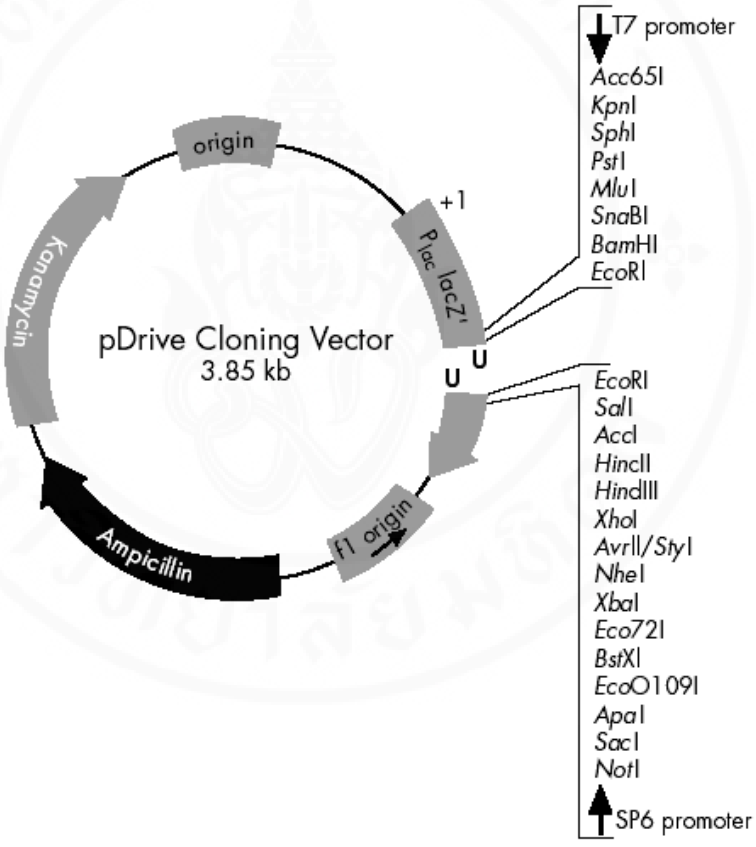

Figure 3.1 The physical map of pDrive cloning vector (QIAGEN)**.** The linearized vector has U overhangs and the restriction endonuclease recognition sites of the cloning site are listed.

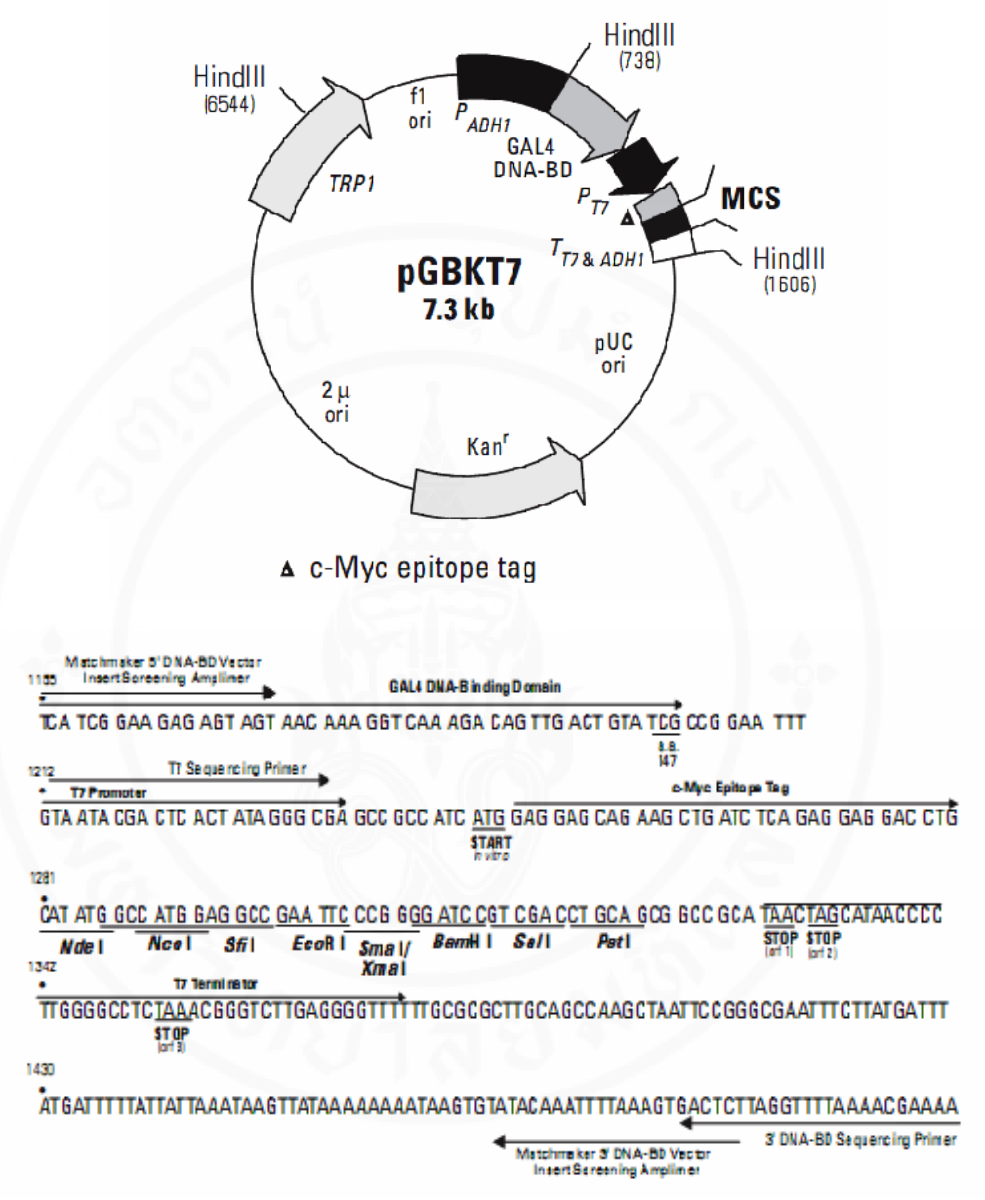

Figure 3.2 The physical map of pGBKT7 (Clontech). The pGBKT7 vector expresses bait proteins fused to the GAL4 DNA binding domain (BD). The vector carries a kanamycin resistance gene (Kan^r) for selection in *E. coli* and the *TRP1* nutritional marker for selection in yeast. It also contains the T7 promoter, a c-Myc epitope tag, and a MCS with restriction endonuclease recognition sites.

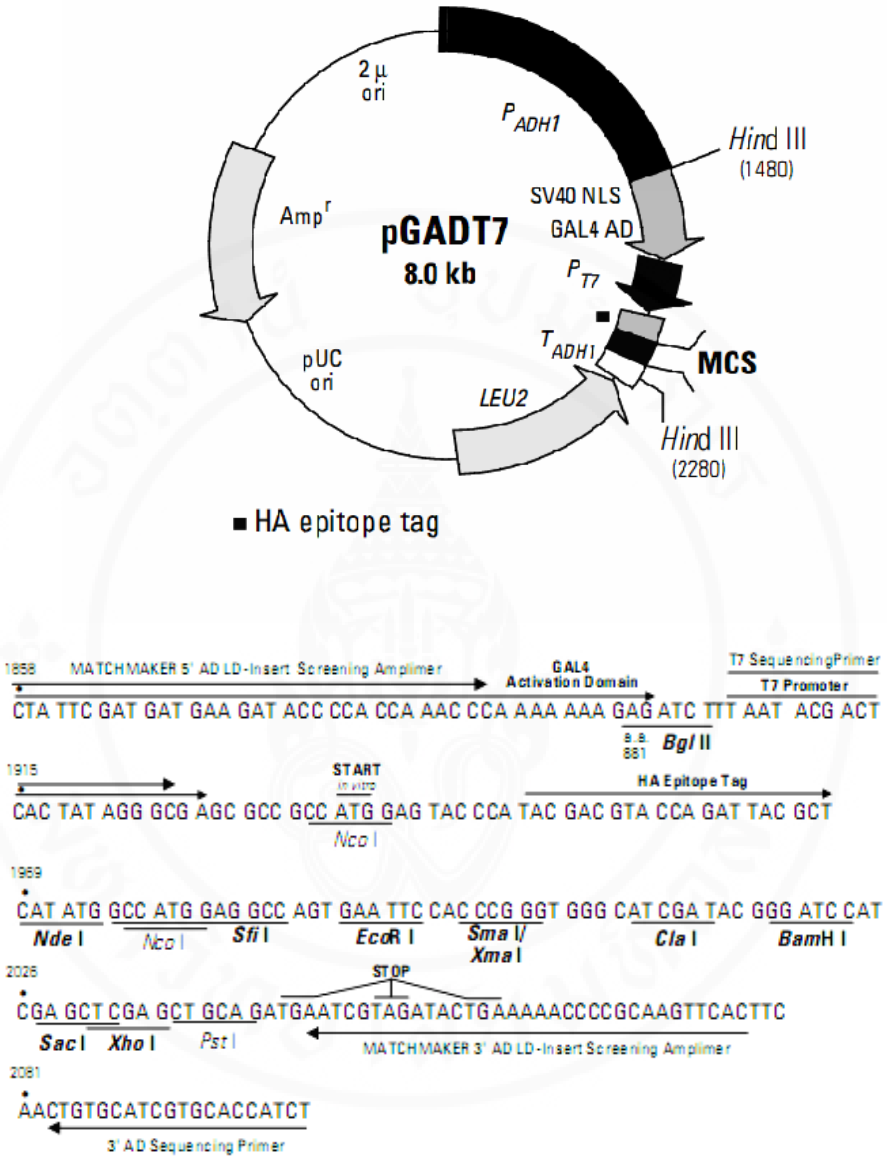

Figure 3.3 The physical map of pGADT7 (Clontech). Vector pGADT7 expresses prey proteins or cDNA library fused to the GAL4 activation domain (AD). The vector carries an ampicillin resistance gene (Amp^r) for selection in *E. coli* and the *LEU2* nutritional marker for selection in yeast. It also contains the T7 promoter, an HA epitope tag, and a MCS with restriction endonuclease recognition sites.

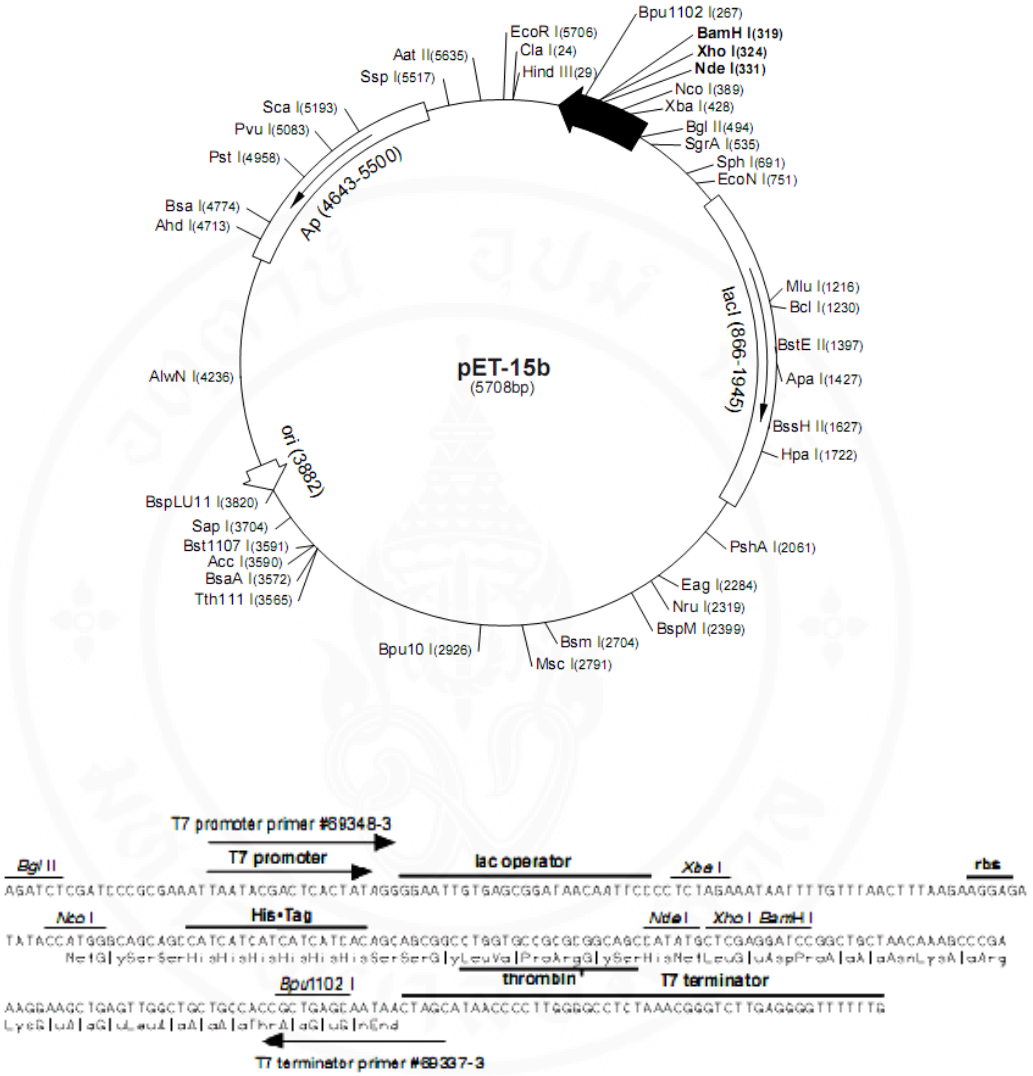

pET-15b cloning/expression region

Figure 3.4 The physical map and cloning sites of pET-15b vector (Novagen). The pET-15b vector carries an N-terminal His•Tag® sequence followed by a thrombin site and three cloning sites. The cloning/expression region of the coding strand transcribed by T7 RNA polymerase is shown.

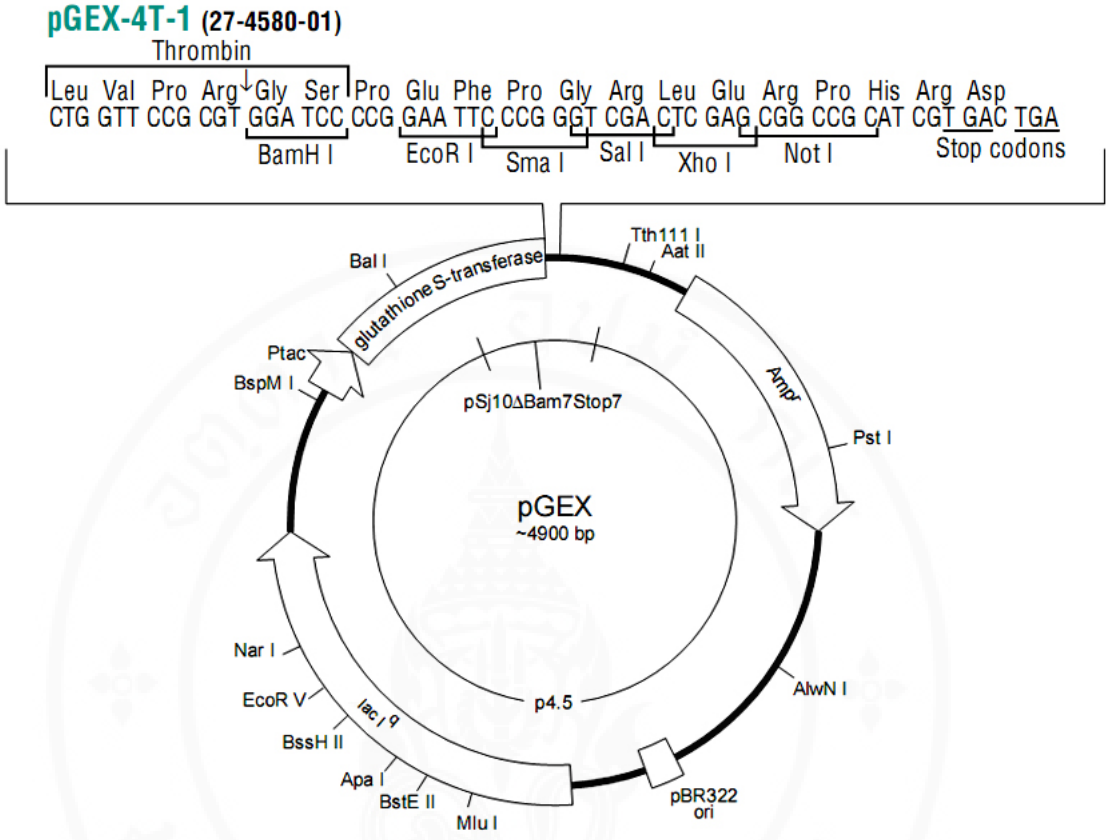

Figure 3.5 The physical map and cloning sites of pGEX-4T-1 vector (Novagen). The pGEX-4T-1 vector carries an N-terminal glutathione S-transferase tag sequence followed by a thrombin site and multiple cloning sites.

Table 3.1 Sequences and names of primers used

Names	Sequences (5' to 3')	Remarks
LRR_R	GCTGTCACATGAGCCTGAACCACAAGCAGT	5'RACE
LRR_N	GGAGCAGCAGGAACAGTGTAAGAGGTGCAG	5'RACE and Full-length amplification
LRR_F	ATGAGAAAGACAGTTAAATCTCGGTCT	Full-length amplification
LRR_inF	GAGCTCCTTGACCTACCACAAAGCGTTGGC	Transcription study
LRR_inR	CCCGAAGCTTGCGTAAGTTGCCTATACTTG	Transcription study
Actin_F	TGACGGCCAGGTGATCACCA	Transcription study
Actin_R	GAAGCACTTCCTGTGAACGA	Transcription study
SPH_5'R1	GGATCCAGTCCGAGGCGTAACCCACGTCGG	5'RACE
SPH_5'R2	TGTCGATCCCCTGCTGGCCGCCAGCGC	5'RACE
SPH_F	ATGCGGGTGTTGGCAGTAGCGCTAGCA	Full-length amplification
SPH_R	TTAAATAAATCTTCCGTAGTCCCAGTCATA	Full-length amplification
SPH_inF	CGCTTCGGAGAGTGGGACACCCAG	Transcription study
SPH_inR	GCACCCGATGCCCCAGGCCACGAT	Transcription study
PSPH_F1	CCGGAATTCCAAAACATCCTCAAGGAGGTG	pGBKT7
PSPH_R1	AAAACTGCAGTTAAATAAATCTTCCGTAGT	pGBKT7
PSPH_F2	GGAATTCCATATGCAAAACATCCTCAAGGA	pET-15b
PSPH_F2	CCGCTCGAGTTAAATAAATCTTCCGTAGTC	pET-15b
SPH_F1	GGAATTCCATATGATGCGGGTGTTGGCAGT	pGADT7 and pGBKT7
SPH_R1	CCGCTCGAGAATAAATCTTCCGTAGTCCCA	pGADT7 and pGBKT7
Pol_F1	CGCGGATCCTAATTCCAAAGATCTCCATCC	pGADT7 and pGBKT7
Pol_R1	GAAAACTGCAGGAAGACTCGCTCGATGAG	pGBKT7
Pol_R2	CCGCTCGAGGAAGACTCGCTCGATGAGGGG	pGADT7
MIB_F1	GCATGCCATGGGAGTATGCTTTGCATGTGG	pGBKT7
MIB_R2	GAAAACTGCAGGTCTAGATGCTGGGCGCA	pGBKT7
MIB_F2	CCGGAATTCGTATGCTTTGCATGTGGT	pGADT7 and pGEX-4T-1
MIB_R2	CCGCTCGAGGTCTAGATGCTGGGCGCAGCG	pGADT7 and pGEX-4T-1
Hel_F1	GCATGCCATGGGAATTCAAGGACCACCTGG	pGBKT7
Hel_R1	GCGCCGTCGACGCAGATACACTGGAAGCG	pGBKT7
Hel_F2	GGGAATTCCATATGATTCAAGGACCACCTG	pGADT7
Hel_R2	CCGCTCGAGGCAGATACACTGGAAGCGGAA	pGADT7
M1_F1	GCATGCCATGGGAATGATCCACAACGCAATC	pGBKT7
M1_R1	GAAAACTGCAGGGTCTTAATTTTCCTGAT	pGBKT7
M1_F2	CGCGGATCCTCAGAAATGGACCAAACAAAT	pGADT7
M1_R2	CCGCTCGAGGTAGATGCATAGTGTCATTGC	pGADT7
M3_F1	GCATGCCATGGGAACAATAATCTCAGACCT	pGBKT7
M3_R1	GAAAACTGCAGAGCAACCCAAAGTTCAGA	pGBKT7
M3_F2	CGCGGATCCTCACAATAATCTCAGACCTCT	pGADT7
M3_R2	CCGCTCGAGAGCAACCCAAAGTTCAGATGT	pGADT7
p20_F1	GCCCACATGTCTAACCGTCGTACACGCAC	pGBKT7
p20_R1	GAAAACTGCAGGACCAATTAATTGGATTA	pGBKT7
p20_F2	CCGGAATTCATGAACCGTCGTACACGCACC	pGADT7 and pGEX-4T-1
p20_R2	CGCGGATCCTTATGATTGTGTTTCCATGGG	pGADT7
p20_R3	CCGCTCGAGTTATGATTGTGTTTCCATGGG	pGEX-4T-1
GP64_F1	GCATGCCATGGGTCTCGCTCCACGACAGGC	pGBKT7
GP64_F2	GCGCCGTCGACCTAGGATCGTTTGGCTTTCGT	pGBKT7
GP64_F2	CCGGAATTCCTCGCTCCACGACAGGCACGT	pGADT7
GP64_R2	GCGCCGTCGACCTAGGATCGTTTGGCTTTCGT	pGADT7

Table 3.1 Sequences and names of primers used (continued)

Names	Sequences (5' to 3')	Remarks
TSV_BIR_F1	GCATGCCATGGGAAATGATTGCATTTTGAA	pGBKT7
TSV_BIR_R1	GAAAACTGCAGGGGGAGCTTAAACTGGACA	pGBKT7
TSV_BIR_F2	GGAATTCCATATGAATGATTGCATTTTGAA	pGADT7 and pET-15b
TSV_BIR_R2	CCGCTCGAGGGGGAGCTTAAACTGGACACA	pGADT7 and pET-15b
TSV_Hel_F1	GCATGCCATGGGATGTGGTGATGGTAGTCG	pGBKT7
TSV_Hel_R1	GAAAACTGCAGAAACTCATCTTTAACATCT	pGBKT7
TSV_Hel_F2	CCGGAATTCTGTGGTGATGGTAGTCGAGTT	pGADT7
TSV_Hel_R2	CCGCTCGAGAAACTCATCTTTAACATCTAC	pGADT7 and pET-15b
TSV_Hel_F3	GGAATTCCATATGTGTGGTGATGGTAGTCG	pET-15b
TSV_Pro_F1	GCATGCCATGGGAGACAGAAACGCTCAAGA	pGBKT7
TSV_Pro_R1	GCGCCGTCGACCCATTATGTCTTCCTGAGT	pGBKT7
TSV_Pro_F2	GGAATTCCATATGGACAGAAACGCTCAAGA	pGADT7 and pET-15b
TSV_Pro_R2	CCG CTCGAGCCATTATGTCTTCCTGAGTAA	pGADT7 and pET-15b
TSV_C-Pro_F	GGAATTCCATATGCGAATGTTGTTGATGCCT	pGADT7 and pGBKT7
TSV_Pol_F	GGAATTCCATATGTTGACGCATGAGGAATC	pGADT7 and pGBKT7 and pET-15b
TSV_Pol_R	CCGCTCGAGGAAATAACCCTTCTCATGCAG	pGADT7 and pGBKT7 and pET-15b
TSV_VP2_F1	GCATGCCATGGGAGCTAACCCAGTTGAAAT	pGBKT7
TSV_VP2_R1	GAAAACTGCAGAAATCCGAACATTGAAGCT	pGBKT7
TSV_VP2_F2	GGAATTCCATATGGCTAACCCAGTTGAAAT	pGADT7 and pET-15b
TSV_VP2_R2	CGCGGATCCAAATCCGAACATTGAAGCTAC	pGADT7 and pET-15b
TSV_VP1_F1	GCATGCCATGGGATCAAAAGATAGGGATAT	pGBKT7
TSV_VP1_R1	GAAAACTGCAGATGTGTGGATGGATATATA	pGBKT7
TSV_VP1_F2	CCGGAATTCTCAAAAGATAGGGATATGACG	pGADT7 and pGEX-4T-1
TSV_VP1_R2	CGCGGATCCATGTGTGGATGGATATATACA	pGADT7
TSV_VP1_R3	CCGCTCGAGATGTGTGGATGGATATATACA	pGEX-4T-1
TSV_N-VP1_R	CGGGATCCCTTAGCAATAACTTTACC	pGADT7 and pGBKT7
TSV_C-VP1_F	GGAATTCCATATGCGTGGAAATATTAACCT	pGADT7 and pGBKT7
TSV_VP3_F1	GCATG CCATGG GA GCTGGTCTGGACTACTC	pGBKT7
TSV_VP3_R1	GAAAA CTGCAG AGCCAATTCGGCAGGTCCA	pGBKT7
TSV_VP3_F2	GGAATTCCATATGGCTGGTCTGGACTACTC	pGADT7 and pET-15b
TSV_VP3_R2	CCGCTCGAGAGCCAATTCGGCAGGTCCAAA	pGADT7 and pET-15b
Ami_R	GTAATCGTCCGCCATTTTGTTATTCCAGAT	5'RACE
Ami_N	GTTATTCCAGATCTGGTATGCTGCGCTCAT	5'RACE
Ami_F	ATGGTTCTGAGCGCTACACTAACATTCC	Full-length amplification
Ami_R2	TCAGTATCTACGATTCATCTGCAGCTCG	Full-length amplification
AmiY2H_F	GGAATTC CATATG GTTCTGAGCGCTACACT	pGADT7 and pGBKT7
AmiY2H_R	G GAATTC CTATGAATCCTTCTTGGAAG	pGADT7 and pGBKT7
T7 promoter	GTAATACGACTCACTATAG	Cloning verification
3'BD	TAAGAGTCACTTTAAAATTTGTAT	Cloning verification
3'AD	AGATGGTGCACGATGCACAG	Cloning verification

Note: Underlines indicate restriction sites.

3.9 Experimental challenge

3.9.1 Shrimp virus detection

3.9.1.1 YHV/GAV detection

Yellow head virus (YHV) diagnosis was carried out using an IQ2000^{TM} YHV/GAV Detection kit (GeneReach Biotechnology Corp.). Total RNA from lymphoid organ and hemocytes were used as the template for YHV detection by RT-PCR. The first RT-PCR reaction mix comprised 7 µl of RT-PCR Premix, 0.5 µl of IQzyme DNA polymerase, 0.5 µl of RT Enzyme Mix and 2 µl of RNA sample. The reaction protocol consisted of 42^{o}C for 30 min followed by 94^{o}C for 2min and then 15 cycles at 94^{o}C for 20 sec, 62^{o}C for 20 sec and 72^{o}C for 30 sec with 72^{o}C for 30 sec and 20^{o}C for 30 sec at the end of the final cycle. Then 8 µl of first RT-PCR product was mixed with 14 µl of nested PCR premix and 1 µl of IQzyme DNA polymerase for 30 cycles of reaction at 94^{o}C for 20 sec, 62^{o}C for 20 sec and 72^{o}C for 30 sec followed by 72^{o}C for 30 sec and 20^{o}C for 30 sec at the end of the final cycle. After the nested PCR reaction, the products were analyzed by agarose gel electrophoresis.

3.9.1.2 WSSV detection

White spot syndrome virus diagnosis was carried out using an IQ2000^{TM} WSSV Detection kit, (GeneReach Biotechnology Corp.). DNA from lymphoid organs was used as the template for WSSV detection by PCR. The first PCR reaction mix contained 7.5 µl of First PCR PreMix, 0.5 µl of IQzyme DNA Polymerase, and 2 µl of DNA sample. The reaction protocol was 5 cycles at 94^{o}C for 30 sec, 62^{o}C for 30 sec and 72^{o}C for 30 sec, followed by 15 cycles at 94^{o}C for 15 sec, 62^{o}C for 15 sec and 72^{o}C for 20 sec and then additional 72^{o}C for 30 sec and 20^{o}C for 30 sec at the end of the final cycle. Then 8 µl of first PCR reaction was added to 14 µl of nested PCR premix and 1 µl of IQzyme DNA polymerase for processing 25 cycles at 94^{o}C for 20 sec, 62^{o}C for 20 sec and 72^{o}C for 30 sec followed by 72^{o}C for 30 sec and 20^{o}C for 30 sec at the end of the final cycle. After nested PCR, the products were analyzed by agarose gel electrophoresis.

3.9.2 Experimental challenge and sample collection

After acclimatization overnight, shrimp (*P. monodon)* were each injected intra-muscularly with 100 µl of YHV or WSSV stock suspension. The control group was injected intra-muscularly with 100 µl of PBS buffer (137 mM NaCl, 10 mM phosphate, 2.7 mM KCl, pH 7.4). They were then reared in an aquarium until samples were collected at 0 h before injection and at time intervals (6-60 h) post-injection (p.i.). The whole experimental challenge was performed three times. Collected samples were lymphoid organs and hemocytes. Lymphoid organs of five shrimp were washed three times with diethyl pyrocarbonate (DEPC)-treated TE buffer (10mM Tris-HCl and 1 mM EDTA, pH 8) before being kept in 500 µl of Trizol^{TM} (Invitrogen) and stored at -80^{o}C. Hemolymph from each shrimp was withdrawn from the ventral sinus with 1 ml syringe containing 0.5 ml of anticoagulant, AC-1 solution (450 mM NaCl, 30 mM Tri sodium-citrate, 26 mM Citric acid, 12.7 mM EDTA, and 1 M Glucose, pH 7) (Soderhall and Smith, 1983). The hemolymph from five shrimp was then pooled and centrifuged at 800 x g for 10 min at 4^{o}C. The resulting hemocyte pellet was resuspended in 500 µl of Trizol^{TM} (Invitrogen) and stored at -80^{o}C. Viral infection was confirmed by IQ2000^{TM} YHV/GAV Detection kit and IQ2000^{TM} WSSV Detection kit as described above.

3.10 DNA manipulation

3.10.1 Agarose gel electrophoresis

To determine the size of DNA fragments, gel electrophoresis was performed. The concentration of agarose depended on the size of DNA to be separated. Generally, a 1.2% (w/v) agarose gel in 1X TBE buffer (89 mM Tris-HCl, 89 mM boric acid, 2.5 mM EDTA, pH 8) was used. The DNA samples were mixed with 1/3 volume of the loading dye (25% (v/v) glycerol, 60 mM EDTA, 0.25% (w/v) Bromophenol Blue) before loading into the gel slots that were submerged in TBE solution in an electrophoresis chamber. The electrophoresis was carried out with constant voltage at 100-120 volts and the running time depended on the size of the

DNA to be fractionated. After electrophoresis, the gel was stained with a staining solution containing 2.5 μg/ml of ethidium bromide solution for 5 min and destained with water for 15-20 min. The DNA patterns were observed under UV light (SYNGENE).

3.10.2 DNA purification from agarose gels

DNA fragments were excised from agarose gels and purified using a QIAquick gel extraction kit (QIAGEN). Three volumes of Buffer QG were added to 1 volume of the gel (such as 100 mg of gel was mixed with 300 μl of Buffer QG) and the mixture was incubated at 50^{o}C for 10 min or until the gel was completely dissolved. Then 1 gel volume of isopropanol was added before transfer to a QIAquick column inserted in a 2 ml collection tube. The column was centrifuged at 13,000 x g for 1 min at room temperature. The flow-through solution was discarded and the column was washed with 0.75 ml of PE Buffer following by centrifugation at 13,000 x g for 1 min. The flow-through was discarded and the column was additionally centrifuged for 1 min. In order to collect the eluted DNA, the column was placed on a fresh microcentrifuge tube and 30 μl of sterile water was applied to the column. Then the column was left at room temperature for 1 min before centrifugation. The eluted DNA was stored at 4^{o}C until used.

3.10.3 Purification of DNA reaction solutions

Purification was conducted using a QIAquick PCR purification kit (QIAGEN). Briefly, one volume of PCR product was mixed with 5 volumes of buffer PB (such as 50 μl of PCR product was mixed with 250 μl of buffer PB) and applied to the QIAquick spin column inserted in a 2 ml collection tube. To bind DNA, the column was centrifuged at 13,000 x g for 1 min and the flow-through was discarded. Then the column was washed with 0.75 ml of buffer PE and centrifuged at 13,000 x g for 1 min. The flow-through was removed and the column was centrifuged for 1 min. The column was placed on a fresh tube and 30 μl of sterile water was applied. Then the column was left at room temperature for 1 min before centrifugation. The eluted DNA was stored at 4^{o}C until used.

3.10.4 Cloning of DNA fragments

A PCR cloning kit (QIAGEN) was used for direct cloning of DNA fragments generated by PCR. The ligation reaction was performed by mixing the following components: 4 µl of purified PCR product, 1 µl of pDrive cloning vector, and 5 µl of 2 X ligation master mix. The reaction was briefly mixed and incubated at 4^{o}C overnight. Then the ligation mixture was used to transform competent *E. coli* cells.

3.10.5 Plasmid construction

3.10.5.1 Construction of plasmids for yeast two-hybrid assay

Seven domains from three open reading frames (ORF) of the YHV genome (RNA dependent RNA polymerase (Pol), metal ion binding domain (MIB), helicase (Hel), Motif 1 (M1) and Motif 3 (M3) from ORF1b; p20 from ORF2; and gp64 from ORF3) were amplified by RT-PCR using total RNA extracted from the YHV virus stock. Primers were designed based on the published sequences of YHV genome (GenBank accession numbers **AY052786** and **AF540644**) and contained appropriate restriction sites (Table 3.1). RT-PCR reactions were carried out in a 25 µl reaction solution containing viral RNA as template, 0.2 µM of each primer, 1 µl of SuperScript One-Step RT/Platinum Taq mix (Invitrogen) and 1X reaction buffer. The reaction protocol comprised reverse transcription at 50°C for 30 min followed by denaturation at 94°C for 2 min followed by 30 PCR cycles of denaturation at 94°C for 30 sec, annealing at 55°C for 30 sec and extension at 68°C for 1 min/1 kbp of amplified gene. Amplified products were inserted downstream of the Gal4-binding domain (BD) and/or Gal4-activation domain (AD) of the vectors pGBKT7 and pGADT7 (Clontech), respectively. In addition to YHV, ten domains of TSV genome (BIR, helicase (Hel), protease (Pro), C-terminal protease (C-Pro), RNA dependent RNA polymerase (Pol) from ORF1; and viral protein 1 (VP1), N-terminal VP1 (N-VP1), C-terminal VP1 (C-VP1), viral protein 2 (VP2) and viral protein 3 (VP3) from ORF2) were also amplified and cloned in a same manner as described in YHV using

total RNA extracted from the TSV virus stock. Primers were designed based on the published sequences of TSV genome (GenBank accession number **AF277675**) (Table 3.1). For interaction study between TSV BIR protein and *Pm*Amidase, the full-length of *PmAmidase* was cloned into both pGBKT7 and pGADT7 vectors by RT-PCR using shrimp hemocytes RNA as template and primer pair of AmiY2H_F and AmiY2H_R (Table 3.1). All constructs were subsequently confirmed for sequences and correct reading frames by DNA sequencing (Macrogen Co. Ltd., South Korea and 1st BASE, Malaysia).

3.10.5.2 Construction of expression plasmids used in the bacterial system

After yeast two-hybrid analysis, *in vitro* pull-down assays were conducted to confirm protein interactions. An SPH516-C fragment representing the last C-terminal 124 amino acids was amplified by PCR using the corresponding yeast two-hybrid identified prey as a template and primers PSPH_F2 and PSPH_R2 (Table 3.1). The YHV MIB and p20 domains were PCR amplified using constructed baits as described above as templates and primers MIB_F2 and MIB_R2, and p20_F2 and p20_R3, respectively (Table 3.1). PCR reactions were performed in 25 µl containing *Taq* DNA polymerase 1X buffer, 200 µM of dNTP mix, 0.2 µM of each primer, 0.5 U of *Taq* polymerase (Platinum®*Taq* DNA polymerase, Invitrogen). The PCR protocol comprised initial activation at 94°C for 5 min followed by 25 cycles at 94°C for 30 sec, annealing at an appropriate temperature depending on the particular primer pair for 30 sec and extension at 72°C for 1 min/1 kbp of amplified product. After appropriate restriction digestion, SPH516-C was cloned into pET-15b (Novagen) whereas MIB and p20 were individually inserted into pGEX4T-1 (GE Healthcare, formerly Amersham Biosciences). The TSV proteins were also constructed in the expression vector pET-15b and pGEX4T-1 in the same manner as described above. TSV VP1 was cloned into pGEX4T-1 to generate GST-tag VP1 whereas BIR, Hel, VP2 and VP3 were individually inserted into pET-15b to generate His-tag proteins. The primers used for this aspect were shown in Table 3.1. Correct sequences and in-frame insertion was then verified by DNA sequencing.

3.10.6 Plasmid DNA extraction

QIAprep Spin Miniprep kits were used to isolate plasmid form transformed bacterial cells. *E. coli* XL1-Blue containing plasmid vector or recombinant plasmid was grown in 3 ml LB broth containing antibiotic at 37^{o}C with shaking for 16 h. The cells were harvested by centrifugation at 16,000 x g for 1 min. The cell pellet was resuspended in 250 µl of buffer P1 and mixed until the cells did not clump. Two hundred and fifty µl of buffer P2 was added and the tube was gently inverted 4-6 times. Then 350 µl of buffer N3 was added and the tube was immediately inverted 4-6 times before centrifugation at 16,000 x g for 10 min. The supernatant was applied to a QIAprep spin column and centrifuged at 16,000 x g for 1 min and then the flow-through was discarded. To wash the column, 0.75 ml of buffer PE was added followed by centrifugation at 16,000 x g for 1 min. The flow-through was discarded followed by additional centrifugation for 1 min to remove residual PE buffer. The QIAprep was placed in a new microcentrifuge tube and 30 µl of sterile water was added to the center of the column. The column was left to stand for 1 min and centrifuged for 1 min.

3.10.7 DNA sequencing

All inserted plasmid fragments were sequenced by Macrogen Co. Ltd. (South Korea) or 1st BASE (Malaysia).

3.10.8 Restriction endonuclease digestion

The digestion was performed in a reaction containing 1-2 µg of ds DNA or vector, 1X buffer, 1X bovine serum albumin (BSA) and 1-10 units of an appropriate restriction enzyme. The reaction was incubated at the optimal temperature of each enzyme for at least 4 h. After digestion had been completed, the digested products were analyzed by gel electrophoresis.

3.10.9 DNA ligation

DNA ligation was carried out by mixing the following components: digested DNA fragment, appropriately linearlized vector, 1X buffer, 1-2 units of T4 DNA ligase (Promega). The molar ratio between inserted DNA to vector was approximately 3:1. The reaction was incubated at 16°C overnight and then the enzyme

was inactivated by heating the reaction at 65°C for 10 min. Then, the ligation mixture was used for transformation into *E. coli* XL1-Blue as described below. The plasmid was isolated and the inserted sequence or orientation and reading frame of the junctions were verified by sequencing.

3.10.10 Shrimp DNA extraction

Shrimp lymphoid organs were removed and put into 500 µl of lysis buffer included in the IQ2000^{TM} WSSV detection kit (GeneReach Biotechnology Corp.). The sample was then ground by using a sterile glass pestle. The ground sample was incubated at 95 ^{o}C for 10 min and subsequently centrifuged at 12,000 x g for 10 min. The upper clear solution was transferred to a fresh 1.5 ml microtube and 400 µl of 95% ethanol was added to the tube. The tube was vortexed briefly and centrifuged at 12,000 x g for 5 min. Then, ethanol was removed from the tube and the DNA pellet was washed with 75% ethanol, dried and then dissolved with distilled water and kept at -20 ^{o}C.

3.11 RNA manipulation

3.11.1 RNA isolation

Total RNA was isolated from the lymphoid organ and hemocytes in Trizol^{TM} (Invitrogen). The tissues were homogenized in 500 µl of Trizol^{TM} and incubated at room temperature for 5 min to permit complete dissociation of nucleoprotein complexes. One hundred µl of chloroform was added and the mixture was shaken vigorously for 15 sec before incubation at room temperature for 2-3 min. The mixture was subsequently centrifuged at 12,000 x g for 15 min at 4^{o}C. After centrifugation, the colorless upper aqueous phase was transferred to a fresh tube and RNA was precipitated by mixing with 250 µl of isopropanol. The mixture was left at room temperature for 10 min and centrifuged at 12,000 x g for 10 min at 4^{o}C. The supernatant was removed and the RNA pellet was washed with 500 µl of 75% ethanol. The sample was mixed and centrifuged at 7,500 x g for 5 min at 4^{o}C, the ethanol was discarded and the pellet was briefly air-dried for 10 min. The RNA pellet was

dissolved in DEPC-treated water. The resulting total RNA was then treated with RNase-free DNase I (Fermentas) to remove contaminating DNA. Briefly, 1 µg of total RNA was treated using 1 U of DNase I at 37°C for 30 min. The treated RNA was subsequently collected using Trizol™ reagent as described previously. Finally, the RNA pellet was dissolved in DEPC-treated water and stored at -80°C.

3.11.2 Isolation of full-length genes by 5'RACE

3.11.2.1 Preparation of RNA template

This step was performed using GeneRacer™ Kit (Invitrogen) and *P. monodon* hemocyte RNA as a starting template. RNA template was first prepared within three steps including dephosphorylating RNA, removing the mRNA cap structure and ligating the RNA oligo to decapped mRNA. Briefly, the dephosphorylating RNA reaction was carried out in 10 µl composing of total RNA (1-5 µg), 1X CIP buffer, 40 U of RNaseOut™ and 10 U of CIP. After incubation at 50°C for 1 h, RNA was isolated with phenol:chloroform solution and then precipitated with 2 µl of 10 mg/ml mussel glycogen, 10 µl of 3 M sodium acetate, pH 5.2, and 95% ethanol. After centrifugation, the RNA pellet was washed with 70% ethanol, dried and then dissolved in 7 µl of DEPC water. This dephosphorylated RNA was then add to the tube containing 10 µl of final volume reaction of 1X TAP buffer, 40 U of RNaseOut™ and 0.5 U of TAP. After incubation at 37°C for 1 h, RNA was isolated and precipitated as described above. The resulting RNA was then subjected to the final step of RNA oligo ligation. The decapped RNA (7 µl) was mixed with lyophilized GeneRacer™ RNA Oligo (0.25 g) and then heated at 65°C for 5 min to relax the RNA secondary structure. After chilling on ice, the RNA was ligated in 10 µl final volume of 1X ligase buffer, 1 µl of 10 mM ATP, 40 U of RNaseOut™ and 5 U of T4 RNA ligase. After incubation at 37°C for 1 h, RNA was isolated, precipitated and dissolved in 10 µl of DEPC water.

3.11.2.2 First strand cDNA synthesis

The first-strand cDNA was synthesized by mixing the following components: 10 µl of ligated RNA from above, 1 µl of GeneRacer™ oligo

dT primer, 1µl of 10 mM dNTP mix and 1 µl of distill water. The contents were mixed and heated at 65°C for 5 min and then placed the tube on ice for 2 min. Then the following components were added: 4 µl of 5X first strand buffer, 1 µl of 0.1 M DTT, 40 U of RNaseOut™ and 1 µl of SuperScript™ III RT and the contents were incubated at 50°C for 1 h followed by 70°C for 15 min. To remove RNA from the first-strand cDNA, 1 µl of RNaseH was added to the reaction mixture followed by mixing before incubating at 37°C for 20 min. The cDNA was kept at -20°C until used for PCR amplification.

3.11.2.3 Rapid Amplification of cDNA Ends (RACE)

PCR reactions were conducted using specific primers (Table 3.1) and adapter primers from the kit. The PCR reaction was performed in 50 µl containing 0.5 µM of each primer, 200 µM of dNTP, 1X Advantage™ 2 PCR buffer, 1X Advantage™ 2 Polymerase Mix and 5 µl of diluted adaptor-ligated cDNA served as the template. The amplification cycle consisted of pre-denaturation at 95°C for 1 min. This was followed by 30 cycles of denaturation at 94°C for 15 sec, annealing at an appropriate temperature depending on the particular primer pair for 30 sec, extension at 72°C for 1 min/1 kbp of amplified product and then final extension at 72°C for 10 min. Amplified products were cloned into pDrive cloning vector (QIAGEN). Recombinant plasmids were sequenced by Macrogen Co. Ltd. (South Korea) or 1st BASE (Malaysia). After sequence analysis, the full-length gene was amplified by RT-PCR using specific primers for full-length amplification (Table 3.1).

3.11.3 Tissue distribution analysis

To study *LRR* and *SPH* expression in different organs of *P. monodon*, RT-PCR was carried out using SuperScript™ III One Step RT-PCR System with Platinum® *Taq* DNA polymerase (Invitrogen). Total RNAs from various tissues of *P. monodon* including eye stalks, gills, the heart, hemocytes, the hepatopancreas, intestine, lymphoid organs, pleopods and muscle were extracted using Trizol™ reagent (Invitrogen) as describe above for use as templates. A partial sequence of 541 bp of *LRR* was amplified using LRR_inF primer and LRR_inR primer (Table 3.1) while a partial sequence of 498 bp of *SPH516* was amplified using SPH_inF primer

and SPH_inR primer (Table 3.1). A partial sequence of 377 bp from the *β-actin* gene was amplified as a control using actin_F and actin_R primers (Table 3.1). RT-PCR reactions were carried out in a 25 µl reaction solution containing 100 ng of total RNA, 0.2 mM of each forward and reverse primer, 0.25 µl of SuperScript One-Step RT/Platinum Taq mix (Invitrogen), and 1X reaction buffer. RT-PCR was performed using a GeneAmp® PCR System 2400 machine using the following protocol: 50°C for 30 min, and 94°C for 2 min, followed by 25 cycles of 94°C for 30 s, 55°C for 30 s and 68°C for 1 min with a final extension at 68°C for 5 min. PCR products were analyzed on 1.2 % agarose gels.

3.11.4 Time-course analysis

Expression profiles of *LRR* transcripts during YHV and WSSV infection were investigated in lymphoid organs and *SPH516* transcriptional profiles after YHV challenge were monitored in hemocytes using SuperScript™ III One Step RT-PCR System. Total RNA of specific shrimp tissues were isolated at indicated time post infection using Trizol™ reagent (Invitrogen) and then they were subjected to RT-PCR analysis using the primer pairs (LRR_inF, LRR_inR and SPH_inF, SPH_inR) as described above. The *β-actin* gene was used to normalize shrimp gene expression. The RT-PCR conditions were the same as in tissue distribution analysis. Finally, band intensities were measured and compared using GeneTools software (SynGene).

3.12 Bacteria manipulation

3.12.1 Preparation of competent *E. coli* cells

A single colony of *E. coli* XL1-Blue was grown in 2 ml of LB broth at 37°C with shaking for 16 h. Two ml of culture was inoculated into 200 ml of LB broth for further growth at 37°C with shaking for 2 h. The culture was placed on ice for 10 min and the cells were collected by centrifugation in 4 sterile 50 ml tubes at 10,000 x g for 10 min. The supernatant in each sterile tube was removed and the cells were resuspended in 10 ml of cold RF1 buffer [30 mM K-Acetate, 10 mM $CaCl_2$, 15% (w/v) glycerol, 100 mM RbCl, and 50 mM $MnCl_2$, pH 5.92], and then placed on ice

for 30 min. The cells were centrifuged at 6,000 x g for 10 min and resuspended in 2.5 ml of cold RF2 buffer [10 mM RbCl, 75 mM $CaCl_2$, 10 mM MOPS, and 15% (w/v) glycerol, pH 6.8]. The cell mixtures were kept on ice for 15 min and aliquoted to 100 µl and then stored at -80°C.

3.12.2 *E. coli* transformation

A volume of 100 µl of *E. coli* competent cells was mixed gently with 2-10 µl of ligation mixture. The mixture was left on ice for 30 min, heat shocked at 42°C for 90 sec, and immediately transferred on ice. The resulting cells were mixed with 250 µl of room temperature S.O.C. medium and incubated at 37°C for 1 h with shaking. The transformed culture was spread on LB agar plates containing appropriate antibiotic and incubated at 37°C for 16 h.

3.12.3 PCR for determining recombinant clones

To check for inserted fragments in cloning vectors, PCR reactions were performed in 25 µl containing *Taq* DNA polymerase 1X buffer, 200 µM of dNTP mix, 0.3 µM of each primer, 0.5 U of *Taq* polymerase (Platinum®*Taq* DNA polymerase, Invitrogen). Each bacterial colony was picked with a toothpick and then dipped in the PCR reaction mix. The PCR protocol comprised initial activation at 95°C for 5 min followed by 30 cycles at 94°C for 30 sec, annealing at an appropriate temperature depending on the particular primer pair for 30 sec, and extension at 72°C for 1 min. The PCR products were analyzed by agarose gel electrophoresis.

3.13 Yeast manipulation

3.13.1 Preparation of yeast competent cells

A single colony of yeast was grown in 2 ml of YPD broth at 30°C with shaking for 16 h. The overnight culture was then inoculated into 50 ml YPD broth and incubated at 30°C with shaking for 3-5 h. The cell pellet was collected by centrifugation at 6,000 x g for 5 min and washed with 10 ml sterile water followed by

centrifugation at 6,000 x g for 5 min. Yeast cells were resuspended in 10 ml LiAc/TE buffer (100 mM LiAc, 10 mM Tris-HCl, pH 8, and 1 mM EDTA). After centrifugation, the cells were resuspended in 500 µl of LiAc/TE buffer with 20% glycerol and aliquoted into 100 µl. Yeast competent cells were kept at -80^{o}C until used.

3.13.2 Yeast transformation

Yeast transformation by the Lithium Acetate-Dimethyl Sulfoxide (DMSO) method was performed as described by Gietz *et al*. (1995). Briefly, for each transformation, 100 µl of yeast competent cells was mixed with 3-10 µl of plasmid and 5 µl of herring testes carrier DNA (Clontech). The control contained transforming carrier DNA only. The cells were mixed thoroughly with 280 µl of PEG solution (50% (w/v) PEG 3350 in LiAc/TE buffer) and incubated at 30°C for 45 min. Then 43 µl of DMSO was added followed by heat-shocking in a 42°C water bath for 5-20 min. Yeast cells were collected by spin down for 5 sec and washed with 1 ml of sterile water. After centrifugation, cells were resuspended in 0.5 ml of YPD and incubated at 30°C for 1 h before plated on selective media.

3.13.3 Verification of recombinant clones by yeast colony PCR

The primers used to verify the bait and prey constructs were T7 promoter, 3'BD and 3'AD (Table 3.1).The PCR reaction was composed of *Taq* DNA polymerase 1X buffer, 1.5 mM $MgCl_2$, 200 µM of dNTP mix, 0.3 µM of each primer, 0.5 U of *Taq* polymerase (Platinum®*Taq* DNA polymerase, Invitrogen). Each yeast colony was picked with a toothpick and then dipped in the PCR reaction. The PCR protocol started with the first denaturation at 95^{o}C for 7 min. Amplification was then performed for 30 cycles of 94^{o}C for 45 sec, 50^{o}C for 45 sec and 72^{o}C for 1 min per 1 kb followed by final extension at 72^{o}C for 5 min. The PCR products were subsequently analyzed by agarose gel electrophoresis.

3.13.4 Screening a shrimp hemocytes cDNA library by yeast mating

This experiment used MIB domain of YHV as bait to screen a shrimp hemocyte cDNA library that was kindly provided by Prof. Amornrat Phongdara, Prince of Songkla University. In addition to YHV protein, TSV proteins which are BIR domain and VP3 were also subjected to screen their interaction partners in the hemocyte cDNA library. All baits were constructed as described in method 3.10.5.1. To screen the library, each bait was grown on SD/-Trp agar at 30°C for few days. A single colony of Y187 containing bait plasmid was inoculated in 50 ml of SD/-Trp containing 20 µg/ml of kanamycin (Kan) and then incubated at 30°C with shaking for 16 h. The cells were collected by centrifugation at 600 x g for 5 min and resuspended in 5 ml of SD/-Trp. Then the bait strain Y187 was mated with the library host strain AH109 by combining the following components in a sterile 2-L flask: 5 ml of Y187 (bait) culture, 1 ml AH109 (library), and 45 ml of 2X YPD/Kan (50 µg/ml). Then the library vial was rinsed twice with 1 ml of 2X YPD/Kan (50 µg/ml) and added to a 2-L flask. The mating flask was incubated at 30°C with gentle swirling (30-50 rpm) for 20-24 h. After zygote formation, the mating mixture was transferred to a sterile 100-ml centrifuge bottle and centrifuged at 1,000 x g for 10 min. Meanwhile, the mating flask was rinsed twice with 50 ml of 0.5X YPD/Kan (50 µg/ml). After centrifugation at 1,000 x g for 10 min, the cells were resuspended in 10 ml of 0.5X YPD/Kan (50 µg/ml). To select diploids expressing interacting proteins, 300 µl of the mating mixture was spread on each medium plate (150 mm diameter) of SD medium lacking adenine, histidine, leucine, and tryptophan (SD/-Ade/-His/-Leu/-Trp). The plates were incubated at 30°C until colonies appeared (~3-6 days). After yeast colonies appeared, the Ade^+/His^+ colonies (white or light pink and 1-2 mm diameter) were streaked out on fresh SD/-Ade/-His/-Leu/-Trp containing 40 µg/ml of X-α-Gal (Apollo Scientific, UK) and grown for 2-4 days at 30°C. These master plates were store at 4°C and used for further analysis.

3.13.5 Total DNA isolation from yeast

Yeast cell pellets from overnight cultures were harvested by centrifugation and washed with sterile water. The following components were added and mixed thoroughly with the cell pellet: 400 µl of 1 M sorbitol, 100 µl of 0.5 M EDTA (pH 8),

and 40 µl of Zymolyase [0.75% (w/v) Zymolyase in 1 M sorbitol], and then incubated at 37°C for 1 h. After centrifugation at 6,000 x g for 5 min, the cells were lysed with 440 µl of lysis buffer [50 mM Tris-HCl, pH 7.4, 20 mM EDTA, 1% (w/v) SDS] and incubated at 65°C for 30 min. To precipitate cell lysates, 160 µl of 5 M potassium acetate (pH 5.5) was added and the mixture was placed on ice for 30 min. After centrifugation, the supernatant was transferred to a fresh tube and mixed vigorously for 20 sec with 500 µl of phenol: chloroform (1:1). The mixture was centrifuged at 16,000 x g for 5 min and the supernatant was transferred to a fresh tube. To obtain DNA, 1 ml of absolute ethanol was added and the mixture was left at room temperature for 2 min. After centrifugation for 10 min, the DNA pellet was washed twice with 1 ml of 75% ice-cold ethanol, briefly air-dried, and dissolved in 30 µl of 1X TE (10 mM Tris-HCl, pH 7.4 and 1mM EDTA) containing 50 µg/ml RNase.

3.13.6 Rescuing of AD/library plasmids

This rescuing step was done via *E. coli* transformation. Each blue colony (putative positive interaction) in the master plate from method 3.13.4 was grown in 3 ml of SD/-Leu/-Trp medium at 30°C with shaking overnight. Then total DNA from the yeast was isolated as described above. To select for the AD/library plasmid only, total yeast DNA was transformed to *E. coli* XL1-Blue and plated on LB medium containing 100 µg/ml of ampicillin. The AD/library plasmid was then isolated from 5 ml overnight culture using the extraction kit mentioned above. To reduce duplicate AD plasmids, restriction digestion was performed and DNA fragments were analyzed by gel electrophoresis. AD plasmids representing unique sequences were subsequently selected. Before determination of AD/library plasmid by DNA sequencing, the rescued AD plasmid was tested for interaction again with the respective bait plasmid via transformation of both plasmids into yeast strain AH109 as described above. The transformants were selected on SD/-Ade/-His/-Leu/-Trp containing 40 µg/ml of X-α-gal and SD/-Leu/-Trp as a control. Yeast cells with a true interaction still grew and turned blue on SD/-Ade/-His/-Leu/-Trp/ X-α-gal.

3.13.7 Screening of TSV protein-protein interaction by yeast mating

The TSV proteins including BIR, Hel, Pro, C-Pro, Pol, VP1, N-VP1, C-VP1, VP2 and VP3 were constructed by fusing with both BD (bait) and AD (prey) vectors as described in method 3.10.5.1. Each bait plasmid and prey plasmid was transformed into yeast Y187 and AH109, respectively. The empty pGBKT7 and pGADT7 were also transformed into yeast Y187 and AH109, respectively, for used as a control. To search for pairwise protein interactions, each bait was screened with each prey by yeast mating. For prey preparation, yeast AH109 harboring recombinant plasmid was cultured in 5 ml of SD medium lacking leucine (SD/-Leu) at 30^{o}C for two nights with shaking at 250 rpm. Then, 2 ml of culture was inoculated into 30 ml of SD/-Leu and also grown for two nights. Cell pellets were collected by centrifugation at 2,000 rpm for 7 min and resuspended in 15 ml of YPD containing 10% glucose and then incubated at 30^{o}C for 1-2 h with gentle agitation. Three µl of cell suspension was dropped onto a YPD agar plate containing 10% glucose. To prepare baits for testing, yeast Y187 harboring recombinant plasmid was cultured in 5 ml of SD medium lacking tryptophan (SD/-Trp) at 30^{o}C for two nights with shaking at 250 rpm and also expanded in SD/-Trp and YPD as described above. The next step was to generate diploid cells by dropping of 2 µl of bait culture as an overlay on the above prey spots. To allow yeast mating, the plates were incubated at 30^{o}C for two nights. The diploids were selected by replica-plating onto SD/-Leu/-Trp. After growing for two nights, cell spots were transferred onto SD/-Ade/-His/-Leu/-Trp containing 40 µg/ml of X-α-gal and incubated at 30^{o}C for two weeks. Growth of blue yeast colonies on this selective medium was scored as a positive interaction. This screening for protein-protein interactions was carried out independently at least twice.

3.14 SDS-PAGE and western blot analysis

3.14.1 Sample preparation for SDS-PAGE

A protein sample was prepared by mixing with sample buffer [60 mM Tris-HCl, pH 6.8, 10% (v/v) glycerol, 2% (w/v) SDS, 5% (v/v) β-mercaptoethanol,

and 0.01% (w/v) bromophenol blue]. The protein sample was denatured by heat at 95^{o}C for 10 min. Then, the protein sample was centrifuged at 12,000 rpm for 5 min and 10-15 µl of the supernatant was subjected for SDS-PAGE.

3.14.2 Analysis of protein on SDS-PAGE

SDS-PAGE was carried out according to Laemmli (1970). The SDS-polyacrylamide slab gel contained a lower separating gel with 12% (w/v) acrylamide, 0.1% (w/v) SDS in 0.375 M Tris-HCl (pH 8.8), 0.1% (w/v) ammonium persulfate, 6 µl of TEMED and an upper stacking gel with 5% acrylamide, 0.1% (w/v) SDS in 0.126 M Tris-HCl (pH 6.8), 0.1% (w/v) ammonium persulfate, and 5 µl of TEMED. The stacking gel and separating gel were prepared to the desired concentration from a stock of 30% (w/v) acrylamide solution with an acrylamide to N,N'-methylene-bis-acrylamide ratio of 29:1. The separating gel mixture was first poured into the casting mold and overlaid with a small volume of distilled water and allowed to polymerize for 20 min. After polymerization, water was removed and the stacking gel solution was prepared and poured on the top of the separating gel. A comb is used to generate wells to hold the samples by plugging into the surface of the stacking gel while it polymerized. The electrophoresis was performed in protein running buffer (25 mM Tris, 193 mM glycine (pH 8.3), 0.1% SDS) at constant voltage of 100-120 volts using a Mini-protein unit (GE Healthcare) until the tracking dye reached the bottom of the separating gel.

3.14.3 Coomassie brilliant blue staining

After gel electrophoresis, the gel was removed from the mold and stained at room temperature for at least 1 h in staining solution [10% (v/v) acetic acid, 50% (v/v) methanol, 0.3% (w/v) Coomassie brilliant blue R-250]. The stained gel was destained with several changes of destaining solution [10% (v/v) acetic acid, 15% (v/v) methanol] until a clear background was obtained and then dried at room temperature between two sheets of cellophane over a glass plate.

3.14.4 Western blot analysis

After separating on SDS-PAGE, protein samples were transferred to Immobilon-P membranes (Millipore) using a Mini Trans-Blot® electrophoresis transfer cell (Bio-Rad) for semi-dry blotting. The membranes were pre-wetted in methanol for a few seconds and the pre-wetted membrane and papers (Whatman® 3 MM) were then soaked in transfer buffer (20% (v/v) methanol in protein running buffer) for 5 min. A sandwich of the components was assembled as follows. Two sheets of saturated blotting paper were placed one by one and the pre-wet membrane was subsequently placed onto the stack of blotting papers. Then the gel which had been soaked in transfer buffer was placed on the membrane and two sheets of blotting paper were placed on top of the gel. The blot was set for a constant current depending on the size of the gel. The current was calculated by measuring the gel surface area (cm^2) and multiplying by $2mA/cm^2$. After the transfer was performed for 1 h, the gel was stained with staining solution to check the efficiency of the transfer. The membrane was lifted and used in the detection step. After transfer, the membrane was incubated in blocking solution prepared from 5% (w/v) skim milk in TBST buffer (10 mM Tris-HCl, pH 7.5, 150 mM NaCl, 0.05% Tween 20) for at least 2 h. Then the membrane was rinsed with TBST buffer before incubation with primary antibody diluted in 2% (w/v) skim milk in TBST buffer at room temperature for 1 h. After incubation, the membrane was washed 3 times for 10 min each with TBST buffer and further incubated with secondary antibody for 1 h with gentle agitation. Then the membrane was washed 3 times for 10 min each with TBST buffer to remove excess antibodies. The antigen-antibody complex was detected by liquid substrate of 3,3',5,5'-Tetramethylbenzidine (TMB) (Sigma) for HRP-conjugated antibody or nitro blue tetrazolium (NBT)-Bromochloroindolyl phosphate (BCIP) (Roche) for AP-conjugated antibody. The reaction was developed in the dark and stopped by rinsing with water.

3.15 Protein expression

3.15.1 Shrimp and viral protein expression in the bacterial system

E.coli strain BL21 carrying an expression plasmid for His-tag proteins and *E.coli* strain XL1-Blue containing an expression plasmid for GST-tag proteins were cultured in 3 ml of LB broth containing ampicillin (50 μg/ml) and chloramphenicol (34 μg/ml) and only ampicillin, respectively. *E. coli* were grown at 37^{o}C overnight with shaking at 200 rpm. Then, the overnight culture was seeded into 100 ml of fresh medium to make up to 1% of the final concentration and then incubated at 37^{o}C until OD_{600} reached 0.3-0.5. After induction with 1 mM IPTG at 37^{o}C for 3 h, the cell pellet was collected by centrifuation at 10,000 rpm for 10 min. The supernatant was discarded and cell pellet was re-suspended in ice-cold PBS buffer containing 1X protease inhibitor (Roche), and then sonicated for 30 min on ice. The insoluble debris was collected by centrifugation and the supernatant was used for protein purification.

3.15.2 Protein purification

Solutions containing His-tag proteins were used to purify proteins by mixing with Ni-NTA agarose beads (QIAGEN). The mixture was incubated on a rotating wheel at 4^{o}C for 3 h. The beads were then washed several times with wash buffer (50 mM NaH_2PO_4, 300 mM NaCl and 20 mM imidazole, pH 8.0) to remove unbound materials. The fusion proteins were eluted directly from the beads with elution buffer (50 mM NaH_2PO_4, 300 mM NaCl and 250 mM imidazole, pH 8.0). For GST-tag proteins, the supernatant was mixed with glutathione sepharose 4B resins (GE Healthcare, formerly Amersham Biosciences) and then incubated on a rotating wheel at room temperature for 1 h. The unbound materials were removed by washing several times with ice-cold PBS buffer and the GST fusion protein was eluted using 10 mM reduced glutathione in 50 mM Tris-HCl (pH 8.0). The purified proteins were subjected to SDS-PAGE and immunoblot assay probing with anti-His antibody (GE Healthcare) or anti-GST antibody (Zymed).

3.15.3 *In vitro* pull-down assays

In vitro pull-down assays between C-terminal SPH516 and MIB were performed using either Ni-NTA or glutathione sepharose 4B beads. The negative control for this test used a combination of His_6-SPH516-C with GST-p20. Binding experiments using His_6-SPH516-C without GST-MIB protein and vice versa were also performed. Purified fusion proteins were mixed and incubated with respective beads for 1 h at 4°C. Samples were washed and eluted as described above. Proteins in the flow-through, washing, and elution fractions were analyzed by SDS-PAGE and western blotting with anti-His and anti-GST antibodies. *In vitro* pull-down among TSV proteins, GST-tag VP1 and its complexes His-tags of BIR, Hel, VP2 and VP3, were performed using glutathione sepharose 4B beads. Each pair of tested proteins or protein complexes were mixed with glutathione sepharose 4B beads and incubated at 4°C for overnight. The protein complexes were washed and eluted and detected with anti-His antibody.

3.15.4 Antibody production

The His-fusion protein of SPH516-C (residues 393 to 516) produced heterologously in *E. coli* as described above was used to produce a polyclonal antiserum in rabbits. Rabbit immunization was performed by injection of 100 µg of purified fusion protein in complete Freund's adjuvant followed by four booster injections in incomplete adjuvant at one-weekly intervals. Serum was collected from the rabbits one week after the last booster.

3.15.5 Detection of SPH expression in shrimp tissues

Hemolymph was withdrawn from the pleopod base of the first abdominal segment using a sterile 1-ml syringe with a 25-guage needle containing an equal volume of anticoagulant AC1 solution (Soderhall and Smith, 1983). After centrifugation at 800 x g for 10 min, the supernatant (hemolymph plus anticoagulant) was collected. The hemocyte pellet as well as gills and heart tissues were homogenized in 100 mM NaCl-50 mM Tris buffer, pH 8 containing 1 mM phenylmethanesulfonyl fluoride (PMSF). The homogenates were centrifuged at 3000 x g for 5 min and the supernatants were collected. Protein concentrations were

determined using a Bio-Rad protein assay kit. Equal amounts of proteins (15 μg) were subjected to 10 % SDS-PAGE and western blotting. Rabbit anti-SPH516-C antibody at a dilution of 1:250 was used as a primary antibody. Subsequently, AP-conjugated goat anti-rabbit IgGs (Zymed) were used and detection was performed with a substrate solution (NBT/BCIP, Roche).

3.16 Immunohistochemistry assay

Tissue sections of SPF shrimp were prepared using Davidson's fixative as described by Bell and Lightner (1988). The sections were deparafinized with xylene (5 min x 3), rehydrated (100% EtOH 1 min x 2, 95% 1 min x 2, 80% EtOH 2 min x 2, 50% EtOH 1 min x 1), rinsed in distilled water x 1 and then blocked with blocking buffer (10% Fetal bovine serum in PBS). After deparaffinization and blocking steps, the tissue sections were incubated with anti-SPH516-C serum (1:50 dilution) overnight at 4°C, washed (PBS 10 min x 3), and incubated with goat anti-rabbit IgGs HRP conjugated for 1 h at 37°C. Slides without first antibody served as negative controls. After washing the unbound secondary antibody (PBS 10 min x 3), signal detection was achieved using Histostain-SP kit (Zymed). The sections were then stained in Mayer's hematoxylin for 4-6 min and passed through tap water for 4-6 min. The sections were further stained in eosin-phloxine for 2 min, dehydrated (70%, 95%, 100% EtOH 1 min x 2 each) and cleared in xylene (2 min x 4). The stained sections were mounted with permount (EMS, England) covered with a coverslip and digital images were captured using an Olympus BX51 microscope.

3.17 Bioinformatics tools for data analysis

DNA and protein analysis were carried out using the EXPASY web server (http://au.expasy.org/). To identify related sequences, a protein-protein basic local alignment search tool (blastp) search was carried out using the NCBI protein database (http://www.ncbi.nlm.nih.gov/BLAST/). Alignments of protein sequences were performed and a phenogram generated by ClustalW (Thompson et al. 1994, http://www.es.embnet. org/ Doc/ phylodendron/ clustal-form.html). An analysis for

protein domains was accomplished by InterPro database (Apweiler et al., 2001, http://www.ebi.ac.uk/ InterProScan/) and SMART (Letunic et al., 2006, http://smart.embl- heidelberg.de/). Molecular modeling of the three-dimensional (3D) structure of LRR protein was performed with the bioinformatics tool server (http://bioserv.cbs.cnrs.fr/). Graphical visualization was performed using RasTop 2.1 program (http://www.geneinfinity. org/rastop/). The protein interaction map was visualized using Cytoscape software (www.cytoscape.org).

CHAPTER IV
RESULTS

4.1 Identification and characterization of *PmLRR*

4.1.1 Cloning and sequence analysis of *PmLRR*

The full-length, leucine-rich repeat (LRR) cDNA sequence from *P. monodon* hemocytes was obtained using 5' RACE (Fig. 4.1) and deposited in GenBank (accession number **DQ355156**). The sequence included 174 nucleotides of 5'-untranslated region, a 1686-nucleotide open reading frame, and a 744-nucleotide 3'-untranslated region. The entire 1686 bp-open reading frame encodes a novel deduced protein of 561 amino acids with a predicted molecular weight of 62.45 kDa and an isoelectric point of 7.26. The *Pm*LRR sequence was leucine-rich, containing 96 leucine residues (17% of total). A GenBank BLAST search (Altschul et al., 1990) revealed strong similarity to leucine-rich repeat proteins of various organisms from bacteria to humans with E-values ranging from 0.0 to 2e-23 (data not shown). Most of the LRR sequences from the BLAST result were not annotated. However, those annotated were mainly named Soc-2, Shoc-2, and Sur-8, proteins involved in intracellular signaling pathways (Selfors et al., 1998; Sieburth et al., 1998). *Pm*LRR showed highest identity (67%) to a non-annotated protein from the honey bee (accession number **XP_396017**). It is not known whether shrimp LRR and the proteins of similar sequence also have functions similar to Soc-2, Shoc-2 or Sur-8 since LRR motifs have been found in a large number of proteins with diverse functions and cellular locations in a variety of organisms (Kobe et al., 1994; Kobe et al., 1995; Buchanan et al., 1996; Kajava, 1998). The BLAST search result revealed that the LRR cDNA sequence described herein is not only the first found from shrimp but also the first found from a crustacean. It would be interesting to know the biological role of this LRR protein in shrimp and closely related species.

For sequence comparison to *Pm*LRR by ClustalW alignment, we selected full-length LRR protein sequences from the first 19 distinct genera giving high similarities (E-values between 0.0 and 3e-56) in the BLAST search. The automatically generated phenogram (Fig. 4.2) showed that *Pm*LRR grouped in a clade that included LRR of other arthropods (i.e., honey bee, mosquito and fruit fly).

4.1.2 Tissue expression

Expression analysis using RT-PCR to determine the distribution pattern of *PmLRR* in different tissues (Fig. 4.3) revealed that *PmLRR* was expressed in all 9 tested tissues but at different levels when compared to the internal β-actin control. *PmLRR* expression was particularly high in hemocytes, the intestine, and the lymphoid organ. The fragment from hemocytes was directly sequenced and found to have the same sequence as the identified cDNA. Weak but detectable signals were found in the gills, heart, muscles, eye stalks, pleopods, and the hepatopancreas. Thus, high *PmLRR* expression was relatively specific to defense-related tissues (i.e., the lymphoid organ and hemocytes), suggesting that *Pm*LRR might play a role in shrimp defense mechanisms (Hasson et al., 1999; Anggraeni et al., 2000; Johansson et al., 2000; van de Braak, 2002). The mucous membrane of intestines is also generally known to act as a defense barrier.

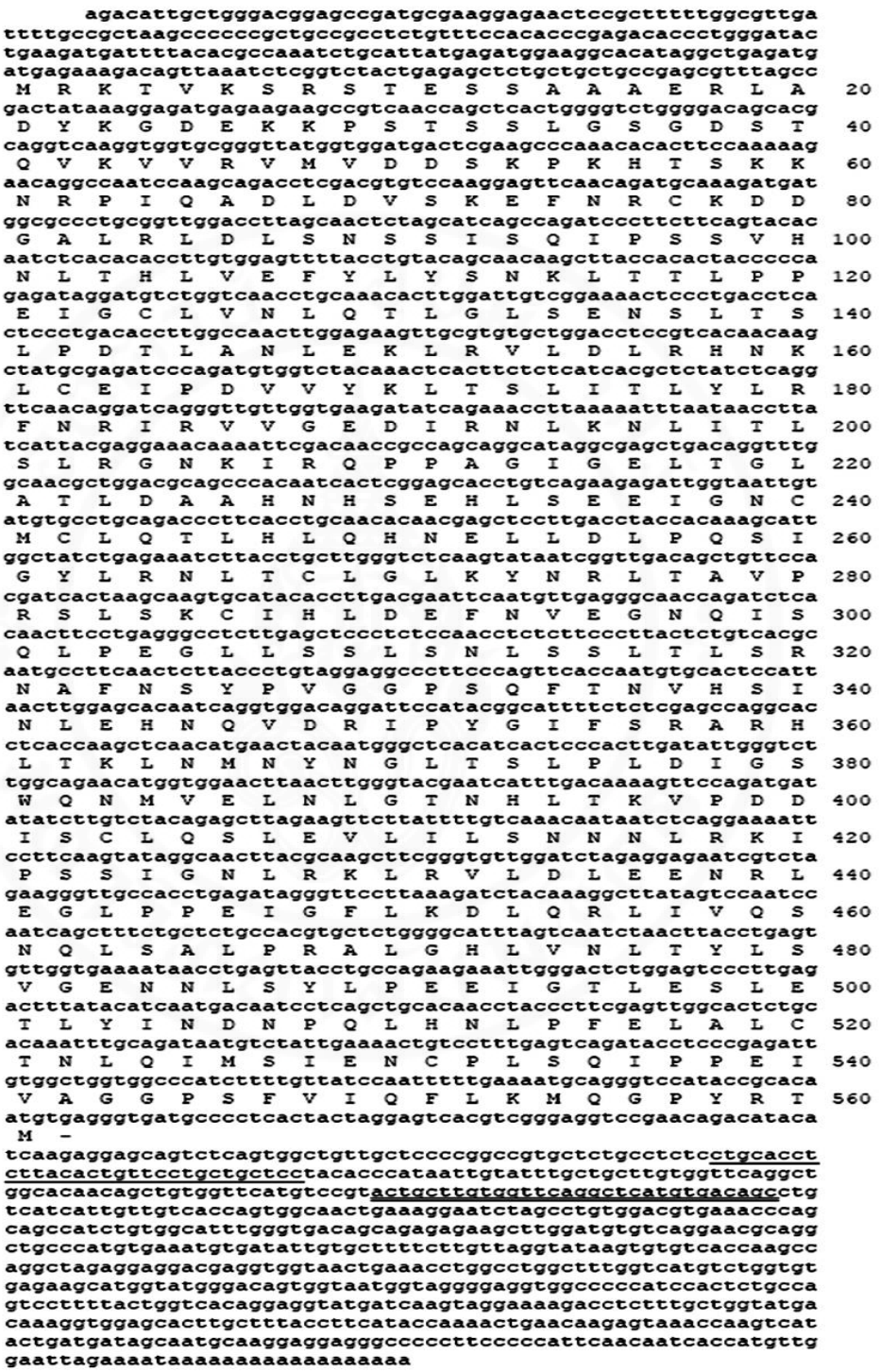

Figure 4.1 The nucleotide and deduced amino acid sequence of full-length *Pm*LRR (GenBank accession no. **DQ355156**). Amino acids are numbered on the right margin. Nested primers and specific primers designed for 5' RACE are underlined and double underlined, respectively.

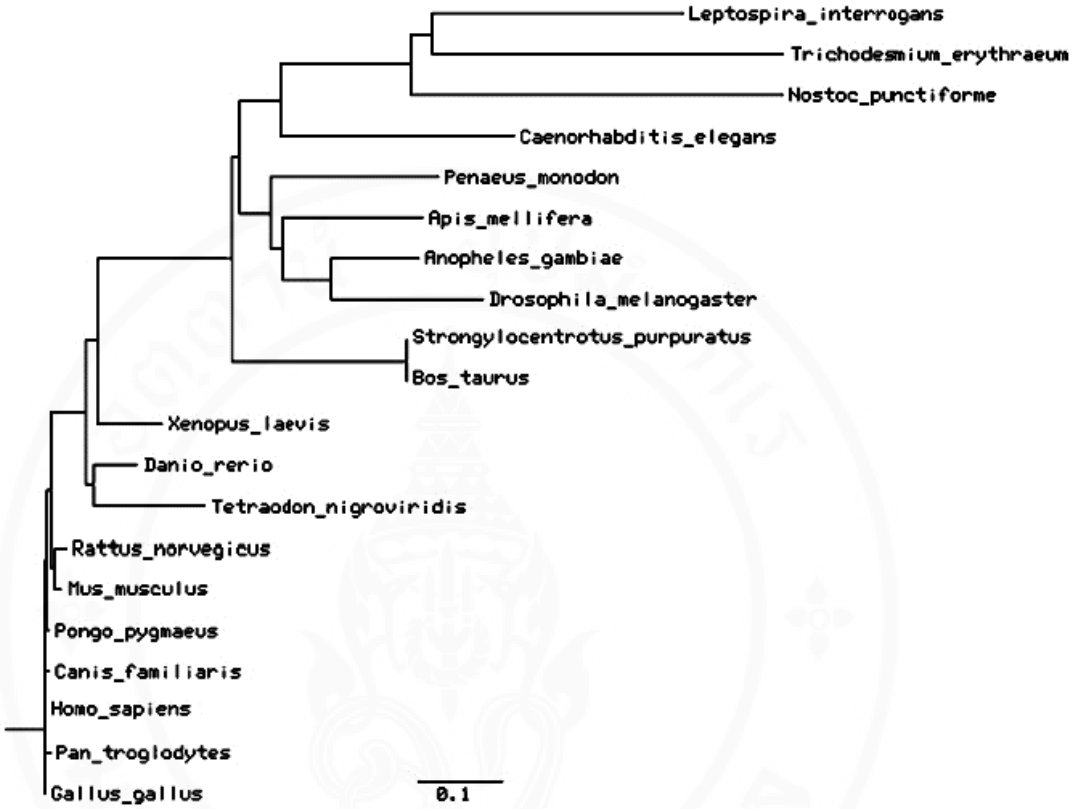

Figure 4.2 Phenogram showing the relationship amongst LRR sequences aligned using ClustalW. Protein sequences from the GenBank database were *L. interrogans* (accession no. **AAS69444**), *T. erythraeum* (accession no. **ZP_00671672**), *N. punctiforme* (accession no. **ZP_00110172**), *C. elegans* (accession no. **AAM81129**), *P. monodon* (accession no. **DQ355156**), *A. mellifera* (accession no. **XP_396017**), *A. gambiae* (accession no. **EAA44595**), *D. melanogaster* (accession no. **AAM75092**), *S. purpuratus* (accession no. **XP_798409**), *B. taurus* (accession no. **XP_588750**), *X. laevis* (accession no. **AAH42263**), *D. rerio* (accession no. **XP_682883**), *T. nigroviridis* (accession no. **CAG01294**), *R. norvegicus* (accession no. **NP_001013173**), *M. musculus* (accession no. **AH83060**), *P. pygmaeus* (accession no. **CAH92905**), *C. familiaris* (accession no. **XP_535013**), *H. sapiens* (accession no. **CAH72812**), *P. troglodytes* (accession no. **XP_521602**), and *G. gallus* (accession no. **CAH72812**).

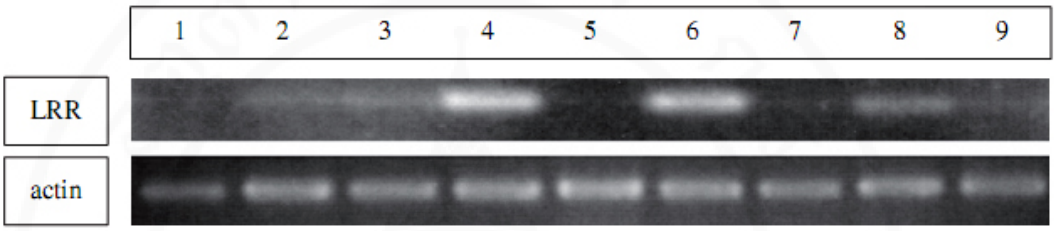

Figure 4.3 Expression analysis of *PmLRR* and β-actin in various tissues. Lanes 1, eye stalks; 2, gills; 3, heart; 4, hemocytes; 5, hepatopancreas; 6, intestine; 7, pleopods; 8, lymphoid organ; 9, muscle.

4.1.3 Time course analysis after YHV and WSSV challenges

For preliminary viral challenge experiments, the lymphoid organ was chosen as the analytical target because it is known to play a role in the shrimp response to viral pathogens (Hasson et al., 1999; Anggraeni et al, 2000) and because it gave high expression levels in the tissue specificity tests. Shrimp challenged with YHV and WSSV died within 60 and 48 h post-injection (h.p.i), respectively, while no mortality was observed in the control groups during the same interval. The infections were confirmed by RT-PCR and PCR using the respective IQ2000 detection kits. Expression profiles of *PmLRR* mRNA after YHV and WSSV challenges are shown for one experiment in Figs. 4.4a and 4.4b, respectively. Band intensity of *PmLRR* transcripts was normalized using β-actin and analysis revealed a general trend towards reduced *Pm*LRR expression after both viral challenges. Results from band intensities from 3 separate tests are summarized in Fig. 4.4c. Thus, the overall results suggested that shrimp mortality caused by viral infection was associated with a general down-regulation of *PmLRR*. Since RT-PCR expression assays based on agarose gel band intensities are relatively crude, apparent differences of a low order of magnitude may not be real. However, the differences seen from the normal state (0 h.p.i.) to the late phase of infection for both viruses are 5-fold or higher and compare to the differences seen for *PmLRR* in various shrimp tissues (Fig. 4.3), suggesting that they indicate a real drop in expression. Despite this, it would be important to carry out more detailed tests using real-time PCR assays or northern blot analysis to confirm these results before doing further work on the potential role of *PmLRR* in the shrimp response to viral pathogens.

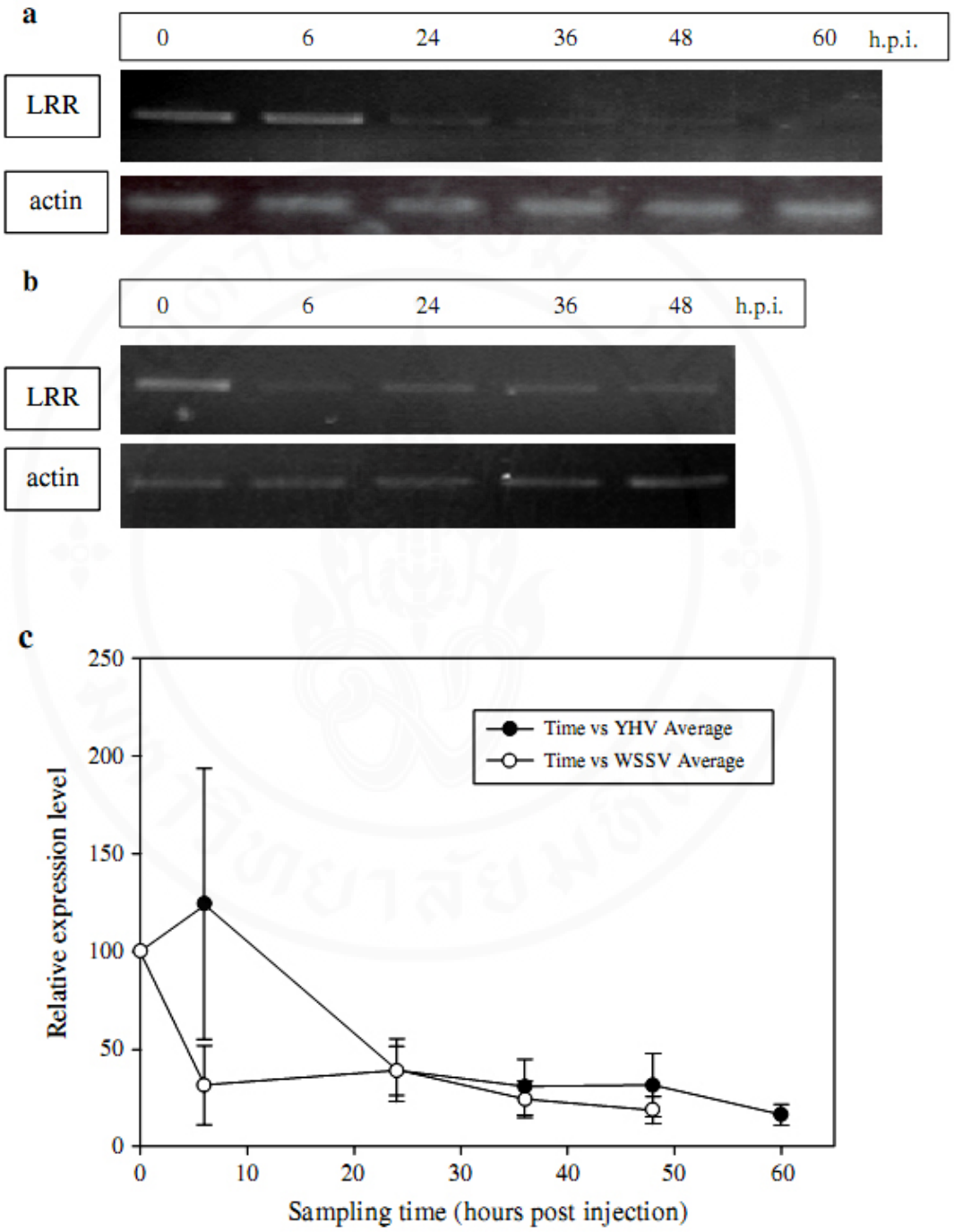

Figure 4.4 Example agarose gel set from one of 3 time-course expression tests for *PmLRR* after challenge with (a) YHV and (b) WSSV (normalized with β-actin). The graph (c) summarizes the results from 3 separate tests.

4.1.4 Structural features of *Pm*LRR

Most LRR-containing proteins contain 2-45 tandem motifs comprising 20-30 amino acids each that are sub-divided into a conserved segment and a variable segment. The conserved segment is characterized by an 11-residue motif of LxxLxLxxNxL, where x can be any amino acid, L indicates leucine or other bulky, non-polar residues, and N asparagine, cysteine, serine or threonine (Kobe et al., 2001). Analysis with InterPro database (Apweiler et al., 2001) revealed that the deduced *Pm*LRR protein contained 16 tandem LRR motifs from amino acids 105 to 498. The motifs are 23-24 amino acids long and form a consensus that is significantly similar to LxxLxLxxNxL (Fig. 4.5a). However, some degenerated LRR motifs were observed. For example, L at position 1 of LRR12 is replaced by methionine, and L at position 4 of LRR1 and LRR9 is replaced by phenylalanine.

So far, at least 7 subfamilies of LRR proteins have been classified based on different lengths and consensus sequences for the variable segments of repeats (Kajava, 1998). The sequence characteristics of *Pm*LRR suggest that it most likely belongs to the 'typical' subfamily (Kobe et al., 2001) in which the variable segment at position 12-22 contains xxLPxxOFxLx, where P indicates proline, O indicates a nonpolar residue, and F indicates phenylalanine or another hydrophobic residue (Fig. 4.5a). Note that F at position 19 is mainly occupied by glycine residues in *Pm*LRR. Similar to the conserved motifs, the variable segments also show some degeneracy.

Because high-resolution work has been carried out on several LRR-containing proteins, 3D structural analysis based on homologous sequence searches could be used to predict a 3D structure for *Pm*LRR using the bioinformatics tool server (http://bioserv.cbs.cnrs.fr/) and visualization by RasTop 2.1 program (http://www.geneinfinity.org/rastop/). The computational result predicted a horseshoe-shaped molecule with a curved parallel β-sheet formed by 16 β-strands on the concave (inner) side and α-helical elements on the convex (outer) side (Fig. 4.5b). The molecular graphic was created from amino acids 83 to 561. The first 82 N-terminal residues were not included in the solenoid shape as they appear to be linear. No signal protein or transmembrane region was identified in this portion. Consistent with prediction from the primary sequence, 16 tandem LRRs are included in amino acids 105 to 498. It is known that the conserved segments of LxxLxLxxNxL represent β-

sheet strands and that the variable segments correspond to α-helixes. This yields a horseshoe structure composed of alternately repeated β-α domains (Kobe et al., 1993).

LRR proteins are thought to play a major role in protein-protein interactions that occur in phenomena such as hormone-receptor interactions, enzyme inhibition, cell adhesion and cellular trafficking (Kobe et al., 1994; Kobe et al., 1995; Buchanan et al., 1996; Kajava, 1998). Atomic resolution structures of LRR-ligand complexes indicated that the ligand-binding site is located on the concave surface of the LRR solenoid (Kobe et al., 1996; Papageorgiou et al., 1997). Certain domains lying in proximity to the convex face have also been suggested to be potential participants in binding (Bell et al., 2003). The undefined region protruding between LRR9 and LRR10 in *Pm*LRR (Fig. 4.5b) is a notable feature that may have some functional significance in protein-protein interactions. With all these characteristics, *Pm*LRR might be a prime candidate for further protein-protein interaction studies in shrimp.

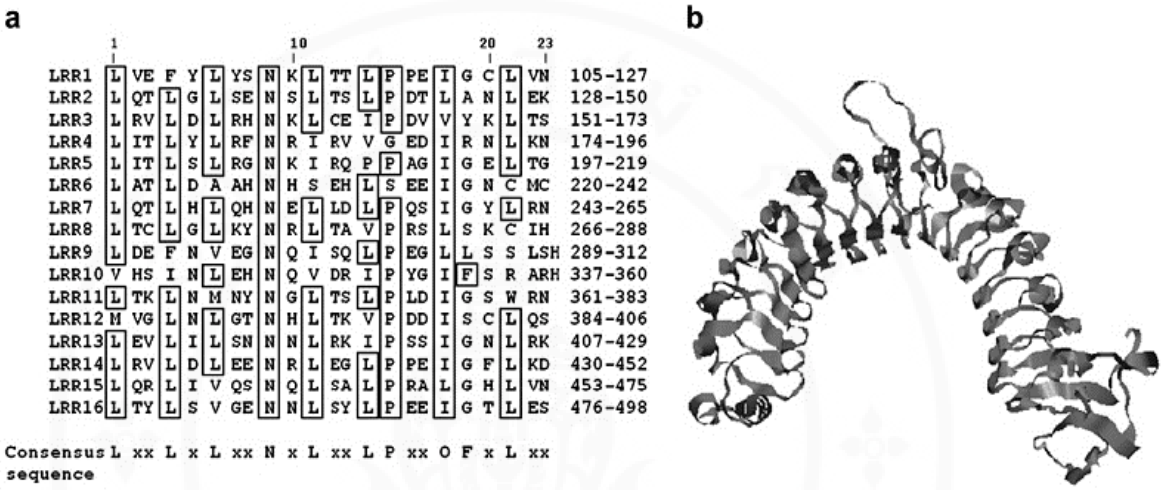

Figure 4.5 (a) Sequence alignment of the individual LRRs in the deduced *Pm*LRR protein. The consensus sequence of the 'typical' LRR subfamily is shown below. X refers to any amino acid, L indicates leucine or bulky, non-polar residues, N indicates asparagine, P indicates proline, O indicates a nonpolar residue, and F indicates phenylalanine and other hydrophobic residue. Position F of *Pm*LRR is mainly occupied by glycine. Boxes denote the positions of the conserved amino acids in the consensus sequence. (b) A schematic representation of the 3D structure of *Pm*LRR protein, consisting of 16 tandem LRRs falling between amino acids 83 to 561.

4.2 Identification and characterization of *PmSPH516*

4.2.1 Identification of SPH516 as a binding protein of YHV MIB domain

Yeast strain Y187 pre-transformed with a shrimp hemocyte cDNA library and yeast strain AH109 containing BD-MIB plasmid were mated and approximately $6.5x10^6$ diploid colonies were screened. The library screening led to the isolation of five independent clones including an in-frame C-terminal sequence of SPH516, called SPH516-C. It was known later when the complete sequence of SPH516 had been obtained (see below) and that yeast two-hybrid analysis had identified SPH516-C clone as containing 124 C-terminal amino acids (residues 393-516). Interaction between SPH516-C and the YHV MIB domain was confirmed both by plasmid switching (i.e., switching the vectors formerly used for cloning of both genes) in the yeast two-hybrid analysis and by *in vitro* pull-down assay (Fig. 4.6). The yeast two-hybrid assays demonstrated that SPH516-C interacted with the YHV MIB domain when carried by either plasmid BD or AD (Fig. 4.6). In addition, no self-activation occurred when SPH516-C or MIB were paired with empty plasmids (i.e., no expression of the reporter genes occurred) (Fig. 4.6). The binding was subsequently reconfirmed using the full-length sequences of SPH516 and the MIB domain in a yeast two-hybrid assay (Fig. 4.6). Binding was also reconfirmed when the vectors containing these full-length sequences were switched.

4.2.2 *In vitro* pull-down assays confirmed the yeast two-hybrid results

Since attempts to express and purify full-length SPH516 protein in *E. coli* and baculovirus systems were not successful (data not shown), we used the C-terminal part of SPH516 that was initially found from the yeast two-hybrid screen for *in vitro* pull-down experiments. The results revealed that the GST-MIB fusion protein could bind to the His_6-SPH516-C fusion protein using Ni-NTA beads and that the bound proteins could be eluted using elution buffer (Fig. 4.7a). SDS-PAGE and western blotting of the eluted proteins gave bands for both His_6-SPH516-C (~13 kDa) and GST-MIB (~34 kDa) in the pull-down product (E fraction, Fig. 4.7a), confirming the binding between the two proteins. It was also observed that approximately 10% of the

total input proteins were recovered (data not shown). A similar result was obtained when glutathione sepharose beads were used (data not shown). GST-p20 was used in a negative control in this experiment because p20 was one of other tested YHV domains that did not bind to SPH516 in the yeast two-hybrid assays (see below). No GST-p20 was found in the pull-down product with His_6-SPH516-C (E fraction, Fig. 4.7b), indicating that the binding between His_6-SPH516-C and GST-MIB was specific and not the result of binding to GST. The possibility that the observed interaction was artifactual was ruled out by further binding tests of His_6-SPH516-C without GST-MIB and vice versa (Figs. 4.7c and 4.7d). The results showed no unspecific binding of GST-MIB to Ni-NTA beads and no cross-reactivity of anti-His and anti-GST antibodies to the GST-MIB and His_6-SPH516-C fusion proteins, respectively.

BD	AD	Interaction
MIB	SPH516-C	+
SPH516-C	MIB	+
empty BD	SPH516-C	–
SPH516-C	empty AD	–
MIB	SPH516	+
SPH516	MIB	+
empty BD	SPH516	–
SPH516	empty AD	–

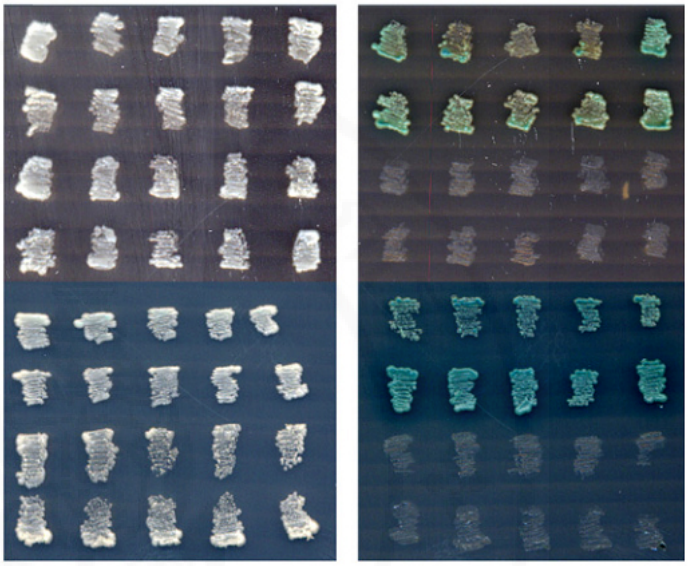

Figure 4.6 Interactions of the full-length and C-terminal region of SPH516 with full-length YHV MIB domain by yeast two-hybrid assay. Results for 5 independent transformants from SD/-Leu/-Trp plates when grown on SD/-Leu/-Trp/-Ade/-His/X-α-gal plates where interaction (+) is indicated by blue yeast colonies and no interaction (-) by no growth. BD and AD constructs co-transformed in yeast AH109 are indicated.

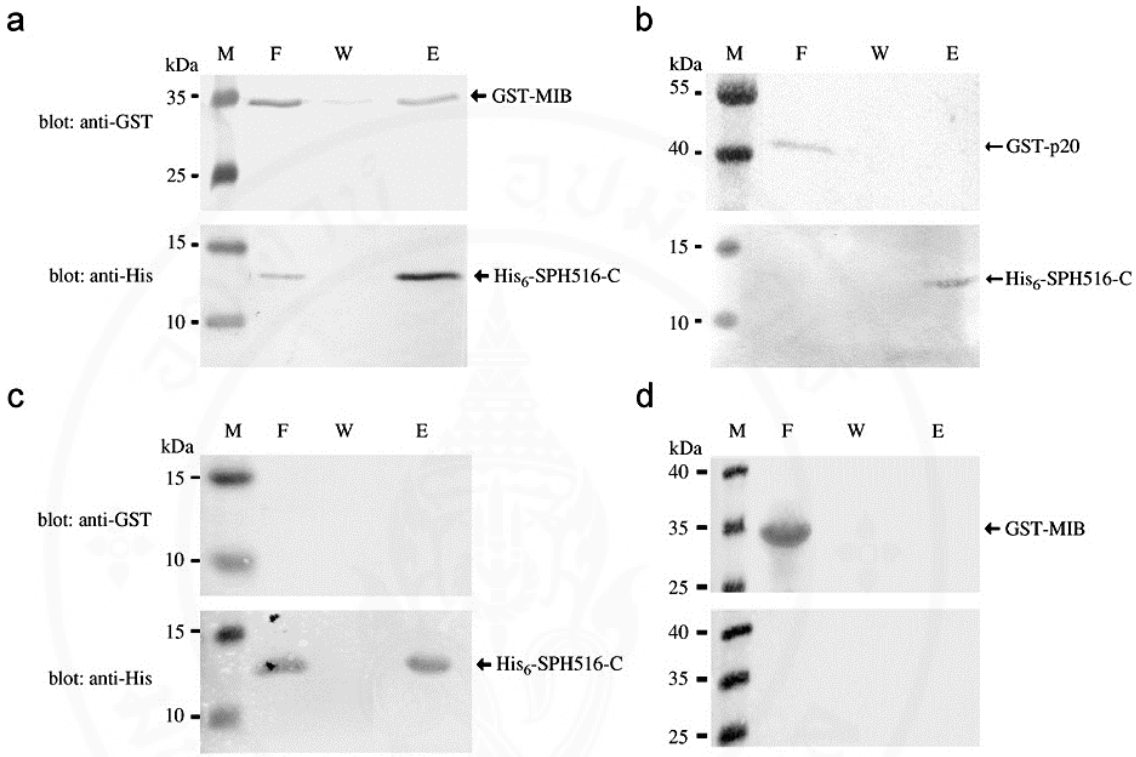

Figure 4.7 Western blot results for *in vitro* pull-down assay components from Ni-NTA beads. (a) Binding test of GST-MIB and His_6-SPH516-C. Lanes M = molecular weight markers; Lane F = flow through excess of GST-MIB and His_6-SPH516-C; Lane W = wash buffer showing absence of His_6-SPH516-C and a very minute quantity of GST-MIB; Lane E = imidazole eluted fraction showing the presence of both GST-MIB and His_6-SPH516-C. (b) Control test of GST-p20 and His_6-SPH516-C pull-down performed as in (a) except GST-p20 was used instead of GST-MIB and no GST-p20 was found in the eluted fraction. (c) and (d) Binding tests of His_6-SPH516-C without GST-MIB, and GST-MIB without His_6-SPH516-C, respectively. Specific binding of His_6-SPH516-C to Ni-NTA beads was demonstrated and no binding of GST-MIB presented alone was detected.

4.2.3 Cloning and molecular characterization of SPH516

Using the 5' RACE method, the full-length SPH516 cDNA sequence of 1,949 bp was obtained from *P. monodon* hemocytes (GenBank accession number **DQ403191**). The sequence included 76 nucleotides of 5'-untranslated region (UTR), a 1,551-nucleotide open reading frame, and a 322-nucleotide 3'-UTR (Fig. 4.8). The entire 1,551 bp-open reading frame encoded a putative protein of 516 deduced amino acids with a theoretical molecular weight of 52.9 kDa. It contained a putative signal sequence of 19 amino acids that would result in a mature SPH516 with a predicted molecular weight of 50.9 kDa and a theoretical pI of 4.94. A potential trypsin-like serine protease domain predicted by InterPro (Apweiler et al., 2001) and SMART databases (Letunic et al., 2006), extended from residue 244 to residue 491. However, this domain lacked the typical catalytic serine protease triad of HDS and showed instead HDG (amino acid residues 194, 344, and 445, respectively) suggesting that it would lack protease activity (Fig. 4.8). In support of this contention, sequence analysis indicated that SPH516 contained a clip domain located from amino acids 159 to 214 that would place it in the clip domain-containing serine protease family. The name of this domain originated from a paper describing a clip like-structure formed by three disulphide bonds of six conserved cysteine residues (Muta et al., 1990). Interestingly, the N-terminus of SPH516 is glycine-rich (contains 101 glycine residues or 19.6% of total). The region is composed of 10 septapeptide repeats of LGGQGGG. However, there are no reports so far on a possible role of this motif.

4.2.4 SPH516 binds specifically to YHV MIB domain

By yeast two-hybrid assay with several YHV gene products, we found that SPH516 bound only to MIB (metal ion binding domain) and not to other proteins including the viral polymerase, helicase, Motif 1 and Motif 3 from ORF1b, p20 from ORF2 and gp64 from ORF3 (Fig. 4.9).

Figure 4.8 Nucleotide and deduced amino acid sequences of a SPH516 cDNA clone. The open reading frame consisted of 1,551 bp encoding 516 deduced amino acids residues. Ten repeats of septapeptide LGGQGGG are inclosed in small boxes. The large, boxed C-terminal domain corresponds to a potential trypsin-like serine protease domain. The shaded amino acid sequence represents a potential signal peptide while the shaded nucleotide sequence indicates the yeast-two-hybrid identified fragment. A predicted clip domain is underlined with dots. Double underlines indicate the sites that were used to design primers for 5'RACE. The three amino acids in the catalytic triad are marked by circles.

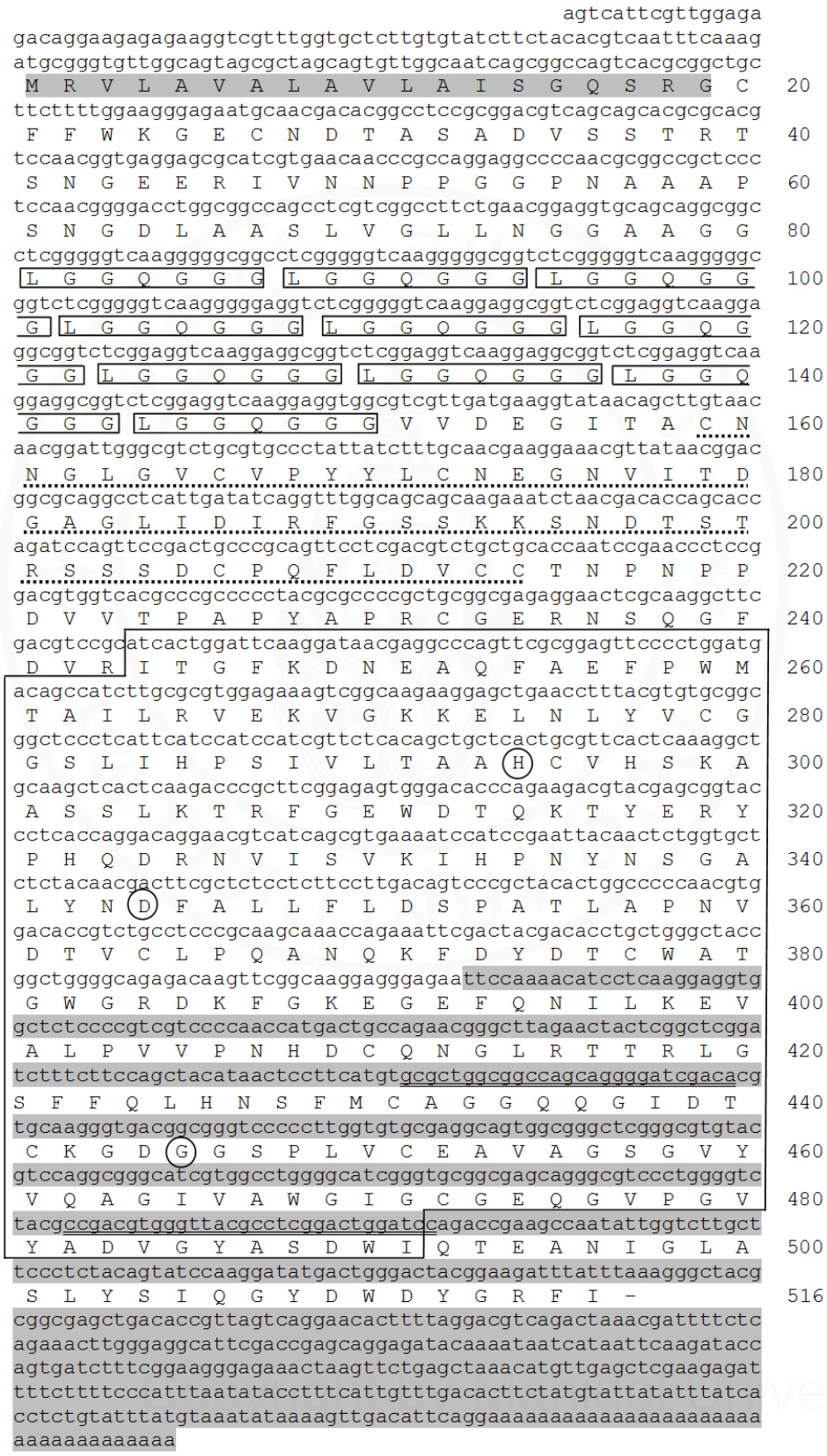
agtcattcgttggaga
gacaggaagagagaaggtcgtttggtgctcttgtgtatcttctacacgtcaatttcaaag
atgcgggtgttggcagtagcgctagcagtgttggcaatcagcggccagtcacgcggctgc
M R V L A V A L A V L A I S G Q S R G C 20
ttcttttggaagggagaatgcaacgacacggcctccgcggacgtcagcagcacgcgcacg
F F W K G E C N D T A S A D V S S T R T 40
tccaacggtgaggagcgcatcgtgaacaacccgccaggaggccccaacgcggccgctccc
S N G E E R I V N N P P G G P N A A A P 60
tccaacggggacctggcggccagcctcgtcggccttctgaacggaggtgcagcaggcggc
S N G D L A A S L V G L L N G G A A G G 80
ctcgggggtcaaggggggcggcctcgggggtcaaggggggcggtctcgggggtcaaggggggc
L G G Q G G G G L G G Q G G G G L G G Q G G 100
ggtctcgggggtcaaggggggaggtctcgggggtcaaggaggcggtctcggaggtcaagga
G L G G Q G G G G L G G Q G G G G L G G Q G 120
ggcggtctcggaggtcaaggaggcggtctcggaggtcaaggaggcggtctcggaggtcaa
G G L G G Q G G G G L G G Q G G G G L G G Q 140
ggaggcggtctcggaggtcaaggaggtggcgtcgttgatgaaggtataacagcttgtaac
G G G L G G Q G G G G V V D E G I T A C N 160
aacggattgggcgtctgcgtgccctattatctttgcaacgaaggaaacgttataacggac
N G L G V C V P Y Y L C N E G N V I T D 180
ggcgcaggcctcattgatatcaggtttggcagcagcaagaaatctaacgacaccagcacc
G A G L I D I R F G S S K K S N D T S T 200
agatccagttccgactgcccgcagttcctcgacgtctgctgcaccaatccgaaccctccg
R S S S D C P Q F L D V C C T N P N P P 220
gacgtggtcacgcccgccccctacgcgccccgctgcggcgagaggaactcgcaaggcttc
D V V T P A P Y A P R C G E R N S Q G F 240
gacgtccgcatcactggattcaaggataacgaggcccagttcgcggagttcccctggatg
D V R I T G F K D N E A Q F A E F P W M 260
acagccatcttgcgcgtggagaaagtcggcaagaaggagctgaacctttacgtgtgcggc
T A I L R V E K V G K K E L N L Y V C G 280
ggctccctcattcatccatccatcgttctcacagctgctcactgcgttcactcaaaggct
G S L I H P S I V L T A A H C V H S K A 300
gcaagctcactcaagacccgcttcggagagtgggacacccagaagacgtacgagcggtac
A S S L K T R F G E W D T Q K T Y E R Y 320
cctcaccaggacaggaacgtcatcagcgtgaaaatccatccgaattacaactctggtgct
P H Q D R N V I S V K I H P N Y N S G A 340
ctctacaacgacttcgctctcctcttccttgacagtcccgctacactggcccccaacgtg
L Y N D F A L L F L D S P A T L A P N V 360
gacaccgtctgcctcccgcaagcaaaccagaaattcgactacgacacctgctgggctacc
D T V C L P Q A N Q K F D Y D T C W A T 380
ggctggggcagagacaagttcggcaaggagggagaattccaaaacatcctcaaggaggtg
G W G R D K F G K E G E F Q N I L K E V 400
gctctccccgtcgtccccaaccatgactgccagaacgggcttagaactactcggctcgga
A L P V V P N H D C Q N G L R T T R L G 420
tctttcttccagctacataactccttcatgtgcgctggcggccagcaggggatcgacacg
S F F Q L H N S F M C A G G Q Q G I D T 440
tgcaagggtgacggcgggtccccccttggtgtgcgaggcagtggcgggctcgggcgtgtac
C K G D G G S P L V C E A V A G S G V Y 460
gtccaggcgggcatcgtggcctggggcatcgggtgcggcgagcagggcgtccctggggtc
V Q A G I V A W G I G C G E Q G V P G V 480
tacgccgacgtgggttacgcctcggactggatccagaccgaagccaatattggtcttgct
Y A D V G Y A S D W I Q T E A N I G L A 500
tccctctacagtatccaaggatatgactgggactacggaagatttatttaaagggctacg
S L Y S I Q G Y D W D Y G R F I - 516
cggcgagctgacaccgttagtcaggaacacttttaggacgtcagactaaacgattttctc
agaaacttgggaggcattcgaccgagcaggagatacaaaataatcataattcaagatacc
agtgatctttcggaagggagaaactaagttctgagctaaacatgttgagctcgaagagat
tttcttttcccatttaatatacctttcattgtttgacacttctatgtattatatttatca
cctctgtatttatgtaaatataaaagttgacattcaggaaaaaaaaaaaaaaaaaaaaaa
aaaaaaaaaaaaa

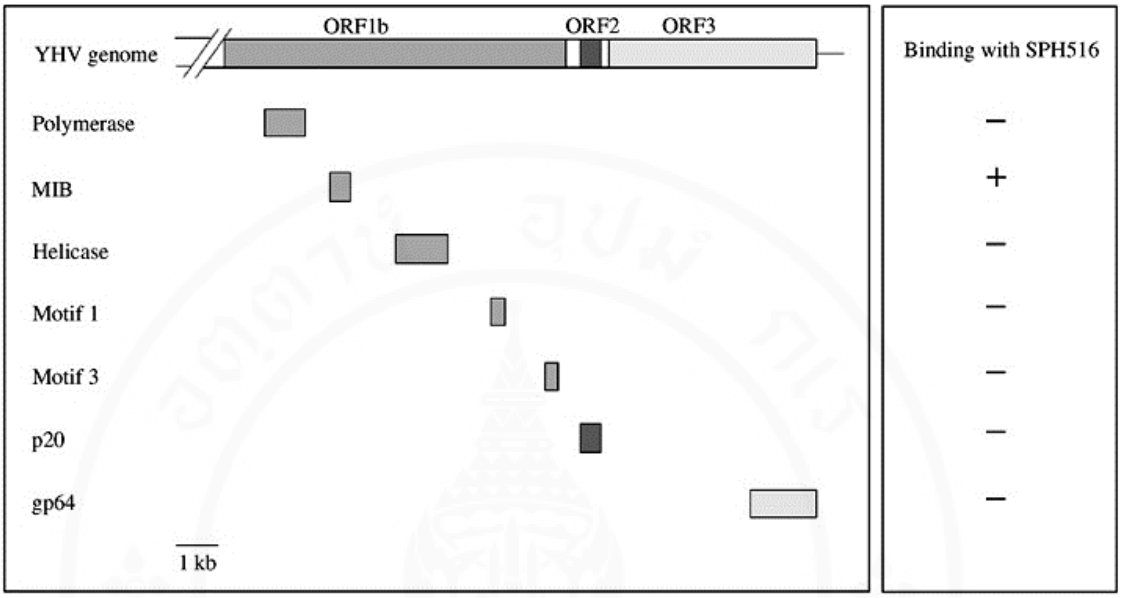

Figure 4.9 Diagrammatic representation of the YHV gene products tested for interaction with SPH516 in the yeast two-hybrid system. The structures of ORF and domains in YHV genome are presented schematically. The symbols indicate positive (+) interactions (i.e., growth and blue color change) and no interaction (-) (i.e., by no growth).

4.2.5 Identification of SPH isoforms

Using RT-PCR with total hemocyte RNA as a template and primers based on the SPH516 coding region, an amplicon of approximately 1.5 kb was obtained and several clones from it were sequenced. In addition to clones of the expected 1,551 bp SPH516, we obtained clones for an additional SPH isoform of 1,527 bp encoding 509 deduced amino acids (GenBank accession number **DQ916148**) that was named SPH509. Recently, two SPH cDNAs, called a masquerade-like serine proteinase homologue (MasSPH; GenBank accession number **DQ455050**) and a clip domain serine protease homologue (c-SPH; GenBank accession number **AY600627**) have been reported from *P. monodon* (Lin et al., 2006; Amparyup et al., 2007). Interestingly, SPH516 and SPH509 show higher identity to MasSPH (99%) than to c-SPH (32% identity). A comparison of the deduced proteins of MasSPH, SPH516 and SPH509 using the ClustalW program (Thompson et al., 1994) (Fig. 4.10) revealed that the SPH isoforms were very similar (i.e., amino acid changes at only six positions). Since we sequenced 2 clones from both strands, it is unlikely that PCR errors or sequencing errors could have produced these differences. This is particularly true for the variation in the number of septapeptide repeats (LGGQGGG), the most noticeable difference amongst MasSPH (11 repeats), SPH516 (10 repeats), and SPH509 (9 repeats) (Fig. 4.10). In addition, one of the repeat motifs of SPH509 is HGGQGGG instead of LGGQGGG. If these differences resulted from PCR or sequencing errors, they would have had to be consistent errors for 21 or more contiguous bases for each form. Thus, it is far more likely that these variants are truly isoforms that originate either from different genes or from post-transcriptional modification of a single gene.

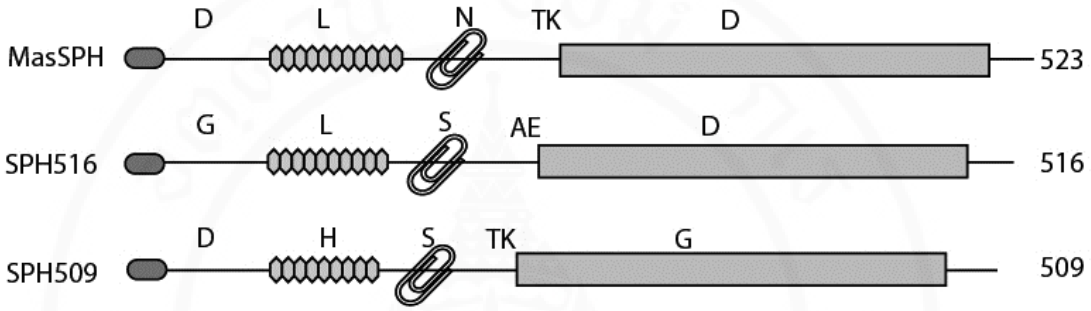

Figure 4.10 Predicted domain structure of *P. monodon* serine protease homologues. GenBank accession numbers of MasSPH, SPH516, and SPH509 are DQ455050, **DQ403191**, and **DQ916148**, respectively. The putative signal peptide (oval) is followed by the glycine-rich region (polygons) and the clip domain (paper clip symbol). The trypsin-like serine protease domain (box) is located at the C-terminus. The number of polygons represents the number of septapeptide motifs of LGGQGGG. Sequence variation among SPH isoforms are shown by single-letter amino acid codes above the domain features. Length of amino acid sequence is indicated on the right margin.

4.2.6 Sequence comparison of SPH516

Comparison of the SPH516 deduced protein sequence with the GenBank database using a BLAST search (Altschul et al., 1990) revealed that SPH516 had significant similarity to proteins annotated as serine proteases, serine protease homologues, trypsin-like serine proteases, tryptase, tryptase precursor, prophenoloxidase-activating factor (PPAF), and masquerade-like proteins of various animals with E-values ranging from 1e-109 to 3e-24 (data not shown). We chose to compare only those reported in crustaceans. Together with this study, there have been 12 serine proteases or serine protease homologues found in shrimp, crabs, lobsters and crayfish. Table 4.1 summarizes species and details of the proteins used for comparison and for phylogenetic tree construction (Fig. 4.11). Interestingly, MasSPH, SPH516, and SPH509 from *P. monodon* are closer to a similar protein of the blue crab PPAF (53% identity) than to c-SPH (32% identity) of the black tiger shrimp that has been reported to be involved in cell adhesion (Lin et al., 2006) (Fig. 4.11, Table 4.1).

Table 4.1 Names and details of serine protease proteins from crustaceans.

Key to phylogenetic tree	Species	Proposed function	Identity to SPH516 (%)	No. of clip domains	Triad	Accession number
SPH516	*P. monodon*	Binding protein of YHV	100	1	HDG	DQ403191
SPH509	*P. monodon*	–	99	1	HDG	DQ916148
MasSPH	*P. monodon*	Immune-related protein	99	1	HDG	DQ455050
c-SPH	*P. monodon*	Cell adhesion	32	1	HDG	AY600627
White shrimp	*P. vannamei*	Serine protease	21	1 Pseudo-clip[a]	HDS	AY368151
Kuruma shrimp	*P. japonicus*	Immune-related protein	27	1	HDG	BAD34945
Lobster	*Panulirus argus*	Serine protease	18	1 Pseudo-clip[a]	HDS	AAK48894
Crayfish1	*Pacifastacus leniusculus*	PPAF	22	1	HDS	AJ007668
Crayfish2	*Pacifastacus leniusculus*	Cell adhesion	31	7	HDG	Y11145
Crayfish3	*Pacifastacus leniusculus*	Immune-related protein	33	1	HDG	AY861652
Blue crab	*Callinectes sapidus*	PPAF	53	1	HDG	AAS60227
Mud crab	*Scylla serrata*	Serine protease	19	1 Pseudo-clip[a]	HDS	AY946200

[a]There are four to five cysteine residues instead of six in the domain.

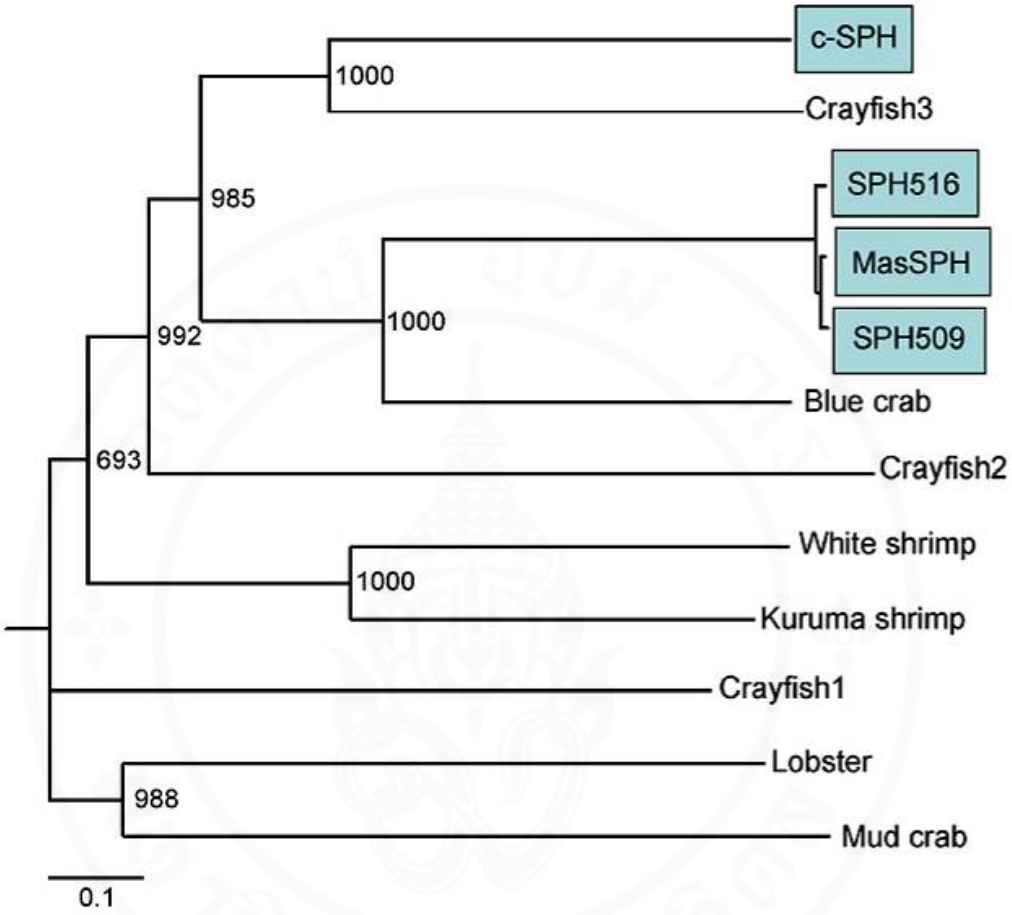

Figure 4.11 Phylogenetic tree showing the relationship amongst serine proteinase proteins reported from crustaceans. See Table 4.1 for keys to protein sequences from the GenBank database. The bootstrap values for 1,000 independent comparisons are added at each branch point. Serine protease and serine protease homologues from *P. monodon* are shaded.

4.2.7 SPHs are strongly expressed in hemocytes and gills

The distribution patterns of SPHs in different shrimp tissues were studied by RT-PCR and compared to the expression level of β-actin as a control. Of the nine tested tissues, SPH cDNAs were highly expressed in hemocytes and gills (Fig. 4.12). Weak but detectable signals were found in pleopods and the lymphoid organ. The amplicon from hemocytes was subjected to sequencing and found to have the same sequence as our SPH cDNAs. With the primers used, we expected to obtain all identified SPH isoforms.

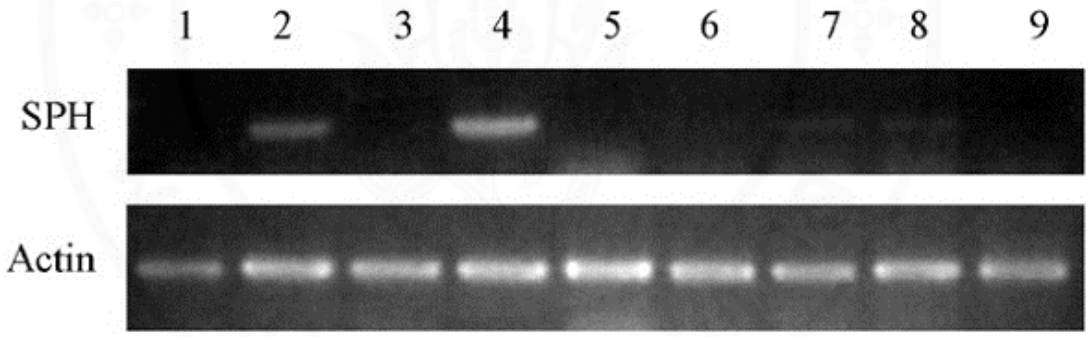

Figure 4.12 Expression of SPHs and β-actin in different shrimp tissues. Lanes 1, eye stalk; 2, gills; 3, heart; 4, hemocytes; 5, hepatopancreas; 6, intestine; 7, pleopod; 8, lymphoid; 9, muscle.

4.2.8 Time course analysis after YHV challenge

Using RT-PCR analyses of shrimp hemocytes from YHV-challenged shrimp to measure SPH516 expression during the course of viral infection, we found that the overall SPH expression generally declined during the course of disease development, except for a slight increase during the first 12 h.p.i. (Fig. 4.13). SPH expression was normalized with respect to β-actin expression with band intensity of SPH transcripts at 0 h set at 100%. Fig. 4.13a summarizes SPH expression profiles from three separate tests and Fig. 4.13b shows band intensities from one of the agarose gel results. As with the tissue expression tests described above, amplified products were likely to represent all reported SPH isoforms.

4.2.9 Tissue localization of SPHs

When total shrimp proteins from hemolymph, hemocytes, gills, and the heart were analyzed for tissue localization of SPH proteins by immunoblotting using anti-SPH516-C antibody, a positive immunoreaction occurred with a band of approximately 72 kDa from hemolymph and hemocytes, while only very faint reactions were detectable from gills and the heart (Fig. 4.14). The immunoreactive band was located at a position indicating higher molecular mass than that predicted from the deduced sequence of SPH516 (52.9 kDa), suggesting possible post-translational modifications of the native protein. Immunohistochemical results confirmed the western blot results (Fig. 4.15) in that strong positive immunoreactions occurred in the hemolymph located in arteries and sinuses surrounding all tissues but not in the tissues themselves. The immunoreaction of individual hemocytes was impossible to distinguish giving the overwhelming reaction of the hemolymph that surrounded them.

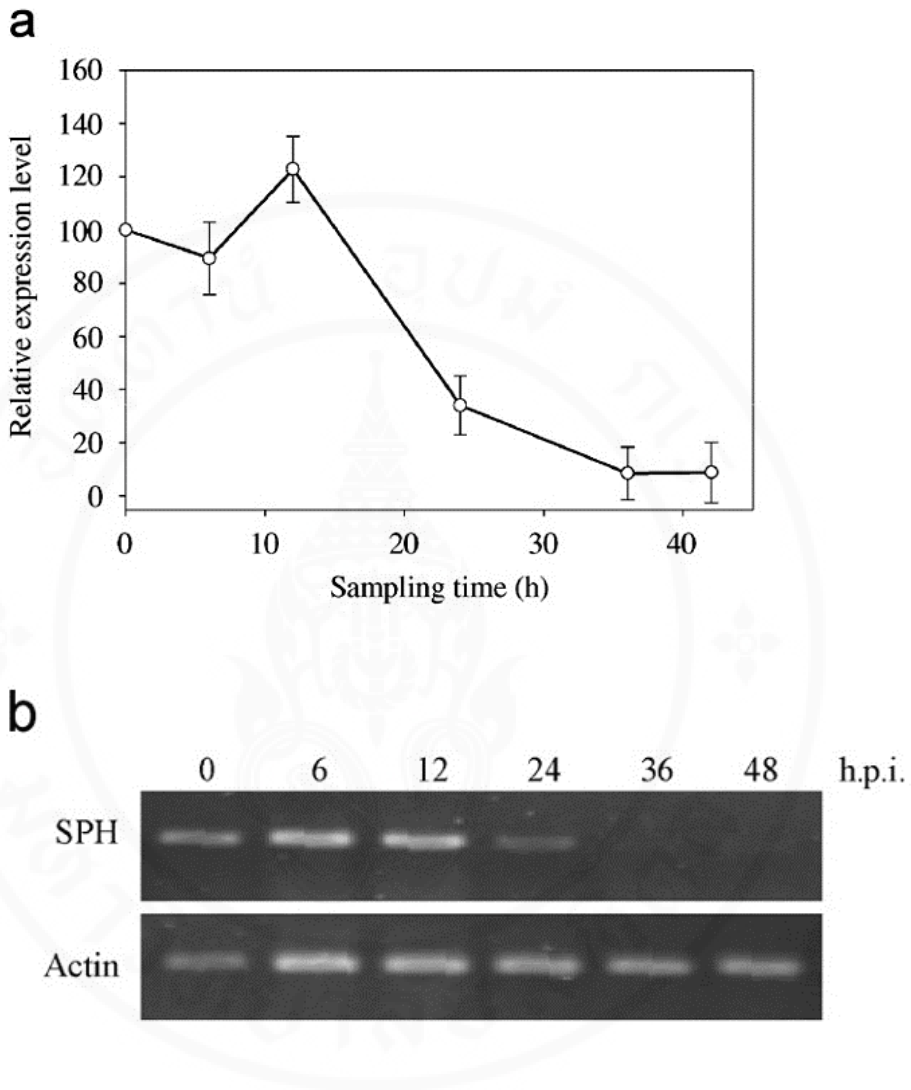

Figure 4.13 Time-course expression profiles of SPHs after YHV challenge. (a) The graph was calculated from expression of SPHs normalized with that of β-actin from three separate tests. (b) Agarose gels of RT-PCR amplicons for SPHs and β-actin at various times post challenge from one of the three experiments.

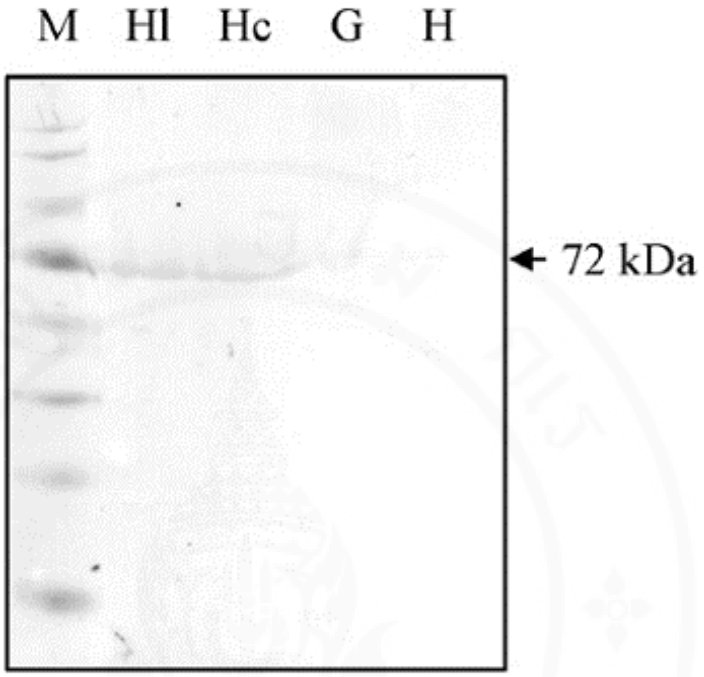

Figure 4.14 Detection of SPH proteins in shrimp tissues. Immunoblot of an SDS-polyacrylamide gel using anti-SPH516-C antibody. Lanes: M, prestained marker (Fermentas); Lane Hl = hemolymph; Lane Hc = hemocytes; Lane G = gills; Lane H = heart. The expected band (72 kDa) for SPH516 protein is indicated.

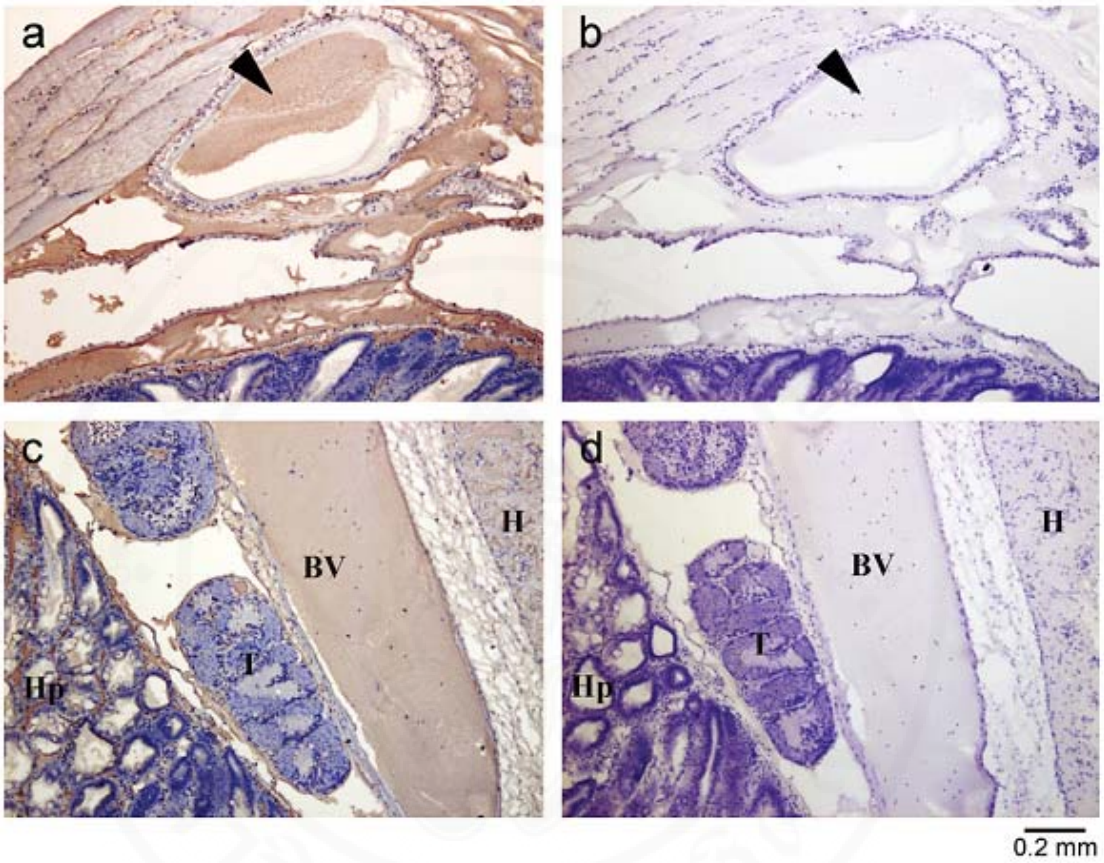

Figure 4.15 Immunohistochemistry for localization of SPH in shrimp tissue sections using anti-SPH516-C as the primary antibody. (a) Tissue section showing an artery containing immunopositive (brown) hemolymph (arrowhead) with muscle above, the hepatopancreas below, all bathed in immunopositive hemolymph. (b) Parallel tissue section processed as in (a) but without anti-SPH516-C antibody. (c) Tissue section showing an artery (BV), the heart (H), testis (T) and hepatopancreas (Hp) all with immunopositive (brown) hemolymph. (d) Parallel tissue section processed as in (c) but without anti-SPH516-C antibody. The scale bars at the bottom right applies to all of the photomicrographs.

4.3 TSV protein-protein interactions

4.3.1 Transmembrane domain analysis

As described in Chapter 3, 7 domains (BIR, Hel, Prot, Pol, VP1, VP2, and VP3) from ORF1 and ORF2 in the TSV genome (GenBank accession number **AF277675**) were subjected to protein-protein interaction study. However, yeast two-hybrid assay could be limited for transmembrane domain containing proteins since these proteins may not be imported to the nucleus where the two hybrid system occurred. Thus, to allow all possible interactions of TSV proteins, we first analyzed all deduced TSV proteins for the presence of transmembrane domains using InterPro software (http://www.ebi.ac.uk). The results showed that among the 7 TSV domains, Prot (221 amino acids in length) and VP1 (492 amino acids in length) were found to contain potential transmembrane domains residing in amino acid residues 15-35 and 103-121, respectively. Therefore Prot and VP1 were additionally expressed as sub-fragments that excluded the transmembrane region as C-terminal Prot (C-Prot; amino acid residues 36-221), N-terminal VP1 (N-VP1; amino acid residues 1-102), and C-terminal VP1 (C-VP1; amino acid residues 122-492) for use in the yeast two-hybrid assay.

4.3.2 Construction of TSV recombinant plasmids

Altogether 10 TSV domains including BIR, Hel, C-Prot, Prot, Pol, N-VP1, C-VP1, VP1, VP2, and VP3 were constructed in-frame with the BD domain and AD domain of pGBKT7 and pGADT7 vectors, respectively. The cloning step was begun by amplification of TSV fragments using the RT-PCR technique. TSV-infected shrimp RNA extracts were used as templates for amplification with specific primers listed in Table 3.1. The amplified products were then analyzed by agarose gel electrophoresis and the results showed successful amplification of all TSV genes with the expected sizes (Fig. 4.16). After restriction digestion and DNA ligation, each of TSV fragment inserted in pGBKT7 and pGADT7 vectors were verified to be correctly in-frame by nucleotide sequencing. The recombinant BD or AD constructs were then transformed into yeast strain Y187 or AH109 and spread onto SD/-Trp or SD/-Leu agar plates, respectively. To select the transformed yeast cells, yeast colony PCR using T7

promoter and 3'BD primers (for BD constructs) and T7 promoter and 3'AD primers (for AD constructs) was performed, respectively. An example of the PCR screening results is shown in Fig. 4.17. In summary from this phase, 10 baits and 10 prey of TSV were successfully generated to be investigated for protein-protein interactions.

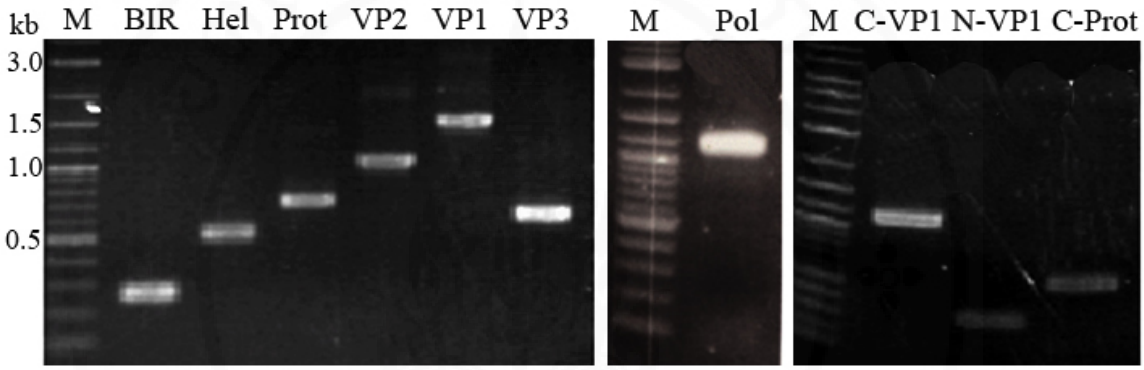

Region	Size (bp)
BIR	222
Hel	468
Prot	664
Prot-C	559
Pol	1,131
VP2	984
VP1	1,476
VP1-N	306
VP1-C	1,113
VP3	567

Figure 4.16 Amplification of 10 TSV domains. Each TSV fragment was amplified by RT-PCR reactions. The products were verified by 1.2% agarose gel electrophoresis. M; 2-log DNA ladder marker (New England Biolabs). Expected sizes of the TSV fragments are summarized in the table below the gel figures.

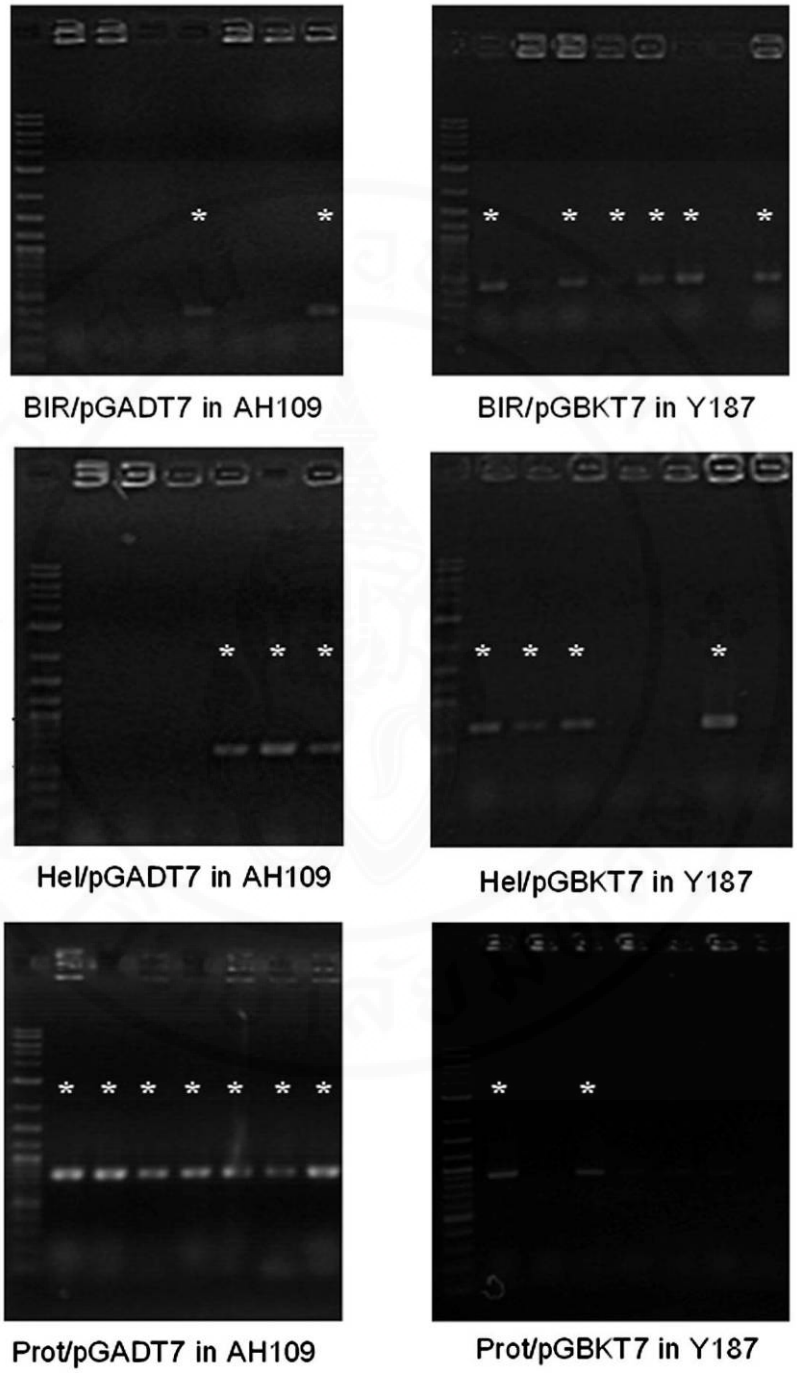

Figure 4.17 Example of yeast colony PCR of recombinant BIR, Hel and Prot constructs. Transformed yeast cells (7-8 colonies) containing indicated BD or AD constructs were individually subjected to PCR screening using vector primers. The products were analyzed by gel electrophoresis. Asterisks above each well represents the correct insert sizes for the TSV fragments.

4.3.3 Autoactivation test

Prior to TSV protein-protein interaction, autoactivation of each bait and prey was examined to exclude false-positive results. This was conducted by mating yeast Y187 bearing each bait with yeast AH109 carrying an empty pGADT7 vector. In addition, yeast AH109 bearing each prey was mated with yeast Y187 carrying an empty pGBKT7 vector. The diploid cells were selected on media SD/-Leu/-Trp. To observe any auto-activation of the reporter genes, *HIS3*, *ADE2* and *MEL1*, the diploids were transferred onto media SD/-Ade/-His/-Leu/-Trp containing of X-α-gal. Recombinant plasmids that yielded yeast colonies able to grow and turn blue were classified as autoactivated constructs. The result showed that only N-VP1 constructs both in pGBKT7 (bait) and in pGADT7 (prey) gave autoactivation (Fig. 4.18). Therefore N-VP1 constructs were excluded from the TSV protein-protein interaction study.

4.3.4 Identification of TSV protein-protein interactions

In this experiment, TSV protein-protein interactions were identified using yeast mating strategy that was conducted on solid YPD agar containing 10% glucose. After obtaining the diploids, they were tested for reporter gene expression on SD/-Ade/-His/-Leu/-Trp/X-α-gal plates. The interactions were independently tested twice since confidence and reliability of the protein interaction data was important. The reproduced results were scored as high confidence (H) results while the results with no reproducibility were referred to as low confidence (L) results (Uetz et al., 2000). The results shown in Fig. 4.19 represent one of the duplicated assays for TSV protein-protein interactions. Specifically, 5-6 individual diploid yeasts from each interaction pair were streaked on selective media and interaction results were scored from SD/-Ade/-His/-Leu/-Trp/X-α-gal plates. For TSV protein fragments lacking transmembrane domains (C-Prot, N-VP1 and C-VP1), the diploids obtained were transferred to selective media by replica plating. The results shown in Fig. 4.20 revealed no true positive interaction. Blue colonies (false positive results) were observed only for autoactivated N-VP1 constructs, confirming the results described above.

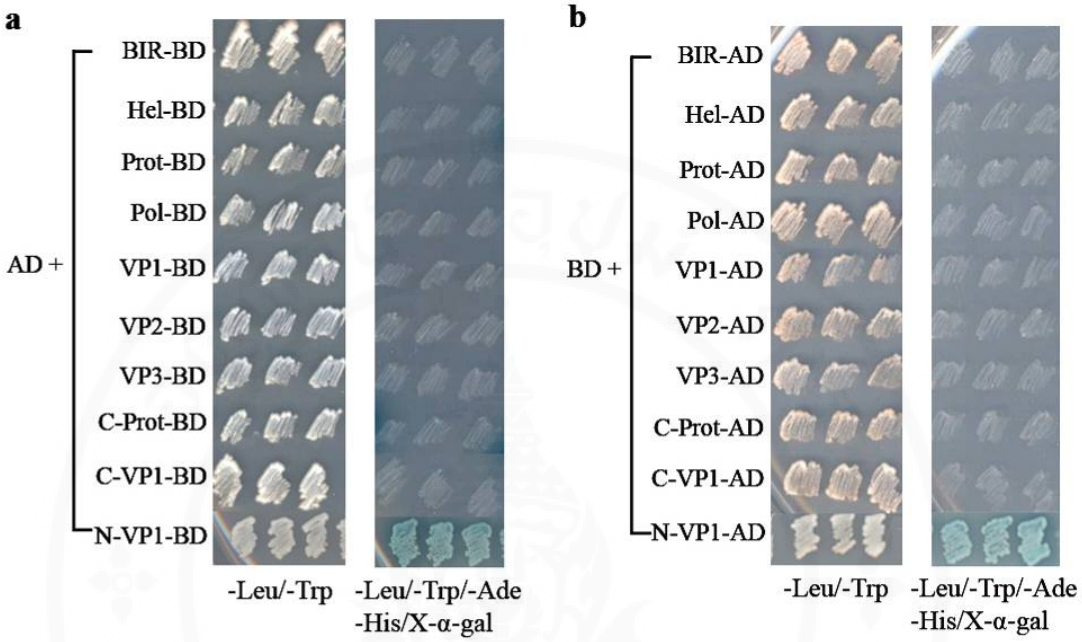

Figure 4.18 Autoactivation test. Each bait (**a**) and prey (**b**) was mated with yeasts carrying empty AD and BD plasmids, respectively. 3 individual diploids were investigated from each interaction pair. Autoactivation activity was indicated by growth and blue color change on the highly selective medium SD/-Leu/-Trp/-Ade/-His/X-α-gal.

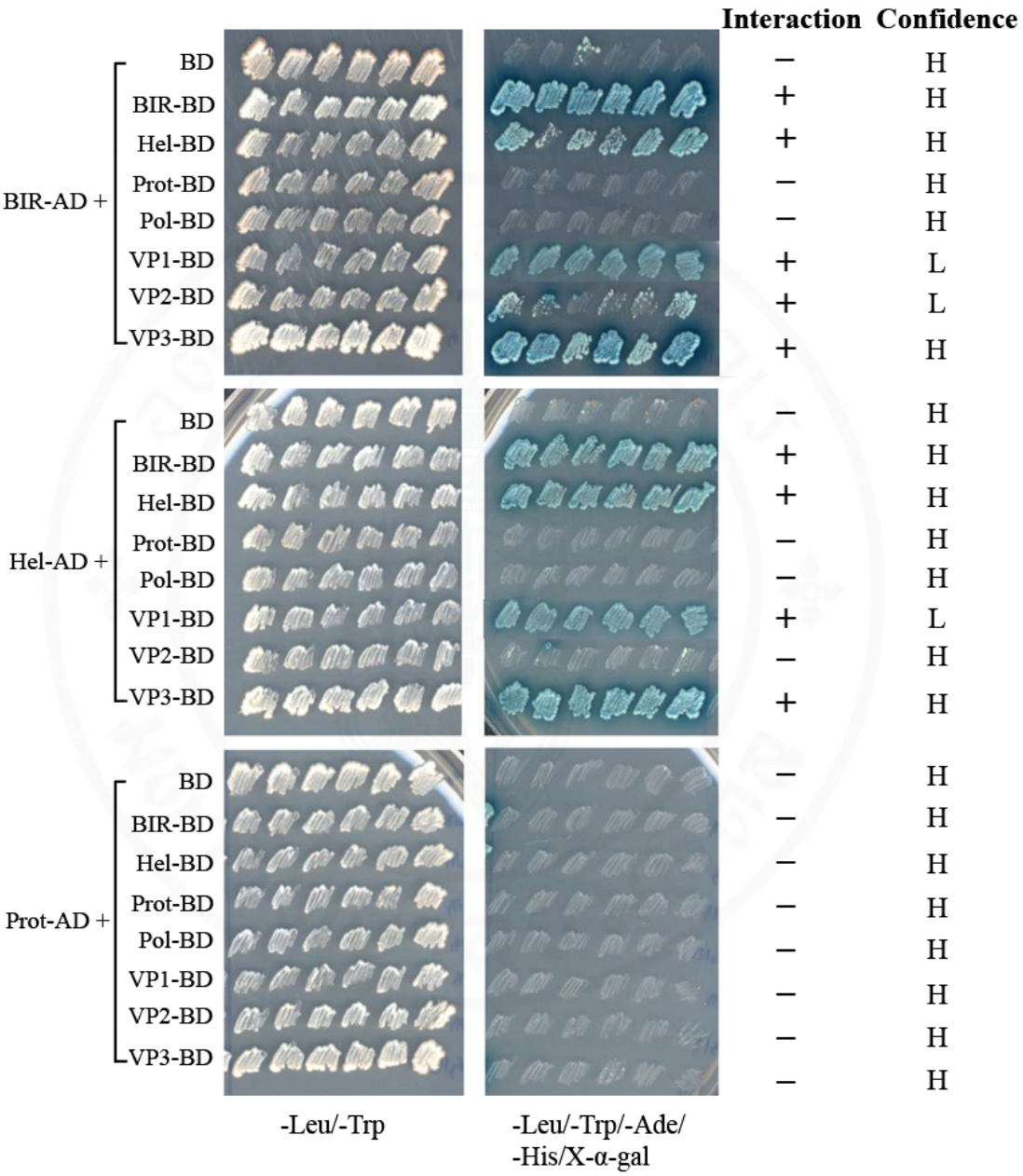

Figure 4.19 TSV protein-protein interaction study. TSV proteins fused with AD were investigated for their interacting proteins constructed in BD. Each protein pair tested was conducted by yeast mating and the resulting diploids (6 individual colonies) were then streaked on selective media. Growth and blue colonies on SD/-Leu/-Trp/-Ade/-His/X-α-gal implied positive interactions which are indicated by (+) while no interactions are indicated by (-). High confidence (H) and low confidence (L) interactions are also indicated.

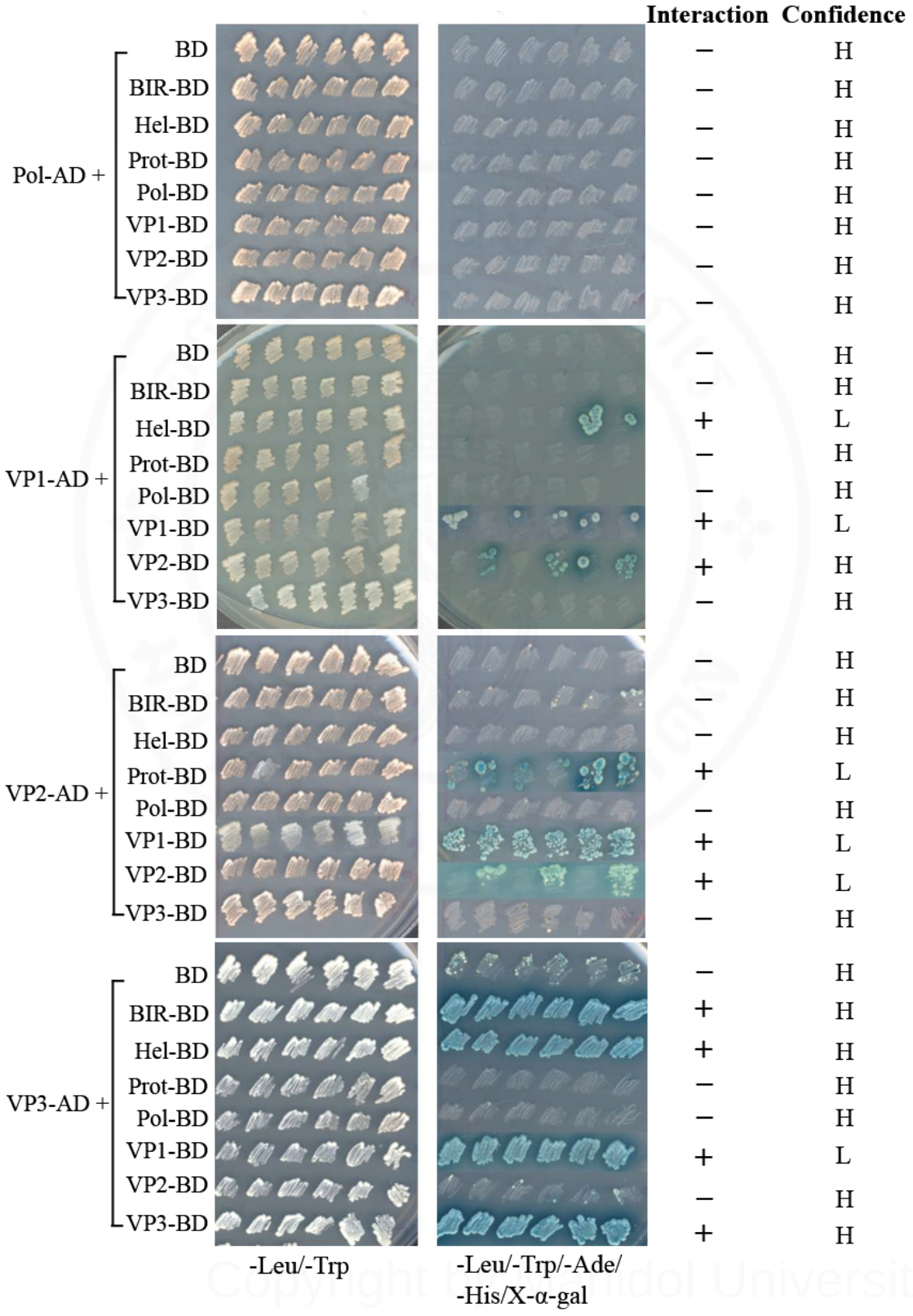

Figure 4.19 TSV protein-protein interaction study (cont.).

Figure 4.20 Interaction studies of TSV proteins lacking transmembrane domains. (**a**) C-Prot, N-VP1 and C-VP1 fused with AD were mated with all TSV proteins constructed in BD. Diploid cells obtained on YPD plate containing 10% glucose were transferred to selective medium SD/-Leu/-Trp/ and SD/-Leu/-Trp/-Ade/-His/X-α-gal by the plate replication technique. Interactions are indicated by growth and blue color change on the latter plate. (**b**) C-Prot, N-VP1 and C-VP1 fused with BD were mated with all TSV proteins constructed in AD. Interaction results are indicated in the same manner as above. Empty vector pGBKT7 (BD) and pGADT7 (AD) were included as negative controls.

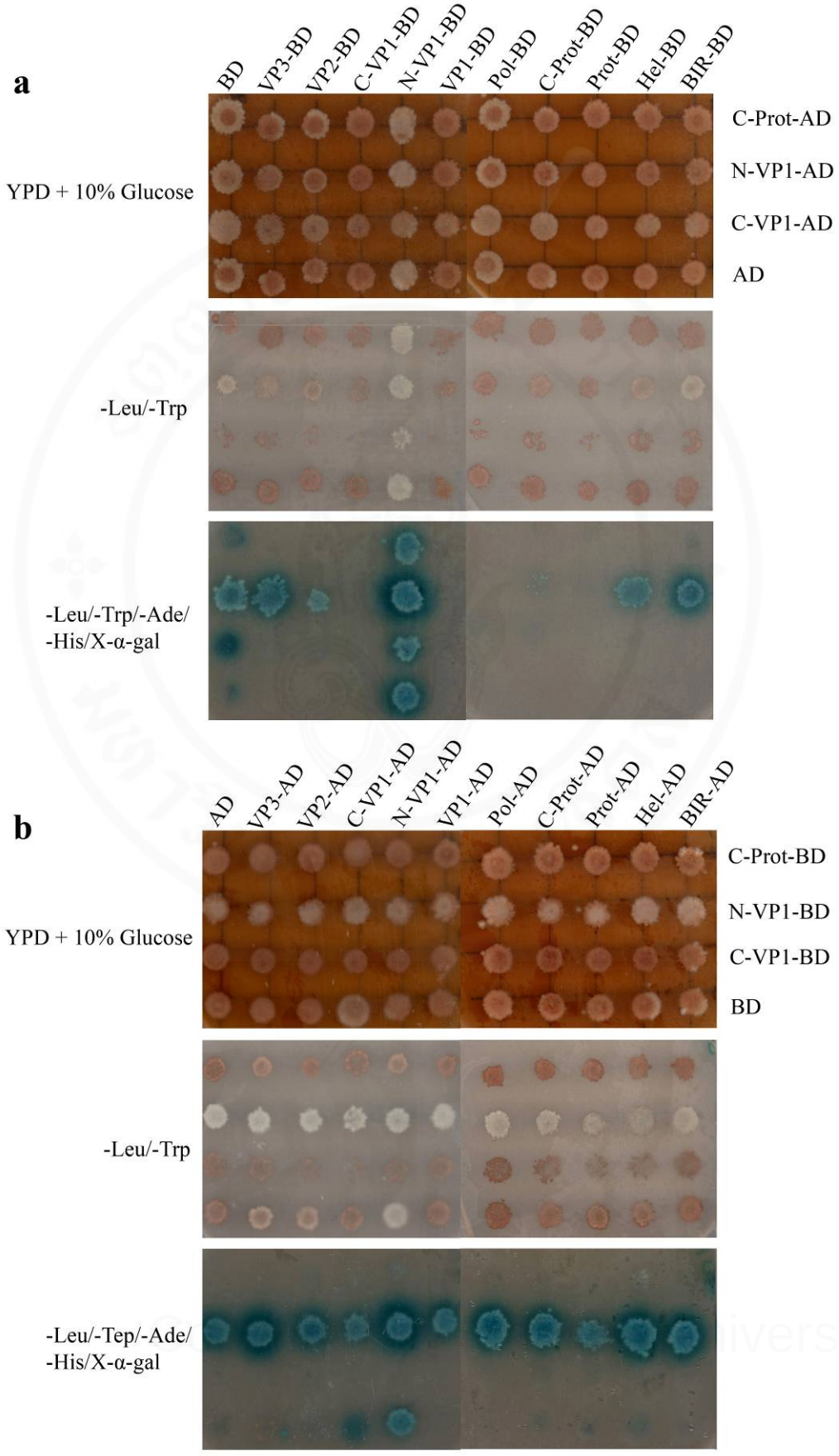
a
BD
VP3-BD
VP2-BD
C-VP1-BD
N-VP1-BD
VP1-BD
Pol-BD
C-Prot-BD
Prot-BD
Hel-BD
BIR-BD
YPD + 10% Glucose
C-Prot-AD
N-VP1-AD
C-VP1-AD
AD
-Leu/-Trp
-Leu/-Trp/-Ade/
-His/X-α-gal
b
AD
VP3-AD
VP2-AD
C-VP1-AD
N-VP1-AD
VP1-AD
Pol-AD
C-Prot-AD
Prot-AD
Hel-AD
BIR-AD
YPD + 10% Glucose
C-Prot-BD
N-VP1-BD
C-VP1-BD
BD
-Leu/-Trp
-Leu/-Tep/-Ade/
-His/X-α-gal

In summary, excluding autoactivated N-VP1, there were 19 positive interactions from the total of 81 interaction pairs (9 BD constructs x 9 AD constructs). There were 10 high confidence interactions and 9 low confidence interactions. The results are summarized in a matrix interaction format in Table 4.2. Previous studies of viral protein interactions have described the ratio between total number of interactions and tested viral ORFs. In this study, the number of baits employed in this study was used in stead of the number of ORFs. Therefore, the ratio of interactions to the total number of examined domains of TSV was calculated as 2.1 (19/9). Our TSV interaction results are compared to those for interactions of proteins from other viruses (Table 4.3).

4.3.5 Building of a TSV protein-protein interaction map

Cytoscape open source software that is used for visualizing networks (Shannon et al., 2003; Cline et al., 2007) was employed to build the TSV protein-protein interaction (PPI) map. In this map, 14 distinct viral protein interactions (subtracting 5 interactions from the reciprocal interaction results) were identified from the yeast two-hybrid assays and these were set as input for the Cytoscape program. TSV proteins are referred to as nodes and the protein interactions as edges. The map illustrated in Fig. 4.21 revealed a total number of 6 proteins (nodes) involved in 14 interactions (edges) in the TSV PPI network. Except for Prot, all of the TSV nodes have self interaction (i.e. binding to themselves). The TSV PPI map showed that BIR and VP1 had the highest number of interactions (5 interactions). The work clearly revealed that high confidence interaction results were obtained for the 3 proteins BIR, Hel and VP3 (Fig. 4.21). Therefore, these proteins and their binding partners were selected for further study of their complex protein interactions by *in vitro* pull-down assay (see below).

Table 4.2 Summary of TSV protein-protein interaction in matrix format

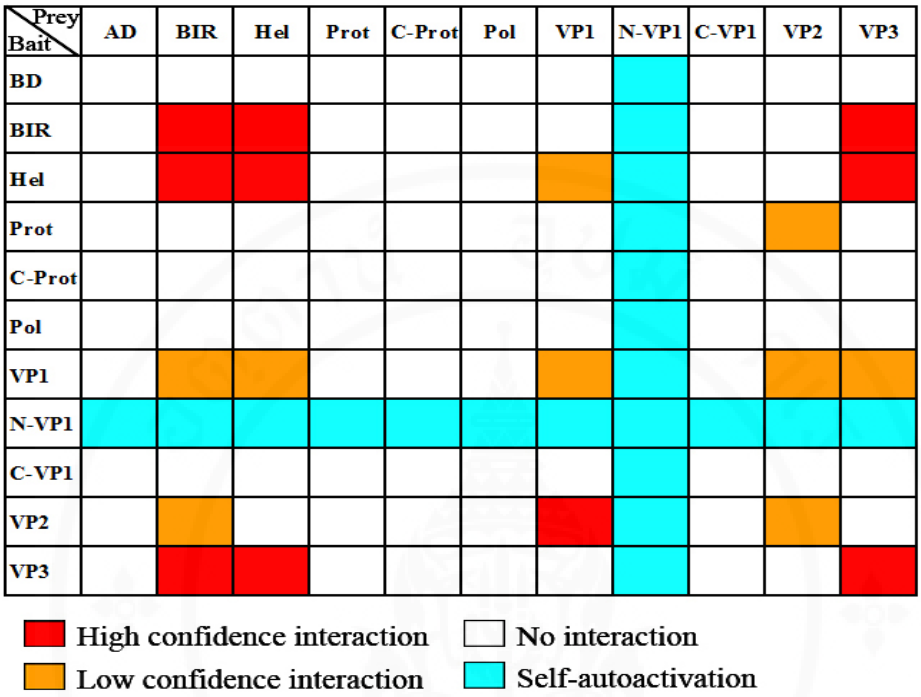

Table 4.3 Comparison of the protein interaction ratio of TSV to those published for other viruses.

Virus	ORF or Bait	Interactions	Interaction/Bait	Reference
Hepatitis C virus (HCV)	10	5	0.50	Flajolet et al., 2000
Vaccinia virus	266	37	0.14	McCraith et al., 2000
T7 bacteriophage	55	25	0.45	Bartel et al., 1996
Kaposi-sarcoma-associated virus (KSHV)	89	123	1.38	Uetz et al., 2006
Varicella-zoster virus (VZV)	69	173	2.50	Uetz et al., 2006
Epstein-Barr virus (EBV)	85	43	0.50	Calderwood et al., 2007
White spot syndrom viru (WSSV)	143	710	4.97	Sangsuriya et al., 2014
TSV	9	19	2.1	This study

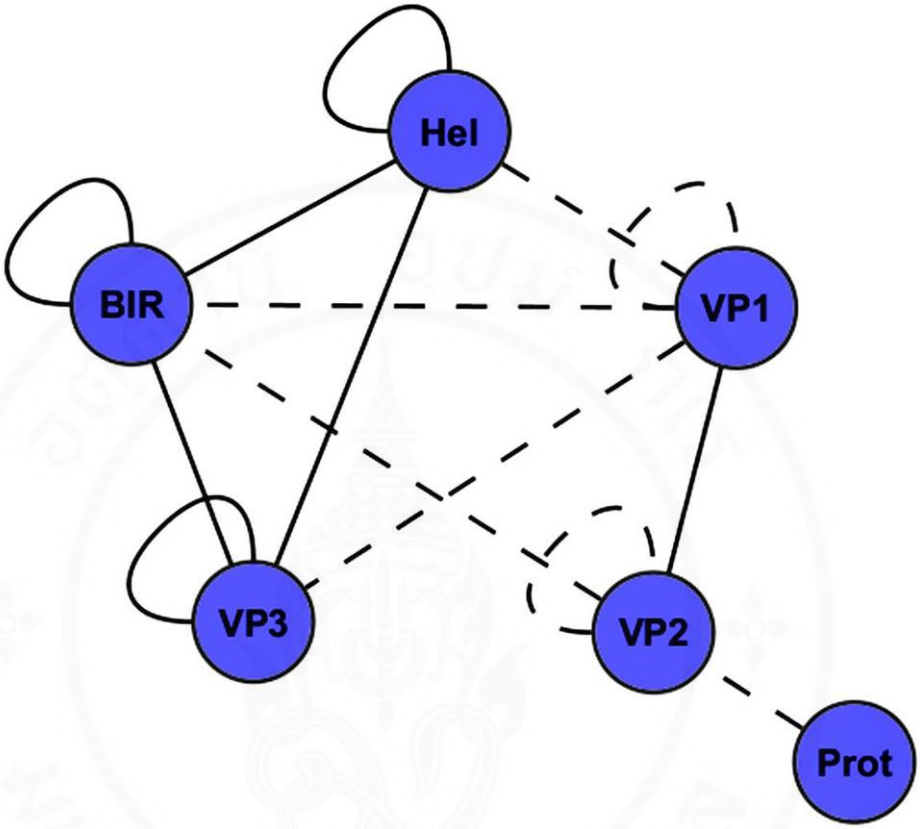

Figure 4.21 TSV protein-protein interaction map. The interaction map for 6 TSV proteins was created using Cytoscape program. TSV proteins are shown as nodes and interactions are shown as edges. High and low confidence interactions were displayed by solid and dash lines, respectively. Loops indicated self-interaction (self-binding).

4.3.6 *In vitro* pull-down assay confirmed TSV protein-protein interactions

The coding regions of *VP1*, *VP2, VP3, BIR* and *Hel* were amplified with specific primers (Table 3.1). *VP1* gene was cloned into pGEX-4T-1 while the rest were cloned into pET-15b plasmid. The resulting recombinant plasmids were transformed into *E.coli* BL21 to express GST tagged VP1 protein (VP1-GST) and His tagged proteins including VP2-His, VP3-His, BIR-His and Hel-His. After induction with IPTG, the bacterial lysates were subjected to SDS-PAGE and immunoblot assay with detection using respective anti-GST or anti-His antibodies. All TSV fusion proteins were successfully expressed in the bacterial system with the expected sizes as shown in Fig.4.22.

In vitro pull-down was conducted using glutathione sepharose beads (GE Healthcare). The bacterial lysate containing VP1-GST was incubated with glutathione sepharose beads and then the beads were washed several times to remove unbound proteins. The resulting VP1-GST pre-coupled with glutathione sepharose beads was then employed for protein complex interaction assays. There were 4 protein mixtures for the interaction assays; 1) VP1 + VP2 + VP3, 2) VP1 + VP2 + VP3 + BIR + Hel, 3) VP1 + VP2 + VP3 + BIR, and 4) VP1 + VP2 + VP3 + Hel. The crude lysate proteins as indicated were incubated with the VP1-GST pre-coupled beads. The presence of protein mixtures in each condition was demonstrated by immunoblot assay with detection using anti-His antibody (Fig. 4.23, loading mixture panel). After washing steps, eluate from each binding assay was subjected to SDS-PAGE and immunoblot detection using the anti-His antibody. Fig. 4.23, lane 1 shows that VP1 could pull-down only VP2 but not VP3. In lane 2, for the protein mixture acontaining mong VP1, VP2, VP3, Hel and BIR it can be seen that only VP2 and Hel were pulled-down together by VP1. In lane 3, only VP2 (not VP3 or BIR) was pulled-down by VP1. In lane 4, VP2, VP3, and Hel were pulled-down by VP1. These results suggested that the structural proteins alone (VP1, VP2 and VP3) could not form a complex by themselves (lane 1). However, in the presence of Hel, the structural protein complex could be formed (lane 4). However, that was not the case for BIR (lane 3) indicating that BIR did not help recruit structural proteins to form a complex. Extrapolation from the yeast two-hybrid assays that showed interaction between BIR and VP3 with high

confidence, suggested (lane 3) that BIR and VP3 bound together leaving VP2 to be pulled-down with VP1. Indeed, in lane 2 (mixture of VP1, VP2, VP3, BIR, and Hel), BIR and VP3 were not found in the complex of VP1-VP2-Hel. Taken together, the results suggested that formation of a structural protein complex containing VP1-VP2-VP3 required Hel but not BIR. In summary, all protein interactions investigated by *in vitro* pull-down assay coincided with the results derived from yeast two-hybrid assay.

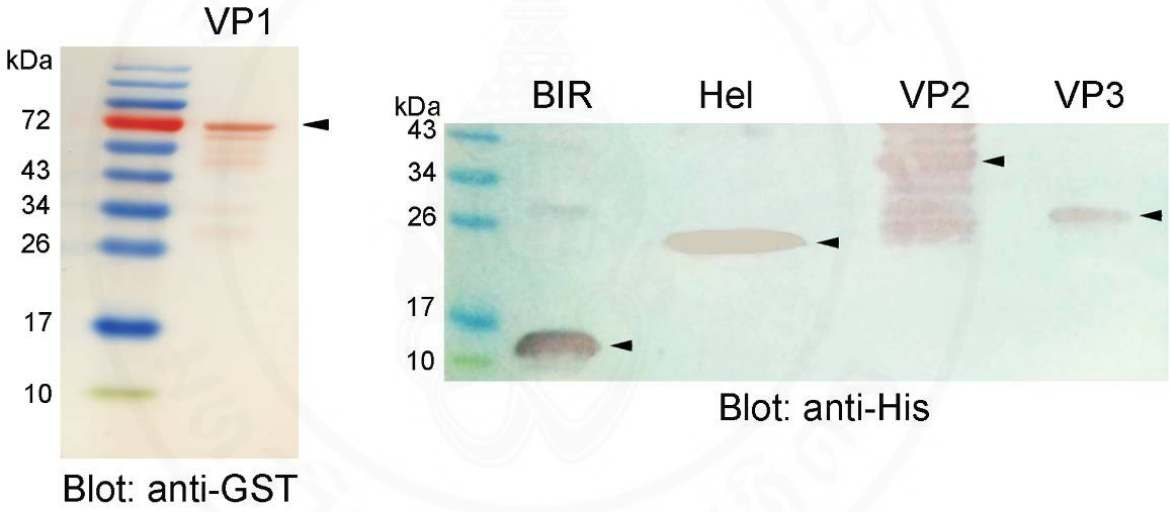

Figure 4.22 Expression of recombinant TSV proteins. TSV fusion proteins were expressed in the bacterial system. Western immunoblots detected by anti-GST or anti-His antibody revealed all the TSV proteins of expected sizes (marked by arrow heads); VP1 (~ 78 kDa), BIR (~ 9 kDa), Hel (~18 kDa), VP2 (36 kDa) and VP3 (21 kDa).

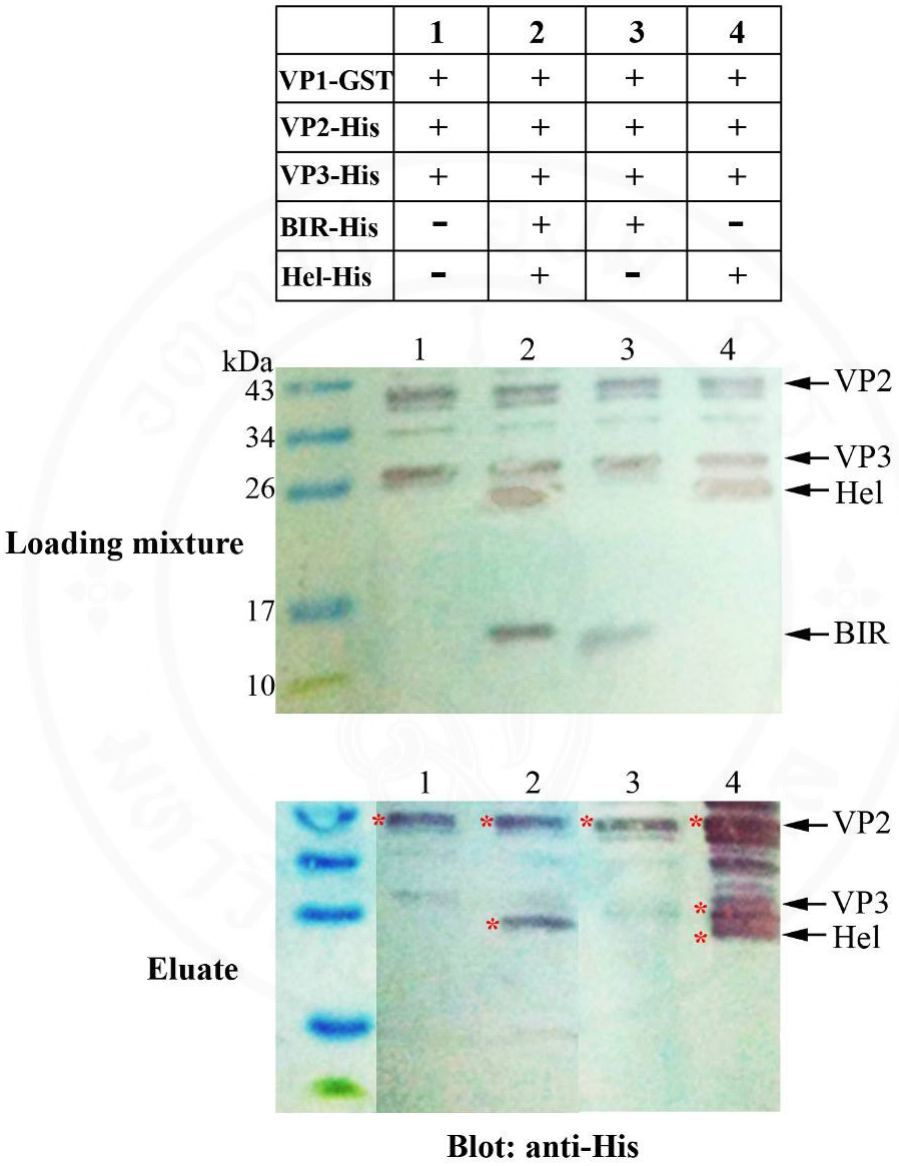

Figure 4.23 *In vitro* pull-down assays. VP1-GST was coupled with glutathione sepharose beads and then incubated with His-tagged TSV proteins as indicated in lanes 1-4. The loading mixture panel shows the input of His-tagged TSV proteins in the reactions. After washing steps, the pulled-down proteins marked by red asterisks were detected by anti-His antibody in the eluate panel.

4.4 Identification and characterization of *PmAmidase*

4.4.1 Cloning and sequence analysis of *PmAmidase*

The study of TSV protein interaction indicated that Hel was important for structural protein interaction (Fig. 4.23, lane 4) and that the presence of BIR may disturb the protein complex (Fig. 4.23, lanes 2, 3). We therefore hypothesized that TSV might exclude BIR from its protein complex by using host factors in order to accomplish the viral assembly process. To further investigate the relationship between host and TSV, BIR was then selected in a search for possible shrimp interacting proteins using the yeast mating strategy. The screen was performed by mating the pre-transformed BIR-BD Y187 strain with AH109 strain harboring the *P. monodon* hemocyte cDNA library (Tonganunt, et al 2005). Among approximately $2.5x10^5$ diploid colonies generated, four different clones that grew and turned blue on the SD/-Leu/-Trp/-Ade/-His/X-α-gal plates were subsequently identified. Sequencing and comparison of deduced amino acid sequences of these clones using BLASTP revealed that 3 of the sequences were unknown genes while 1 matched the previously reported protein sequence of fatty-acid amide hydrolase 2-like proteins from various organisms (data not shown). The in-frame sequence contained a partial amidase domain (pfam01425), for which the clone was named as Amidase-P (i.e. P for partial).

Subsequently 5'RACE amplification was performed to obtain a 5' end fragment of the Amidase sequence while bioinformatics analysis was conducted to search for the 3'end sequence. The 5'RACE using specific primers (Table 3.1) yielded a fragment of ~1.2 kb whereas a BLAST search tool using Amidase-P sequence against the *P.monodon* EST database hit one overlapping sequence of 720 bp (clone HC-N-N01-3827-LF-rev). The assembled sequence appeared to cover the complete *Amidase* sequence of *P. monodon*. Primers were then designed (Table 3.1) and used to amplify the full-length sequence of *PmAmidase* from shrimp gill RNA. As shown in Fig. 4.24, the full-length *Amidase* cDNA sequence of 1,961 bp included 167 nucleotides of 5'-UTR, a 1,602-nucleotide ORF, and a 192-nucleotide 3'-UTR. The entire *PmAmidase* ORF encoded a putative protein of 533 deduced amino acids with a theoretical molecular weight of 58.5 kDa and an isoelectric point 8.76. BLASTP and InterPro analysis revealed that it contained the amidase superfamily domain of 442

amino acids (residues 63 to 504) and a potential signal peptide at amino acid residues 1-32 (Fig. 4.24). BLASTP analysis of the PmAmidase deduced protein sequence against the GenBank database revealed that PmAmidase had significant similarity to proteins annotated as fatty-acid amide hydrolase 2, amidase and amidotransferase of various animals with E-values ranging from 1e-116 to 9e-116 (data not shown). To evaluate the evolutionary relationships of PmAmidase, ClustalW alignment and phenogram construction were to compare PmAmidase with homologues from 17 distinct genera including mammals (*Pan troglodytes*, GenBank accession number **XP_003317540**; *Homo sapiens*, GenBank accession number **NP_777572**; *Monodelphis domestica*, GenBank accession number **XP_001375446**), avians (*Taeniopygia guttata*, GenBank accession number **XP_002194510**), reptiles (*Anolis carolinensis*, GenBank accession number **XP_003227851**), fish (*Danio rerio*, GenBank accession number **NP_001002700**), amphibians (*Xenopus* (*Silurana*) *tropicalis*, GenBank accession number **XP_002940451**), a nematode (*Caenorhabditis briggsae*, GenBank accession number **XP_002631704**) and insects (*Apis mellifera*, GenBank accession number **XP_392277**; *Nasonia vitripennis*, GenBank accession number **XP_001601890**; *Drosophila melanogaster*, GenBank accession number **NP_610764**; *Anopheles gambiae*, GenBank accession number **XP_309335**; *Aedes aegypti*, GenBank accession number **XP_001650937**; *Tribolium castaneum*, GenBank accession number **XP_967443**; *Acyrthosiphon pisum*, GenBank accession number **XP_001946922**; *Pediculus humanus corporis*, GenBank accession number **XP_002424410**). A phylogenetic tree was generated by MEGA software (Tamura et al., 2007) using the Neighbor-Joining method is shown in Fig. 4.25. PmAmidase grouped in a clade of proteins from insects and was linked most closely to proteins from *T. castaneum* (red flour beetle), *A. pisum* (pea aphid) and *P. humanus corporis* (human louse).

The full-length sequence of *PmAmidase* was subsequently inserted into the yeast two-hybrid vectors, pGBKT7 and pGADT7, for protein interaction assays with BIR and other TSV proteins (described below).

4.4.2 Identification of protein interaction between PmAmidase and TSV proteins

To investigate whether full-length PmAmidase interacted with the BIR domain or other TSV domains, yeast two-hybrid assays were carried out via co-transformation. PmAmidase in AD and BD plasmids were designated Ami-AD and Ami-BD, respectively. All 7 domains of TSV (BIR, Hel, Prot, Pol, VP2, VP1 and VP3) were also constructed in AD and BD plasmids as previously described. Pairwise interactions between AD and BD constructs were investigated using yeast AH109 strain. Interaction between BIR-BD and Ami-P-AD (first identified from the yeast two-hybrid screen) was used as a positive control while Amidase-AD with empty plasmid BD and Amidase-BD with empty plasmid BD were used as negative controls. Growth of six individual colonies from each combination pair were observed on SD/-Leu/-Trp and SD/-Leu/-Trp/-Ade/-His/X-α-gal. The results (Fig. 4.25) revealed that the full-length Amidase did not interact with any of the TSV proteins, and this contrasted with the previous result that a partial amidase sequence (Ami-P) could interact with the BIR domain.

Figure 4.24 Sequence analysis of *PmAmidase*. The *PmAmidase* ORF consisted of 1,602 bp encoding 533 deduced amino acid residues. The nucleotide sequence originally identified from the yeast two-hybrid screen is shown as italics while the sequence identified from *P. monodon* EST database is double underlined. The solid and dash arrows represent primers and nested primers, respectively, used in te 5'RACE assay. A potential signal peptide is highlighted in grey. The bold capital letters in the sequence indicate the Amidase superfamily domain.

```
                gaaaagtgtccacggagacgcggagggagagagacgggctagtgaag
tctctgtggactgtgacctgttttgtcccttgaggtgggcggggctatcagctggcgtga
cgcgagaagccctgaaagtattgtcatctgagtgaggggcagagtgaccacctgttagcc
atggttctgagcgctacactaacattcctccgaggagtgtacaagttggcagtgcgggcg
 M  V  L  S  A  T  L  T  F  L  R  G  V  Y  K  L  A  V  R  A   20
ttttatgggcgctgtggtcgttcaggtcgcccgcccgcccactgcgcccagtcacagac
 F  L  W  A  L  W  S  F  R  S  P  A  R  P  L  R  P  V  T  D   40
ccggtgttggtgcagcccgcccacgtgctcgcagaatggattcggaggggggaaggtgacg
 P  V  L  V  Q  P  A  H  V  L  A  E  W  I  R  R  G  K  V  T   60
tcctacgccgtcgtggaggcctacatcgaccgcatcggcgtcgtgaaccccgtcctcaac
 S  Y  A  V  V  E  A  Y  I  D  R  I  G  V  V  N  P  V  L  N   80
gccgtggtggacgaccgcttccgacaggcgctgacggaggcccgggaggtggaccgcgtc
 A  V  V  D  D  R  F  R  Q  A  L  T  E  A  R  E  V  D  R  V  100
ctcgcctccagctcgccggaggagaaggagcgcctcgtcgcctccaagccgttcttgggc
 L  A  S  S  S  P  E  E  K  E  R  L  V  A  S  K  P  F  L  G  120
gtgccgttcacgacgaaggagaacgtgcgggtgaagggtctaagtcacacgggcggatta
 V  P  F  T  T  K  E  N  V  R  V  K  G  L  S  H  T  G  G  L  140
gtcgcgcggatcggaaggcgagcgaaggaagatgcagttgtggtcacgttgatgaaggat
 V  A  R  I  G  R  R  A  K  E  D  A  V  V  V  T  L  M  K  D  160
gcaggcgccataccttgtgcgtgtcgaacgtccccgagctgggcatctggtgggagacg
 A  G  A  I  P  L  C  V  S  N  V  P  E  L  G  I  W  W  E  T  180
gcgaatcaagtctacggcaggacctccagcgctcacgatatctccaggacgccgggagga
 A  N  Q  V  Y  G  R  T  S  S  A  H  D  I  S  R  T  P  G  G  200
tcctctgggggcgaggcggcactgctggcgagttgcgggtcacccctgagcatcgggacg
 S  S  G  G  E  A  A  L  L  A  S  C  G  S  P  L  S  I  G  T  220
gacgtgggaggctccatcagggttcccgcttattgctctggggtttacgggcataaaccc
 D  V  G  G  S  I  R  V  P  A  Y  C  S  G  V  Y  G  H  K  P  240
acgtctggatgggtatccttagaaggcgccggtctttataccgagaagctgaagaaagga
 T  S  G  W  V  S  L  E  G  A  G  L  Y  T  E  K  L  K  K  G  260
ggagtacttgtggcaggccctcttggacgctgcgtgaaggacctcatcctcgcactgcaa
 G  V  L  V  A  G  P  L  G  R  C  V  K  D  L  I  L  A  L  Q  280
gtcctggcgccacaggatgcaacaggactccaagataagatagagaaaacggaactctcc
 V  L  A  P  Q  D  A  T  G  L  Q  D  K  I  E  K  T  E  L  S  300
aagaccaaagtgtggtgggcggaggaactagggtctcccctgtactcctccgtggatttc
 K  T  K  V  W  W  A  E  E  L  G  S  P  L  Y  S  S  V  D  F  320
cggttacgtaaccttctccacagggttctgcatttccttgatcactccaacgctgcttac
 R  L  R  N  L  L  H  R  V  L  H  F  L  D  H  S  N  A  A  Y  340
gtcgccaagtggcccgtcgatatgagcgcagcataccagatctggaataacaaaatggca
 V  A  K  W  P  V  D  M  S  A  A  Y  Q  I  W  N  N  K  M  A  360
gacgattacagcggcgaacctagcctgacttgtgacatggcggacagaaaggggagatt
 D  D  Y  S  G  E  P  S  L  T  C  D  M  A  D  R  K  G  E  I  380
aacctggcgtgggagtggatgctgtggctggtgggtcgcggccgccacactttcccacc
 N  L  A  W  E  W  M  L  W  L  V  G  R  G  R  H  T  F  P  T  400
ctcttccaggccgtcctccacaaggtttcggggcagaagaagaagcctgaaacttctccc
 L  F  Q  A  V  L  H  K  V  S  G  Q  K  K  K  P  E  T  S  P  420
ttttactggaagactcaccaagagaagttcaaggaggtaatggggaatgacggtgtgttg
 F  Y  W  K  T  H  Q  E  K  F  K  E  V  M  G  N  D  G  V  L  440
atcatgcctgtcctgcctatcgtgtccccttaccacaacgagccgattctcaaccccttc
 I  M  P  V  L  P  I  V  S  P  Y  H  N  E  P  I  L  N  P  F  460
gattactgctactccggaatgttcaacgccatcgagtttccaagtacggctgtgacgctt
 D  Y  C  Y  S  G  M  F  N  A  I  E  F  P  S  T  A  V  T  L  480
ggccagacgagtgatggttgtcccataggcctacagattgtaactacaccagggaacgat
 G  Q  T  S  D  G  C  P  I  G  L  Q  I  V  T  T  P  G  N  D  500
cacttaagtttagcagtggctacggtttctcgagagaaagtttggtggttgggtcccccct
 H  L  S  L  A  V  A  T  V  L  E  R  K  F  G  G  W  V  P  P  520
tttgaactacaattcccgtcttcttccaagaaggattcatagaaaatgctccggtttatt
 F  E  L  Q  F  P  S  S  S  K  K  D  S  -                    533
aaattttctggagtaactttattaatttatatggaggtgatattttgattcatagaaaat
gttccgaaagatcagtgttgtggagggacttaattaacttatatggaaatgatttttttt
ccattcgaatatatactttgttttatatatgttgagcaagaacatatttcatat
```

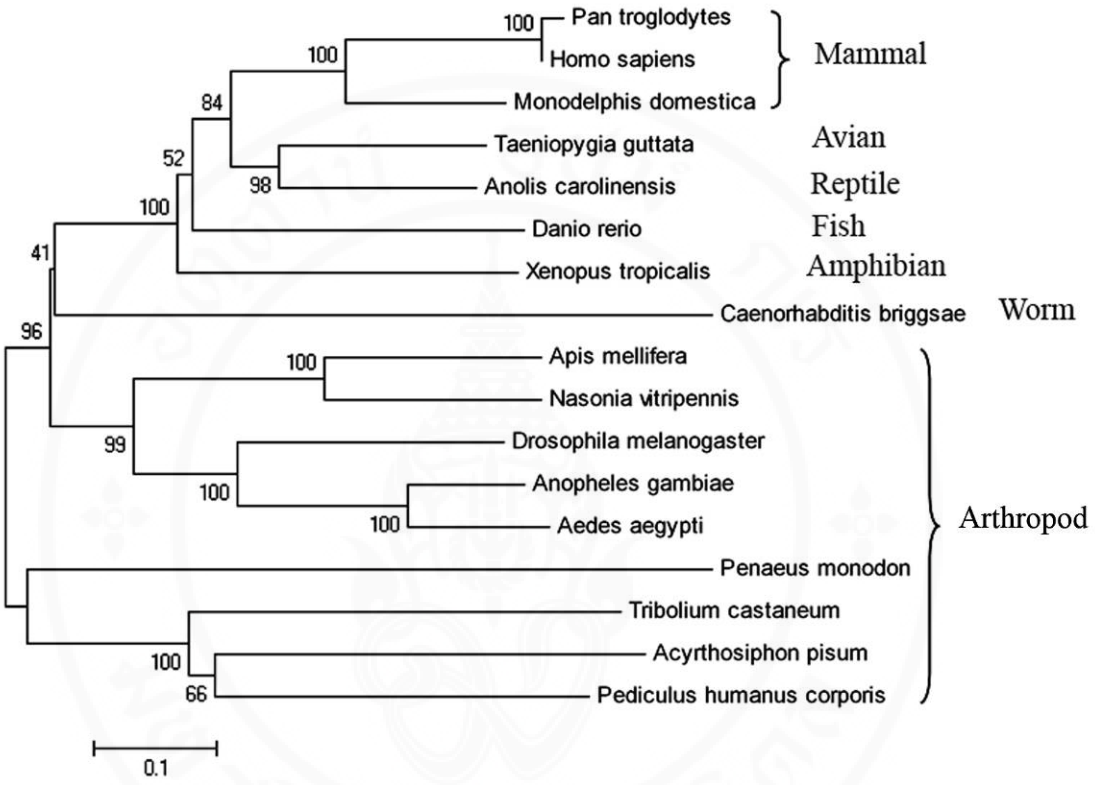

Figure 4.25 Phylogenetic relationships among amidase amino acid sequences from various species demonstrated by a neighbor-joining method. Percentage bootstrap values (1000 replicates) are shown at each branch point

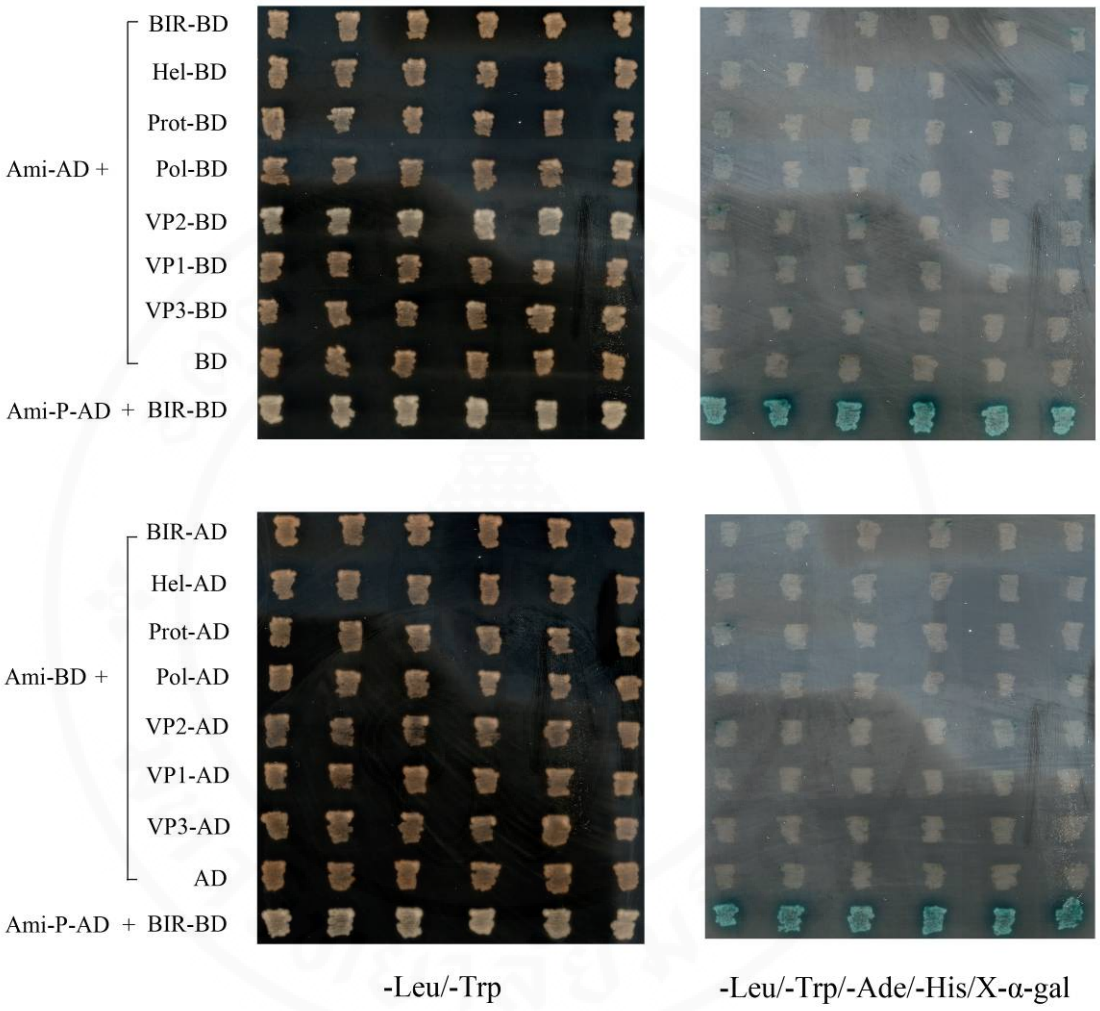

Figure 4.26 Interaction study between PmAmidase and TSV proteins by yeast two-hybrid assay. The upper panel shows yeast cells from co-transformation between a full-length *PmAmidase* fused with AD (Ami-AD) and TSV proteins fused with BD. The lower panel shows co-transformation using plasmid switching constructs.
Yeast containing Ami-P-AD and TSV BIR-BD served as the positive control whereas yeast harboring a full-length Amidase and respective empty plasmids served as the negative control.

CHAPTER V
DISCUSSION

5.1 General comments

Viruses are a major cause of production losses to the global shrimp culture industry. Despite this, little is known about viral-host interactions in shrimp due in part to the lack of continuous shrimp cell lines. Initial work in this thesis focused on two novel proteins identified by yeast two-hybrid screens for study interactions between proteins from yellow head virus (YHV) and proteins from a cDNA library of the black tiger shrimp *Penaeus monodon*. Several domains of YHV were used as baits and subsequently the yeast two-hybrid screens identified two positive preys both binding to MIB (the metal ion binding) domain of the virus. Full-length identification of the two preys revealed novel *P. monodon* cDNA sequences coding for putative leucine-rich repeat (LRR) protein and a serine protease homolog (SPH516). Investigation was then conducted to explain the involvement of SPH516 in the defense mechanisms of *P. monodon* by determining the tissue distribution, tissue localization, and transcription expression upon viral challenges and the results are discussed in section 5.3 below. However, identification of the full-length LRR revealed that the partial sequence initially isolated from the yeast two-hybrid screen was not in-frame with the AD domain of pGADT7. Thus, interaction was not observed between the full-length LRR and YHV MIB domain. However, the LRR protein was examined for tissue expression in normal shrimp and shrimp challenged with YHV and WSSV and the results are discussed below in section 5.2. Section 5.4 discusses the thesis work done to develop a protein-protein interaction (PPI) network for Taura syndrome virus and Section 5.5 discusses the results of studies on the interaction between the BIR domain protein of TSV and host shrimp proteins.

5.2 Identification and characterization of *PmLRR*

PmLRR identified in this study is not only the first found from shrimp but also the first found from a crustacean. The signature for the *Pm*LRR gene sequence is leucine enrichment (i.e., it contains 96 leucine residues, constituting 17% of the total amino acid composition). Although a comparison of *PmLRR* with proteins in databases using BLASTp (Altschul et al., 1990) showed strong similarity to many non-annotated proteins with leucine-rich repeats, there were some records for annotated proteins such as Soc-2, Shoc-2, and Sur-8 that are involved in intracellular signaling pathways (Selfors et al., 1998; Sieburth et al., 1998). LRR motif-containing proteins have diverse functions and cellular locations in a variety of organisms (Kobe et al., 1994; Kobe et al., 1995; Buchanan et al., 1996; Kajava, 1998). Thus, it was of interest to investigate whether shrimp LRR might have functions similar to Soc-2, Shoc-2 or Sur-8.

PmLRR expression was relatively strong in defense-related tissues (i.e., the lymphoid organ and hemocytes), suggesting that *Pm*LRR might play a role in shrimp defense mechanisms (Hasson et al., 1999; Anggraeni et al., 2000; Johansson et al., 2000; van de Braak, 2002). Intestinal tissue that is generally known to act as a defense barrier also showed high expression of *PmLRR*.

The lymphoid organ was chosen for further investigation as a representative defense tissue with high *PmLRR* expression, particularly with respect to to the effect of yellow head virus (YHV) and white spot syndrome virus (WSSV) infection on *PmLRR* expression, since it is known to play a role in the shrimp response to viral pathogens (Hasson et al., 1999; Anggraeni et al, 2000). Analysis carried out based on agarose gels of RT-PCR assays clearly revealed that *PmLRR* expression in normal, uninfected shrimp was 5-fold higher than that in shrimp during the late phase of infection for both viruses. Since RT-PCR expression assays based on agarose gel band intensities are relatively crude, low orders of difference may not indicate real differences in expression. However, the large difference in intensity for *PmLRR* suggested that the drop in expression was real and that shrimp mortality caused by viral infection was associated with a general down-regulation of *PmLRR*. However, more detailed experiments such as real-time PCR assays or northern blot analysis

would be advisable to confirm this down-regulation before investing time on further work regarding the potential role of *PmLRR* in the shrimp response to viral pathogens.

Analysis of the structural features of *Pm*LRR using the InterPro database (Apweiler et al., 2001) revealed 16 tandem LRR motifs in the deduced protein and this corresponded with the general characteristic of most LRR-containing proteins that contain 2-45 tandem LRR motifs (Kobe et al., 2001). In addition, *Pm*LRR revealed the conserved pattern of LRR motifs consisting of an 11-residue motif of LxxLxLxxNxL, where x can be any amino acid. L indicates leucine or other bulky, non-polar residues, and N represents asparagine, cysteine, serine or threonine (Kobe et al., 2001). In addition to the conserved segment, variable segments in motifs are also used to classify LRR proteins into at least 7 subfamilies based on different lengths and consensus sequences (Kajava, 1998). *Pm*LRR most likely belongs to the 'typical' subfamily (Kobe et al., 2001). A 3D model of *Pm*LRR was constructed had a horseshoe-shape. It is known that the conserved segments of LxxLxLxxNxL in the protein constitute β-sheet strands and that the variable segments correspond to α-helixes and this yields a horseshoe structure composed of alternately repeated β-α domains (Kobe et al., 1993).

LRR proteins are thought to play a major role in protein-protein interactions that occur in phenomena such as hormone-receptor interactions, enzyme inhibition, cell adhesion and cellular trafficking (Kobe et al., 1994; Kobe et al., 1995; Buchanan et al., 1996; Kajava, 1998). The undefined region protruding between LRR9 and LRR10 in *Pm*LRR is of interest for further investigation into possible functional significance in protein-protein interactions. Overall, *Pm*LRR is a prime candidate for further protein-protein interaction studies in shrimp.

5.3 Identification and characterization of *PmSPH516*

*Pm*SPH516 was found to bind only to MIB (metal ion binding domain) and not to other proteins from yellow head virus (YHV). Although the function of YHV MIB has not been reported, it is known that MIB domains are present in many viruses since the proteins they encode are required to interact with metal ions that assist in maintaining viral structure and function (for a review see Chaturvedi and

Shrivastava, 2005). Metal ions are also important for various host cell functions. For example, serine proteases and serine protease homologues participate in a variety of cellular activities and are often metal ion dependent. Specific examples include the pro-phenoloxidase (pro-PO) activating system in arthropods (Perazzolo and Barracco, 1997; Lee et al., 2002) and blood coagulation in mammals (Davie et al., 1979). Understanding the role of SPH binding to YHV MIB will require a better understanding of the SPH themselves.

Even though the role of SPH in arthropod defense mechanisms against bacteria and fungi has been fairly well described for the pro-PO activating system, functions related to viral defenses have been less well studied. So far, a role for serine protease protein in arthropod antiviral activity has been reported only against nucleopolyhedrovirus in the silkworm *Bombyx mori* (Nakazawa et al., 2004). The fact that our SPH516 binds specifically to YHV MIB suggests that it may also play some role in viral defense mechanisms. Since MasSPH (Amparyup et al., 2007) also from *P. monodon* has very high identity to SPH516 and SPH509 and has an identical C-terminal region to that of SPH516 that binds to YHV MIB, it is likely that they are isoforms of the same protein and that all will be capable of binding to YHV MIB. SPH isoforms in some insect species have been published (Adams et al., 2000; Christophides et al., 2002). Given the similarity in sequences, it is perhaps surprising that MasSPH was not recovered in our screening. It is possible that it would have been obtained if more clones had been sequenced. With c-SPH (Lin et al., 2006) from *P. monodon* sharing only 38% identity with SPH516, binding to YHV MIB is less certain. In any case, it would be worthwhile carrying out the relevant pull-down assays to be certain.

Among the three SPH isoforms, the major sequence difference is the variation in the number of LGGQGGG repeats at the N-terminal glycine-rich domain. Amparyup et al (2007) suggested that this region might have antimicrobial peptide activity by reference to the function of glycine-rich antimicrobial peptides from the spider *Acanthoscurria gomesiana*. Although transcriptional expression of SPH in shrimp hemocytes during bacterial (Amparyup et al., 2007) and viral infection (this study) have been examined, the amplification primers used in both studies were designed from conserved SPH regions so that the amplified transcripts were likely to

represent at least the three SPH isoforms in *P. monodon*. The previous results showed up-regulation of SPH after *Vibrio harveyi* (bacteria) injection whereas we found down-regulation after YHV injection. The reason for the difference is intriguing and deserves further attention. Generally, viruses are known to shut off host transcription and/or translation to avoid metabolic competition while facilitating their own propagation, thereby affecting cellular gene expression and cell functions (Lyles, 2000; Bushell and Sarnow, 2002). Molecular responses of host cells against viral pathogens have been well investigated for various mammalian and plant viruses, but little is known about the interaction between shrimp and their viruses. The down-regulation of shrimp SPH after YHV infection may be the result of a direct or indirect virus shut off mechanism or may be the result of an unsuccessful host defense response.

Our results on transcription expression, western blotting, and immunohistochemistry strongly suggest that SPH in *P. monodon* are transcribed in hemocytes and then secreted into the hemolymph. This is consistent with the presence of a putative signal peptide in the deduced protein sequence. To our knowledge, this is the first evidence of such a phenomenon in shrimp. The molecular weight discrepancy between the deduced mass of SPH516 (52.9 kDa) and the band detected in our immunoblots (72 kDa) could be due to post-translational modifications such as glycosylation and phosphorylation. However, study of an *Anopheles gambiae* clip domain serine protease suggested that N-linked glycosylation was not the major contributor to this effect (Volz et al., 2005). Rather, it resulted from the formation of a protein complex that was resistant to SDS-induced denaturation (Arakawa et al., 1992; Tong et al., 2005). In addition, since the polyclonal antibody was raised against SPH516-C (residues 393-516) located in the conserved trypsin-like serine protease domain, it is possible that the antibody also cross-reacted with other serine protease proteins. Examination of the sequences of serine proteases (SP) identified to date from crustaceans revealed that none contain more than one clip domain although SP from other arthropods do contain more than one (Satoh et al., 1999; Jiang et al., 2003). On the other hand, one crustacean serine protease homologue (SPH) has been reported to contain 7 clip domains [GenBank accession number **Y11145** (Huang et al., 2000)]. It is not known whether SP with more than one clip domain exist in crustaceans. If they do exist, they await discovery.

Given the poor understanding of the role of SPH516 itself in cellular function, it is difficult to speculate on the role of its binding to YHV MIB. The fact that the two proteins bind specifically suggests that the role of YHV MIB is unlikely to be simple competition with SPH for available metal ions in the cell, especially since it appears to be largely an extracellular protein. On the other hand, it is probable that binding between YHV MIB and SPH516 is mediated through metal ion(s). Further studies will be required to test this hypothesis and to identify possible natural metal co-factors that might be involved in the interaction. However, even if that turned out to be the case, it would not give us a reason for the binding. Is it possible that SPH516 plays a role in shrimp defenses and that binding with YHV MIB somehow limits or overcomes that role to allow for viral replication? Although this may be an appealing concept, we are left with the problem that the two proteins seem to be in largely different compartments in the shrimp, YHV MIB inside the cell and SPH516 outside. In addition, the immunohistochemical results indicated that SPH516 was present in the hemolymph of normal *P. monodon* suggesting that it is constitutively produced and released into the hemolymph where it should have an important extracellular function(s).

5.4 TSV protein-protein interactions

Taura syndrome virus (TSV) is a serious shrimp pathogen that has caused economic losses in cultivation of especially the Pacific white shrimp, *Penaeus (Litopenaeus) vannamei*. Although TSV genome has been characterized (Mari et al., 2002) and some host-TSV interactions have been documented (Senapin and Phongdara, 2006), the function of each viral protein and the mechanism of pathogenesis are not fully characterized. This study examined the interaction among the viral proteins themselves with the objective of constructing a viral protein-protein interaction (PPI) map.

Based on predicted TSV ORFs, all 7 domains and transmembrane-truncated forms were subjected to interaction analysis by yeast two-hybrid assay. They were generated as fusion proteins with both BD (as bait) and AD (as prey) domains. Identification of auto-activation proteins of both bait and prey constructs was first

conducted prior to interaction screening in order to minimize false positive results. It was revealed that only N-VP1 had self-activation activity in both BD and AD orientations. The auto-activation of N-VP1 might be due to different protein folding since the full-length VP1 was not auto-activating.

Except for N-VP1, thorough interaction screening was carried out among all the TSV domains in a matrix format. This gave a combination of 81 pairwise protein interactions (9 BD x 9 AD). Among these tested interactions, 19 positive interactions were revealed with the ratio of interaction to total ORF of approximately 2.1 (19/9). This ratio is consistent with those found for other viral networks (ranging from 0.14 to 2.5) (Bartel et al., 1996; Calderwood et al., 2007; Flajolet et al., 2000; McCraith et al., 2000; Uetz et al., 2006). However, some reports suggested that the use of two-hybrid libraries made from random viral genome fragments increases the possibility of identifying additional protein interactions that might not occur in a matrix of defined full-length polypeptides (Bartel, et al, 1996, Flajolet et al., 2000).

Among the TSV bait collection, the 3 baits, C-Prot, C-VP1, and Pol, yielded no interactions using TSV proteins as prey. The lack of interactions may have arisen due to incorrect protein folding of truncated protein forms. In addition, Pol or RNA polymerase may tend to interact with host proteins rather than viral proteins. Viral RNA polymerase is often associated with host components that facilitate replication or assist in evasion of host RNA degradation pathways. Several components of the host translational apparatus (e.g., elongation factor EF-1a) have been reported to be co-opted by RNA polymerase of diverse RNA viruses (see review in Li and Nagy, 2011).

The TSV PPI map presented in this study includes a total number of 6 proteins (nodes) involved in 14 interactions (edges). The BIR and VP1 proteins had the highest number of interactions (5 interactions) in the map, suggesting important roles in the TSV life cycle and marking them as prime candidates for further investigation. For example, knocking down BIR and VP1 might be expected to deter TSV propagation and protect shrimp against viral disease. However, knocking down BIR might not be practical since BIR domains are also found in shrimp proteins such as IAPs (inhibitor of apoptosis proteins) and Survivin (Leu et al., 2012). Thus, VP1 might be a better candidate for this purpose. Previous work to test the protective effect

of knocking down a putative shrimp receptor for TSV (Lamr/p40) that could bind to TSV VP1 (i.e., to inhibit TSV entry to the host cells) resulted in shrimp mortality even without viral challenge (Senapin and Phongdara, 2006). The TSV PPI map also revealed interactions among the three proteins, BIR, Hel and VP3 with high confidence and stimulated further study of their complex protein interactions by *in vitro* pull-down assay.

By *in vitro* pull-down assay, it was shown that the structural proteins alone (VP1, VP2 and VP3) could not form a complex without Hel protein involvement. The question as to how Hel (helicase) might be involved in TSV virion protein formation remains obscure. However, recent work has provided evidences for interaction between a viral helicase and a viral structural protein (Mousseau et al., 2011; Jones et al., 2011). Specifically, a capsid protein (also called core protein) of Hepatitis C virus (HCV) interacts directly with the helicase portion of HCV non-structural protein 3 (NS3h)(Mousseau et al., 2011). The findings suggested that NS3 had an additional role in viral particle assembly apart its previously known role in viral replication. However, little is known for viral assembly in the Dicistroviridae, although the crystal structure of the Cricket paralysis virus (CrPV) virion has been solved (Tate et al, 1999). Recent works on Triatoma virus (TrV), another Dicistrovirus, demonstrated that naturally occurring empty particles lacking their RNA genome were non-infectious and that the empty particles resulted from defective processing of the capsid protein precursor (Agirre et al, 2011). It is not known whether any other viral components participate in TrV capsid assembly. With respect to TSV, the putative complex interaction between helicase and the structural proteins would need to be confirmed by other methods and its significance examined. Use of highly purified recombinant viral proteins should also be employed in order to avoid interaction interference from other contaminating proteins. This should shed more light on the mechanism of viral infection and the molecular events associated with capsid assembly in a non-enveloped virus.

5.5 Identification and characterization of *PmAmidase*

Using the BIR domain of TSV to screen for interacting proteins from a *P. monodon* hemocyte cDNA library, a partial cDNA sequence of the amidase domain was identified. The full-length of *PmAmidase* cDNA sequence was then successfully identified. It contained a putative signal sequence, a potential amidase superfamily domain, and a unique highly conserved Ser-Ser-Lys catalytic triad used for amide hydrolysis. Among more than 80 proteins that contain the amidase superfamily domain (Chebrou et al., 1996; Patricelli et al., 1999; Cai et al., 2005; Gopalakrishna et al., 2004; Labahn et al., 2002; Neu et al., 2007), the first amidase found from shrimp was closely similar to glutamyl-tRNA amidotransferase, an enzyme generally known to be involved in protein synthesis.

Attaching the correct amino acid to its cognate tRNA is critical in protein synthesis. This step involves an enzyme called aminoacyl tRNA synthetase (aaRS) that catalyzes the esterification of a specific amino acid to its compatible cognate tRNA to form an aminoacyl-tRNA (Ibba and Söll, 2000). For example, Ala-tRNA^{Ala} is catalysed by alanyl-tRNA synthetase (AlaRS) and Gly-tRNA^{Gly} is formed by glycyl-tRNA synthetase (GlyRS). However, there are some organisms that lack specific synthetase activities for a subset of the 20 amino acids. For example, *Bacillus subtilis* and most Gram-positive bacteria do not harbor glutaminyl-tRNA synthetase (GlnRS) (reviewed in Ibba et al, 1997). Thus, these organisms synthesize Gln-tRNA^{Gln} indirectly by two consecutive enzymatic reactions. Firstly, GluRS attaches tRNA^{Gln} to Glu forming Glu-tRNA^{Gln}, then the tRNA-bound Glu is transamidated into Gln by the enzyme glutamyl-tRNA amidotransferase. The fact that *Pm*Amidase has similar features to glutamyl-tRNA amidotransferase suggests that shrimp may also lack a functional GlnRS enzyme and that *Pm*Amidase is used to assist in the formation of Gln-tRNA^{Gln}.

It is known that viruses are dependent on host protein synthesis machinery to synthesize their viral proteins. Although no link between the aminoacyl tRNA amidotransferase and a virus has been reported so far, several works have shown that host translational machinery components are targeted by viruses. For example, it was demonstrated that human Lys-tRNA^{Lys} and LysRS are incorporated into human immunodeficiency virus type 1 (HIV-1) virions because Lys-tRNA^{Lys} serves as the

primer for reverse transcriptase (Jiang et al., 1993, Cen et al, 2001). Since protein interaction between PmAmidase and TSV BIR was observed using a partial sequence (i.e., not a full-length sequence) of *Pm*Amidase, other methods might be required to confirm the interaction, to prove that *Pm*Amidase is a as glutamyl-tRNA amidotransferase and to determine the significance of its interaction with TSV BIR.

CHAPTER VI
SUMMARY

This research discovered two immune-related genes, *PmLRR* and *PmSPH516*, from the black or giant tiger shrimp *P. monodon*. Their distribution and transcription expression profiles in normal and viral challenged shrimp were investigated. In addition, a study of interactions among TSV proteins was carried out, resulting in construction of a protein-protein interaction (PPI) map. Briefly, *PmLRR* cDNA was cloned from *P. monodon* hemocyte RNA by 5' rapid amplification of cDNA ends (5' RACE). The full-length of *PmLRR* consisted of 2,604 bp with a 1,686-bp open reading frame, encoding 561 amino acids. The deduced protein sequence revealed a high proportion of leucine residues (17%) and showed sixteen tandem LRR motifs of 23-24 amino acids in length. The computed 3D structure revealed a horseshoe shape consisting of alternately repeated strand and helical domains. Such structures are generally considered to mediate protein-protein interactions, and to our knowledge, this is the first report of an LRR protein from crustaceans. *PmLRR* expression was tissue-specific (i.e., highest in hemocytes, the intestine and the lymphoid organ) suggesting that it may play some role in the shrimp defense against pathogens. Preliminary tests revealed that *PmLRR* was down-regulated after challenge with WSSV and YHV indicating possible involvement in the shrimp response to viral pathogens.

PmSPH516 was identified via a yeast two-hybrid screen between YHV proteins and hemocyte proteins of *P. monodon*. Initially, the C-terminal region of SPH516 (SPH516-C) was found to interact with the putative metal ion binding domain (MIB) encoded by ORF1b in the YHV genome. Subsequently, the full-length of *PmSPH516* cDNA was obtained using 5' RACE and it was also shown to bind specifically to the MIB protein of YHV. The SPH516 isoform named SPH509 was additionally identified from shrimp hemocytes using RT-PCR. All shared the same domain features including a putative signal peptide, glycine-rich repeat motifs, a clip

domain, an HDG triad and a trypsin-like serine protease domain. Phylogenetic analysis revealed that *Pm*SPH516 and its isoform were closer to a prophenoloxidase-activating factor (PPAF) from blue crab than to another SPH from the black tiger shrimp reported to be involved in cell adhesion. SPH transcripts were highly expressed in hemocytes and gills and were found to be down-regulated after YHV infection. Immunohistochemistry using a polyclonal antibody raised against the shrimp protein SPH516-C revealed that SPH516 was present almost exclusively in the shrimp hemolymph.

A viral protein-protein interaction (PPI) map of TSV was constructed using yeast two-hybrid analysis based on a matrix approach. Among 7 TSV genome domains (BIR, Hel, Prot, Pol, VP1, VP2, and VP3) and transmembrane-truncated forms (C-Prot, N-VP1 and C-VP1), only N-VP1 showed self-activation activity in both BD and AD orientations. After interaction screening, there were 19 positive interactions from the total of 81 interaction pairs (9 BD constructs x 9 AD constructs). The 3 baits, C-Prot, C-VP1 and Pol, yielded no interactions with TSV proteins. The ratio of interactions to the total number of examined domains of TSV was calculated as 2.1 (19/9). A TSV PPI map was constructed with a total number of 6 proteins (nodes) involved in 14 interactions (edges). The highest number of interactions (5 interactions) occurred for the BIR and VP1 proteins. High confidence was established for the interaction among the three proteins, BIR, Hel and VP3 in the TSV PPI map. *In vitro* pull-down assays indicated that a structural protein complex of VP1-VP2-VP3 required Hel but not BIR. It was likely that Hel was important for assembly of the structural protein complex and that the presence of BIR could interfere with its assembly. To test the hypothesis that isolation of BIR to permit TSV virion formation was achieved by interaction with a host protein, BIR was employed as bait to search for possible shrimp interacting proteins using the yeast two-hybrid assay. As a result, a partial cDNA sequence of an amidase domain protein was identified as a candidate BIR-interacting protein from a *P. monodon* hemocyte library. Subsequently, the full-length *Amidase* cDNA sequence revealed a 1,602-nucleotide ORF encoding a putative protein of 533 deduced amino acids. This novel shrimp amidase protein showed signatures of a potential signal peptide (residues 1-32), an amidase superfamily domain (residues 63 to 504), and a unique and highly conserved Ser-Ser-Lys catalytic

triad used for amide hydrolysis. BLASTP analysis of the deduced protein sequence revealed that *Pm*Amidase had significant similarity to the proteins fatty-acid amide hydrolase 2, amidase and amidotransferase from various animals. By phylogenetic tree analysis, *Pm*Amidase grouped together with related proteins from insects and was linked most closely to proteins from *T. castaneum* (red flour beetle), *A. pisum* (pea aphid) and *P. humanus corporis* (the human louse). Nevertheless, protein interaction between the full-length of *Pm*Amidase and BIR from TSV could not be demonstrated by the yeast two-hybrid assay and other methods may be required to determine whether interaction occurs and has any biological significance for shrimp.

Altogether, the work in this thesis contributes to the accumulating database on the identity and functional characteristics of immune-related genes in shrimp and to the increasing knowledge regarding shrimp viruses and the host response to them.

REFERENCES

Adams, M. D., Celniker, S. E., Holt, R.A., Evans, C.A., Gocayne, J.D., Amanatides, P.G., et al. (2000). The genome sequence of *Drosophila melanogaster*. *Science*, 287, 2185-2195.

Agirre, J., Aloria, K., Arizmendi, J.M., Iloro, I., Elortza, F., Sánchez-Eugenia, R., et al. (2011). Capsid protein identification and analysis of mature Triatoma virus (TrV) virions and naturally occurring empty particles. *Virology*, 409, 91-101.

Altschul, S.F., Gish, W., Miller, W., Myers, E.W. & Lipman, D.J. (1990). Basic local alignment search tool. *J Mol Biol*, 215, 403-410.

Amparyup, P., Jitvaropas, R., Pulsook, N. & Tassanakajon A. (2007). Molecular cloning, characterization and expression of a masquerade-like serine proteinase homologue from black tiger shrimp *Penaeus monodon*. *Fish Shellfish Immunol*, 22, 535-546.

Anggraeni, M.S. & Owens, L. (2000). The haemocytic origin of lymphoid organ spheroid cells in the penaeid prawn *Penaeus monodon*. *Dis Aquat Organ*, 40, 85-92.

Apweiler, R., Attwood, T.K., Bairoch, A., Bateman, A., Birney, E., Biswas, M., et al. (2001). The InterPro database, an integrated documentation resource for protein families, domains and functional sites. *Nucleic Acids Res*, 29, 37-40.

Arakawa, T., Hung, L., McGinley, M.G., Rohde, M.F. & Narhi, L. O. (1992). Induced resistance of trypsin to sodium dodecylsulfate upon complex formation with trypsin inhibitor. *J Protein Chem*, 11, 171-176.

Assavalapsakul, W., Tirasophon, W. & Panyim, S. (2005). Antiserum to the gp116 glycoprotein of yellow head virus neutralizes infectivity in primary lymphoid organ cells of *Penaeus monodon*. *Dis Aquat Organ*, 63, 85-88.

Auerbach, D. & Stagljar, I. (2005). Yeast two-hybrid protein-protein interaction networks. In: Waksman, G. (Eds.), Proteomics and Protein-Protein

Interactions: Biology, Chemistry, Bioinformatics, and Drug Design. Springer, New York.

Bartel, P.L., Roecklein, J.A., SenGupta, D. & Fields, S. (1996). A protein linkage map of *Escherichia coli* bacteriophage T7. *Nature Gen*, 12, 72-77.

Bell, T.A. & Lightner, D.V. (1988). A handbook of normal shrimp histology. World Aquaculture Society, Baton Rouge, LA, USA.

Bonami, J.R., Hasson, K.W., Mari, J., Poulos, B.T. & Lightner, D.V., (1997). Taura syndrome of marine penaeid shrimp: characterization of the viral agent. *J Gen Virol*, 78, 313-319.

Boonyaratpalin, S., Supamattaya, K., Kasornchandra, J., Direkbusaracom, S., Ekpanithanpong, U. & Chantanachooklin, C. (1993). Non-occluded baculo-like virus, the causative agent of yellow head disease in the black tiger shrimp (*Penaeus monodon*). *Fish Pathol*, 28, 103-109.

Brock, J.A. (1997). Special topic review: Taura syndrome, a disease important to shrimp farms in the Americas. *World J Microb Biot*, 13, 415-418.

Buchanan, S.G., & Gay, N.J. (1996). Structural and functional diversity in the leucine-rich repeat family of proteins. *Prog Biophys Mol Biol*, 65, 1-44.

Bushell, M. & Sarnow, P. (2002). Hijacking the translation apparatus by RNA viruses. *J Cell Biol*, 158,395-399.

Cai, G., Zhu, S., Wang, X. & Jiang, W. (2005). Cloning, sequence analysis and expression of the gene encoding a novel wide-spectrum amidase belonging to the amidase signature superfamily from *Achromobacter xylosoxidans*. *FEMS Microbiol Lett*, 249, 15-21.

Calderwood, M.A., Venkatesan, K., Xing, L., Chase, M.R., Vazquez, A., Holthaus, A.M., et al. (2007). Epstein-Barr virus and virus human protein interaction maps. *Proc Natl Acad Sci USA*, 104, 7606-7611.

Castro-Longoria, R., Quintero-Arredondo, N., Grijalva-Chon, J.M. & Ramos-Paredes, J. (2008). Detection of the yellow-head virus (YHV) in wild blue shrimp, *Penaeus stylirostris*, from the Gulf of California and its experimental transmission to the Pacific white shrimp, *Penaeus vannamei*. *J Fish Dis*, 31, 953-956.

Causier, B. & Davies, B. (2002). Analysing protein-protein interactions with the yeast

two-hybrid system. *Plant Mol Biol*, 50, 855-870.

Causier, B. (2004). Studying the interactome with the yeast two-hybrid system and mass spectrometry. *Mass Spectrom Rev*, 23, 350-367.

Cedano-Thomas, Y., de la Rosa-Vélez, J., Bonami, J.-R. & Vargas-Albores, F. (2009). Gene expression kinetics of the yellow head virus in experimentally infected *Litopenaeus vannamei*. *Aquacult Res*, 111, 1-12.

Cen, S., Khorchid, A., Javanbakht, H., Gabor, J., Stello, T., Shiba, K. et al., (2001). Incorporation of lysyl-tRNA synthetase into human immunodeficiency virus type 1. *J Virol*, 75**,** 5043-5048.

Chaivisuthangkura, P., Tejangkura, T., Rukpratarnporn, S., Longyant, S., Sithigorngul, W. & Sithigorngul, P. (2006). Polyclonal antibodies specific for VP1 and VP3 capsid proteins of Taura syndrome virus (TSV) produced via gene cloning and expression. *Dis Aquat Org*, 69, 249-253

Chantanachookin, C., Boonyaratpalin, S., Kasornchandra, J., Direkbusarakorn, S., Ekpanithanpong, U., Supamataya, K., et al. (1993). Histology and ultrastructure reveal a new granulosis-like virus in *Penaeus monodon* affected by yellow-head disease. *Dis Aquat Organ*, 17, 145-157.

Chaturvedi, U. C. & Shrivastava R. (2005). Interaction of viral proteins with metal ions: role in maintaining the structure and functions of viruses. *FEMS Immunol Med Microbiol*, 43, 105-114.

Chebrou, H., Bigey, F., Arnaud, A., & Galzy, P. (1996). Study of the amidase signature group. *Biochim Biophys Acta*, 1298, 285-293.

Cline, M.S., Smoot, M., Cerami, E., Kuchinsky, A., Landys, N., et al. (2007). Integration of biological networks and gene expression data using Cytoscape. *Nat Protoc*, 2, 2366-2382.

Christophides, G. K., Zdobnov, E., Barillas-Mury, C., Birney, E., Blandin, S., Blass, C., et al. (2002). Immunity-related genes and gene families in *Anopheles gambiae*. *Science*, 298, 159-165.

Cowley, J.A., Dimmock, C.M., Wongteerasupaya, C., Boonsaeng, V., Panyim, S. & Walker, P.J. (1999) Yellow head virus from Thailand and gill-associated virus from Australia are closely related but distinct prawn viruses. *Dis Aquat Organ*, 36, 153-157.

Cowley, J.A., Dimmock, C.M., Spann, K.M. & Walker, P.J. (2000). Gill-associated virus of *Penaeus monodon* prawns: an invertebrate virus with ORF1a and ORF1b genes related to arteri and coronaviruses. *J Gen Virol*, 81, 1473-1484.

Cowley, J.A. & Walker, P.J. (2002). The complete genome sequence of gill-associated virus of *Penaeus monodon* prawns indicates a gene organization unique among nidoviruses. *Arch Virol*, 147, 1977-1987.

Cowley, J.A., Cadogan, L.C., Wonteerasupaya, C., Hodgson, R.A., Boonsaeng, V. & Walker, P.J. (2004). Multiplex RT-nested PCR differentiation of gill-associated virus (Australia) from yellow head virus (Thailand) of *Penaeus monodon*. *J Virol Methods*, 117, 49-59.

Davie, E. W., Fujikawa K., Kurachi K. & Kisiel W. (1979). The role of serine proteases in the blood coagulation cascade. *Adv Enzymol Relat Areas Mol Biol*, 48, 277-318.

de la Rosa-Vélez, J., Cedano-Thomas, Y., Cid-Becerra, J., Méndez-Payán, J.C., Vega-Pérez, C., Zambrano-García, J. & Bonami, J.-R. (2006). Presumptive detection of yellow head virus by reverse transcriptase-polymerase chain reaction and dotblot hybridization in *Litopenaeus vannamei* and *L. stylirostris* cultured on the Northwest coast of Mexico. *J Fish Dis*, 29, 717-728.

FAO. (2012). The State of the World Fisheries and Aquaculture 2012. World review of fisheries and aquaculture.

Fields, S. & Song, O.-K. (1989). A novel genetic system to detect protein-protein interactions. *Nature*, 340, 245-246.

Flajolet, M., Rotondo, G., Daviet, L., Bergametti, F., Inchauspe, G., Tiollais, P., Transy, C. & Legrain, P. (2000). A genomic approach of the hepatitis C virus generates a protein interaction map. *Gene*, 242, 369-379.

Flegel, T.W. (2006). Detection of major penaeid shrimp viruses in Asia, a historical perspective with emphasis on Thailand. *Aquaculture*, 258, 1-33.

Flegel, T.W. (2012). Historic emergence, impact and current status of shrimp pathogens in Asia. *J Invertebr Pathol*, 110, 166-173.

Formstecher, E., Aresta, S., Collura, V., Hamburger, A., Meil, A., Trehin, A., Reverdy,

C., et al. (2005). Protein interaction mapping: A *Drosophila* case study. *Genome Res*, 15, 376-384.

Gietz, R.D., Schiestl, R.H., Willems, A.R. & Woods, R.A. (1995). Studies on the transformation of intact yeast cells by the LiAc/SS-DNA/PEG procedure. *Yeast*, 11, 355-360.

Giot, L., Bader, J.S., Brouwer, C., Chaudhuri, A., Kuang, B., Li, Y., Hao, Y.L., et al. (2003). A protein interaction map of *Drosophila melanogaster*. *Science*, 302, 1727-1736.

GOAL. (2013). The global aquaculture advocate. January/February 2013.

Gopalakrishna, K.N., Stewart, B.H., Kneen, M.M., Andricopulo, A.D., Kenyon, G.L., & McLeish, M.J. (2004). Mandelamide hydrolase from *Pseudomonas putida:* characterization of a new member of the amidase signature family. *Biochemistry*, 43, 7725-7735.

Hasson, K.W., Lightner, D.V., Mohney, L.L., Redman, R.M. & White, B.M. (1999). Role of lymphoid organ spheroids in chronic Taura syndrome virus (TSV) infections in *Penaeus vannamei*. *Dis Aquat Organ*, 38, 93-105.

Hirono, I., Fagutao, F.F., Kondo, H. & Aoki, T. (2011). Uncovering the mechanisms of shrimp innate immune response by RNA interference. *Mar Biotechnol*, 13, 622-628.

Huang, T.S., Wang, H., Lee, S.Y., Johansson, M.W., Soderhall, K. & Cerenius, L. (2000). A cell adhesion protein from the crayfish *Pacifastacus leniusculus*, a serine proteinase homologue similar to *Drosophila masquerade*. *J Biol Chem*, 275, 9996-10001.

Ibba, M., Curnow, A.W & Söll, D. (1997). Aminoacyl-tRNA synthesis: Divergent routes to a common goal. *Trends Biochem Sci*, 22, 39-42.

Ibba, M. & Söll, D. (2000). Aminoacyl-tRNA synthesis. *Annu Rev Biochem*, 69, 617-650.

Ito, T., Chiba, T., Ozawa, R., Yoshida, M., Hattori, M. & Sakaki, Y. (2001). A comprehensive two-hybrid analysis to explore the yeast protein interactome. *Proc Natl Acad Sci USA*, 98, 4569-4574.

Jaroenram, W., Arunrut, N. & Kiatpathomchai, W. (2012). Rapid and sensitive detection of shrimp yellow head virus using loop-mediated isothermal amplification and a colorogenic nanogold hybridization probe. *J Virol Methods*, 186, 36-42.

Jiang, M., Mak, J., Ladha, A., Cohen, E., Klein, M., Rovinski, B. & Kleiman, L. (1993). Identification of tRNAs incorporated into wild-type and mutant human immunodeficiency virus type 1. *J Virol*, 67, 3246-3253.

Jiang, H., Wang, Y., Yu, X.Q. & Kanost, M.R. (2003). Prophenoloxidase-activating proteinase-2 from hemolymph of *Manduca sexta*. A bacteria-inducible serine proteinase containing two clip domains. *J Biol Chem*, 278, 3552-3561.

Jitrapakdee, S., Unajak, S., Sittidilokratna, N., Hodgson, R.A.J., Cowley, J.A., Walker, P.J., et al. (2003). Identification and analysis of gp116 and gp64 structural glycoproteins of yellow head nidovirus of *Penaeus monodon* shrimp. *J Gen Virol*, 84, 863-873.

Johansson, M., Keyser, P., Sritunyalucksana, K. & Soderhall, K. (2000). Crustacean haemocytes and haematopoiesis. *Aquaculture*, 191, 45-52.

Jones, D.M., Atoom, A.M., Zhang, X., Kottilil, S. & Russell, R.S. (2011). A genetic interaction between the core and NS3 proteins of hepatitis C virus is essential for production of infectious virus. *J Virol*, 85, 12351-12361.

Kajava, A.V. (1998). Structural diversity of leucine-rich repeat proteins. *J Mol* Biol, 227, 519-527.

Kiatpathomchai, W., Jitrapakdee, S., Panyim, S. & Boonsaeng, V. (2004). RT-PCR detection of the yellow virus (YHV) infection in *Penaeus monodon* using dried haemolymph spots. *J Virol Methods*, 119, 1-5.

Kiatpathomchai, W., Jareonram, W., Jitrapakdee, S. & Flegel, T.W. (2007). Rapid and sensitive detection of Taura syndrome virus by reverse transcription loop-mediated isothermal amplification. *J Virol Methods*, 146,125-128.

Kiatpathomchai, W., Jaroenram, W., Arunrut, N., Jitrapakdee, S. & Flegel, T.W. (2008). Shrimp Taura syndrome virus detection by reverse transcription loop-mediated isothermal amplification combined with a lateral flow dipstick. *J Virol Methods*, 153, 214-217.

Kobe, B. & Deisenhofer, J. (1993). Crystal structure of porcine ribonuclease inhibitor, a protein with leucine-rich repeats. *Nature*, 366, 751-756.

Kobe, B. & Deisenhofer, J. (1994). The leucine-rich repeat: a versatile binding motif. *Trends Biochem Sci*, 19, 415-421.

Kobe, B. & Deisenhofer, J. (1995). Proteins with leucine-rich repeats. *Curr Opin Struct Biol*, 5, 409-416.

Kobe, B. & Kajava, A.V. (2001). The leucine-rich repeat as a protein recognition motif. *Curr Opin Struc Biol*, 11, 725-732.

Labahn, J., Neumann, S., Buldt, G., Kula, M.R. & Granzin, J. (2002). An alternative mechanism for amidase signature enzymes. *J Mol Biol*, 322, 1053-1064.

LaCount, D.J., Vignali, M., Chettier, R., Phansalkar, A., Bell, R., Hesselberth, J.R., Schoenfeld, L.W., et al. (2005). A protein interaction network of the malaria parasite *Plasmodium falciparum*. *Nature*, 438, 103-107.

Laemmli, U.K. (1970). Cleavage of structural proteins during the assembly of the head of bacteriophage T4. *Nature*, 227, 680-685.

Lee, K. Y., Zhang R., Kim M. S., Park J. W., Park H. Y., Kawabata S., et al. (2002). A zymogen form of masquerade-like serine proteinase homologue is cleaved during pro-phenoloxidase activation by Ca2+ in coleopteran and *Tenebrio molitor* larvae. *Eur J Biochem*, 269, 4375-4383.

Letunic, I., Copley, R.R., Pils, B., Pinkert, S., Schultz, J., Bork, P. (2006). SMART 5: domains in the context of genomes and networks. *Nucleic Acids Res*, 34, 257-260.

Leu, J.-H., Chen, Y.-C., Chen, L.-L., Chen, K.-Y., Huang, H.-T., Ho, J.-M. & Lo, C.-F. (2012). *Litopenaeus vannamei* inhibitor of apoptosis protein 1 (LvIAP1) is essential for shrimp survival. *Dev Comp Immunol*, 38, 78-87.

Li, S., Armstrong, C.M., Bertin, N., Ge, H., Milstein, S., Boxem, M., Vidalain, P.-O., et al. (2004). A map of the interactome network of the metazoan *C. elegans*. *Science*, 303, 540-543.

Li, Z. & Nagy, P.D. (2011). Diverse roles of host RNA binding proteins in RNA virus replication. *RNA Biol*. 8, 305-315.

Lightner, D.V. (1996). A Handbook of Pathology and Diagnostic Procedures for Diseases of Penaeid Shrimp. World Aquaculture Society, Baton Rouge, LA.

Lightner, D.V. (2011). Virus diseases of farmed shrimp in the Western Hemisphere (the Americas):a review. *J Invertebr Pathol*, 106, 110-130.

Lightner, D.V, Redman, R.M., Pantoja, C.R., Tang, K.F., Noble, B.L., Schofield, P., et al. (2012). Historic emergence, impact and current status of shrimp pathogens in the Americas. *J Invertebr Pathol*, 110, 174-183.

Lin, C.Y., Hu, K.Y., Ho, S.H. & Song, Y.L. (2006). Cloning and characterization of a shrimp clip domain serine protease homolog (c-SPH) as a cell adhesion molecule. *Dev Comp Immunol*, 30, 1132-1144.

Lu, Y., Tapay, L.M., Brock, J.A. & Loh, P.C. (1994). Infection of the yellow head baculolike virus (YBV) in two species of penaeid shrimp *Penaeus stylirostris* (Stimpson) and *Penaeus vannamei* (Boone). *J Fish Dis*, 17, 649-656.

Lyles, D. S. (2000). Cytopathogenesis and inhibition of host gene expression by RNA viruses. *Microbiol Mol Biol Rev*, 64, 709-724.

Mari, J., Bonami, J.R. & Lightner, D.V. (1998). Taura syndrome of penaeid shrimp: cloning of viral genome fragments and development of specific gene probes. *Dis Aquat Org*, 33, 11-17.

Mari, J., Poulos, B.T., Lightner, D.V. & Bonami, J.R. (2002). Shrimp Taura syndrome virus: genomic characterization and similarity with members of the genus Cricket paralysis-like viruses. *J Gen Virol*, 83, 915-926.

Mayo, M.A. (2002a). Virus taxonomy -Houston 2002. *Arch Virol*, 147, 1071-1076.

Mayo, M.A. (2002b). A summary of taxonomic changes recently approved by ICTV. *Arch Virol*, 14, 1655-1656.

McCraith, S., Holtzman, T., Moss, B. & Fields, S. (2000). Genome-wide analysis of vaccinia virus protein-protein interactions. *Proc Natl Acad Sci USA*, 97, 4879-4884.

Mouillesseaux, K.P., Klimpel, K.R., Dhar, A.R. (2003). Improvement in the specificity and sensitivity of detection for Taura syndrome virus and

Yellow head virus of penaeid shrimp by increasing the amplicon size in SYBR green Real-time RT-PCR. *J Virol Methods*, 111, 121-127.

Mousseau, G., Kota, S., Takahashi,V., Frick, D.N. & Strosberg, A.D. (2011). Dimerization-driven interaction of hepatitis C virus core protein with NS3 helicase. *J Gen Virol*, 92, 101-111.

Nadala, E.C., Tapay, L.M. & Loh, P.C. (1997). Yellow-head virus: a rhabdovirus-like pathogen of penaeid shrimp. *Dis Aquat Org*, 31, 141-146.

Nakazawa, H., Tsuneishi E., Ponnuvel K. M., Furukawa S., Asaoka A., Tanaka H., et al. (2004). Antiviral activity of a serine protease from the digestive juice of *Bombyx mori* larvae against nucleopolyhedrovirus. *Virology*, 321, 154-162.

Neu, D., Lehmann, T., Elleuche, S. & Pollmann, S. (2007). *Arabidopsis* amidase 1, a member of the amidase signature family. *FEBS J*, 274, 3440-3451.

Nunan, L.M., Poulos, B.T. & Lightner, D.V. (1998). Reverse transcription polymerase chain reaction (RT-PCR) used for the detection of Taura Syndrome virus (TSV) in experimentally infected shrimp. *Dis Aquat Org*, 34, 87-91.

Nunan, L.M., Tang-Nelson, K. & Lightner, D.V. (2004). Real-time RT-PCR determination of viral copy number in Penaeus vannamei experimentally infected with Taura syndrome virus (TSV). *Aquaculture*, 229, 1-10.

OIE (Office International des Epizooties) (2006). Manual of diagnostic tests for Aquatic Animal diseases, fifth ed. Office International des Epizooties, Paris, France. 467p.

OIE (Office International des Epizooties) (2010). Aquatic Animal Health Code, 13th ed. World Organization for Animal Health, Paris, France, 301p.

Overstreet, R.M., Lightner, D.V., Hasson, K.W., McIlwain, S. & Lotz, J., (1997). Susceptibility to TSV of some penaeid shrimp native to the Gulf of Mexico and southeast Atlantic Ocean. *J Invertebr Pathol*, 69, 165-176.

Patricelli, M.P., Lovato, M.A. & Cravatt, B.F. (1999). Chemical and mutagenic investigations of fatty acid amide hydrolase: evidence for a family of serine hydrolases with distinct catalytic properties. *Biochemistry*, 38, 9804-9812.

Perazzolo, L. M. & Barracco M. A. (1997). The prophenoloxidase activating system of the shrimp *Penaeus paulensis* and associated factors. *Dev Comp Immunol*, 21, 385-395.

Phalitakul, S., Wongtawatchai, J., Sarikaputi, M. & Viseshakul, N. (2006). The molecular detection of Taura syndrome virus emerging with White spot syndrome virus in penaeid shrimp of Thailand. *Aquaculture*, 260, 77-85.

Poulos, B.T., Kibler, R., Bradley-Dunlop, D., Mohney, L.L. & Lightner, D.V. (1999). Production and use of antibodies for the detection of the Taura syndrome virus in penaeid shrimp. *Dis Aquat Org*, 37, 99-106.

Rain, J.-C., Selig, L., De Reuse, H., Battaglia, V., Reverdy, C., Simon, S., Lenzen, G., et al. (2001). The protein-protein interaction map of *Helicobacter pylori*. *Nature*, 409, 211-215.

Robalino, J., Bartlett, T.C., Chapman, R.W., Gross, P.S., Browdy, C.L. & Warr, G.W. (2007). Double-stranded RNA and antiviral immunity in marine shrimp: inducible host mechanisms and evidence for the evolution of viral counter-responses. *Dev Comp Immunol*, 31, 539-547.

Robles-Sikisaka, R., Garcia, D.K., Klimpel, K.R. & Dhar, A.K. (2001). Nucleotide sequence of 30-end of the genome of Taura syndrome virus of shrimp suggests that it is related to insect picornaviruses. *Arch Virol*, 146, 941-952.

Rual, J.-F., Venkatesan, K., Hao, T., Hirozane-Kishikawa, T., Dricot, A., Li, N., Berriz, G.F., et al. (2005). Towards a proteome-scale map of the human protein-protein interaction network. *Nature*, 437, 1173-1178.

Sánchez-Barajas, M., Linán-Cabello, M.A. & Mena-Herrera, A. (2009). Detection of yellow-head disease in intensive freshwater production systems of *Litopenaeus vannamei*. *Aquacult Int*, 17, 101-112.

Satoh, D., Horii, A., Ochiai, M. & Ashida, M. (1999). Prophenoloxidase-activating enzyme of the silkworm, *Bombyx mori*. Purification, characterization, and cDNA cloning. *J Biol Chem*, 274, 7441-7453.

Selfors, L.M., Schutzman, J.L., Borland, C.Z. & Stern, M.J. (1998). Soc-2 encodes a leucine-rich repeat protein implicated in fibroblast growth factor receptor signaling. *Proc Natl Acad Sci USA*, 95, 6903-6908.

Senapin, S. & Phongdara, A. (2006). Binding of shrimp cellular proteins to Taura syndrome viral capsid proteins VP1, VP2 and VP3. *Virus Res*, 122, 69-77.

Shannon, P., Markiel, A., Ozier, O., Baliga, N.S., Wang, J.T., Ramage, D., Amin, N., Schwikowski, B. & Ideker, T. (2003). Cytoscape: a software environment for integrated models of biomolecular interaction networks. *Genome Res*, 13, 2498-2504.

Sieburth, D.S., Sun, Q. & Han, M. (1998). SUR-8, a conserved Ras-binding protein with leucine-rich repeats, positively regulates Ras-mediated signaling in *C. elegans*. *Cell*, 94, 119-130.

Sithigorngul, P., Chauychuwong, P., Sithigorngul, W., Longyant, S., Chaivisuthangkura, P. & Menasveta, P. (2000). Development of a monoclonal antibody specific to yellow head virus (YHV) from *Penaeus monodon*. *Dis Aquat Organ*, 42, 27-34.

Sithigorngul, P., Rukpratanporn, S., Longyant, S., Chaivisuthangkura, P., Sithigornkul, W., Menasveta, P. (2002). Monoclonal antibodies specific to yellow-head virus (YHV) of *Penaeus monodon*. *Dis Aquat Organ*, 49, 71-76.

Sithigorngul, W., Rukpratanporn, S., Sittidilokratna, N., Pechraburanin, N., Longyant, S., Chaivisuthangkura, P. & Sithigorngul, P. (2007). A convenient immunochromatographic test strip for rapid diagnosis of yellow head virus infection in shrimp. *J Virol Methods*, 140, 193-199.

Sittidilokratna, N., Cowley, J.A., Jitrapakdee, S., Boonsaeng, V., Panyim, S. & Walker, P.J. (2002). Complete ORF1b-gene sequence indicates yellow head virus is an invertebrate nidovirus. *Dis Aquat Organ*, 50, 87-93.

Sittidilokratna, N., Phetchampai, N., Boonsaeng, V. & Walker, P.J. (2006). Structural and antigenic analysis of the yellow head virus nucleocapsid protein p20. *Virus Res*, 116, 21-29.

Sittidilokratna, N., Dangtip, S., Cowley, J.A. & Walker, P.J. (2008). RNA transcription analysis and completion of the genome sequence of yellow head nidovirus. *Virus Res*, 136, 157-165.

Soderhall, K. & Smith, V.J. (1983). Separation of the haemocyte populations of *Carcinus maenas* and other marine decapods, and prophenoloxidase distribution. *Dev Comp Immunol*, 7, 229-239.

Soowannayan, C., Sithigorngul, P., Slater, J., Hyatt, A., Cramerri, S., Wise, T., et al. (2003). Detection and differentiation of yellow head complex viruses using monoclonal antibodies. *Dis Aquat Organ*, 57, 193-200.

Soowannayan, C., Cowley, J.A., Pearson, R.D., Wallis, T.P., Gorman, J.J., Michalski, W.P. & Walker, P.J. (2010). Glycosylation of gp116 and gp64 envelope proteins of yellow head virus of *Penaeus monodon* shrimp. *J Gen Virol*, 91, 2463-2473.

Spann, K.M, Cowley, J.A., Walker, P.J. & Lester, R.J.G. (1997). Gill-associated virus (GAV), a yellow head-like virus from *Penaeus monodon* cultured in Australia. *Dis Aquat Org*, 31, 169-79.

Stanyon, C., Liu, G., Mangiola, B., Patel, N., Giot, L., Kuang, B., Zhang, H., et al. (2004). A *Drosophila* protein-interaction map centered on cell-cycle regulators. *Genome Biol*, 5, R96.

Stelzl, U., Worm, U., Lalowski, M., Haenig, C., Brembeck, F.H., Goehler, H., Stroedicke, M., et al. (2005). A human protein-protein interaction network: a resource for annotating the proteome. *Cell*, 122, 957-968.

Tang, K.F. & Lightner, D.V. (1999). A yellow head virus gene probe: nucleotide sequence and application for in situ hybridization. *Dis Aquat Org*, 35, 165-173.

Tassanakajon, A., Somboonwiwat, K., Supungul, P. & Tang, S. (2013). Discovery of immune molecules and their crucial functions in shrimp immunity. *Fish Shellfish Immunol*, 34, 954-967.

Tate, J., Liljas, L., Scotti, P., Christian, P., Lin, T. & Johnson, J.E. (1999). The crystal structure of cricket paralysis virus: the first view of a new virus family. *Nat Struct Biol*, 6, 765-774.

Thompson, J.D., Higgins D.G. & Gibson, T.J. (1994). CLUSTAL W: improving the sensitivity of progressive multiple sequence alignment through sequence weighting, position-specific gap penalties and weight matrix choice. *Nucleic Acids Res*, 22, 4673-4680.

Tong, Y., Jiang, H. & Kanost, M.R. (2005). Identification of plasma proteases inhibited by *Manduca sexta* serpin-4 and serpin-5 and their association

with components of the prophenol oxidase activation pathway. *J Biol Chem*, 280, 14932-14942.

Tonganunt, M., Phongdara, A., Chotigeat, W., Fujise, K. (2005). Identification and characterization of syntenin binding protein in the black tiger shrimp *Penaeus monodon*. *J Biotechnol*, 120, 135-145.

Uetz, P. & Hughes, R.E. (2000). Systematic and large-scale two-hybrid screens. *Curr Opin Microbiol*, 3, 303-308.

Uetz, P., Dong, Y.-A., Zeretzke, C., Atzler, C., Baiker, A., Berger, B., Rajagopala, S.V., Roupelieva, M., Rose, D., Fossum, E. & Haas, J. (2006). Herpesviral protein networks and their interaction with the human proteome. *Science*, 311, 239-242.

van de Braak, K.(2002). Haemocytic defence in black tiger shrimp (*Penaeus monodon*). PhD thesis, Wageningen University.

Volz, J., Osta, M.A., Kafatos, F.C. & Muller, H.M. (2005). The roles of two clip domain serine proteases in innate immune responses of the malaria vector *Anopheles gambiae*. *J Biol Chem*, 280, 40161-40168.

Walhout, A.J., Sordella, R., Lu, X., Hartley, J.L., Temple, G.F., Brasch, M.A., et al. (2000) Protein interaction mapping in *C. elegans* using proteins involved in vulval development. *Science*, 287, 116-122.

Walker, P.J., Cowley, J.A., Spann, K.M., Hodgson, R.A.J., Hall, M.R. & Withyachumnarnkul, B. (2001). Yellow head complex viruses: transmission cycles and topogtraphical distbibution in the Asia-Pacific region. In: Browdy, C.L., Jory, D.E. (Eds.), *The New Wave, Proceedings of the Special Session on Sustainable Shrimp Culture, Aquaculture 2001*. The World Aquaculture Society, Baton Rouge, LA, USA, pp. 292-302.

Walker, P.J. & Mohan, C.V. (2009). Viral disease emergence in shrimp aquaculture: origins, impact and the effectiveness of health management strategies. *Rev Aquacult*, 1, 125-154.

Wertheim, J.O., Tang, K.F.J., Navarro, S.A. & Lightner, D.V. (2009). A quick fuse and the emergence of Taura syndrome virus. *Virology*, 390, 324-329.

Wijegoonawardane, P.K.M., Cowley, J.A., Phan, T., Hodgson, R.A.J., Nielsen, L., Kiatpathomchai, W. & Walker, P.J. (2008). Genetic diversity in the yellow head nidovirus complex. *Virology*, 380, 213-225.

Wongteerasupaya, C., Sriurairatana, S., Vicker, J.E., Akrajamorn, S., Boonsaeng, V., Panyim, S., Tassanakajon, A., et al. (1995). Yellow-head virus of *Penaeus mon*odon is an RNA virus. *Dis Aquat Org*, 22, 45-50.

Wongteerasupaya, C., Tongchuea, W., Boonsaeng, V., Panyim, S., Tassanakajon, A., Withyachumnarnkul, B. & Flegel, T.W. (1997). Detection of yellow-head virus (YHV) of *Penaeus monodon* by RT-PCR amplification. *Dis Aquat Organ*, 31, 181-186.

BIOGRAPHY

NAME	Mr. Thanawat Sriphaijit
DATE OF BIRTH	7 March 1983
PLACE OF BIRTH	Ratchaburi, Thailand
INSTITUTION ATTENDED	Mahidol University, 2003: Bachelor Degree of Science (Biotechnology) Doctor of Philosophy, 2014: (Biotechnology)
SCHOLARSHIP	Thailand Graduate Institute of Science and Technology Scholarship The Royal Golden Jubilee Ph.D. Program
HOME ADRESS	18/302 Ratchaprarop Road, Ratchathewi Bangkok 10400, Thailand

PUBLICATIONS

1. Senapin, S., Phiwsaiya, K., Anantasomboon, G., Sriphaijit, T., Browdy, C.L., Flegel, T.W. (2010). Knocking down a Taura syndrome virus (TSV) binding protein Lamr is lethal for the whiteleg shrimp *Penaeus vannamei*. Fish Shellfish Immunol, 29, 422-429.
2. Sriphaijit, T., Flegel, T.W. & Senapin, S. (2007). Characterization of a shrimp serine protease homolog, a binding protein of yellow head virus. Dev Comp Immunol, 31, 1145-1158.
3. Sriphaijit, T. & Senapin, S. (2007). High expression of a novel leucine-rich repeat protein in hemocytes and the lymphoid organ of the black tiger shrimp *Penaeus monodon*. Fish Shellfish Immunol, 22, 264-271.
4. Sangsuriya P, Phiwsaiya K, Pratoomthai B, Sriphaijit T, Amparyup P, Withyachumnarnkul B, Senapin S. (2014). Knockdown of a novel G-

protein pathway suppressor 2 (GPS2) leads to shrimp mortality by exuvial entrapment during ecdysis. Fish Shellfish Immunol, 37, 46-52.